Controlling Bacterial Super-infection During Influenza

by

Helen Eva Adams Rich

BA, Oberlin College, 2014

Submitted to the Graduate Faculty of

School of Medicine in partial fulfillment

of the requirements for the degree of

Doctor of Philosophy

University of Pittsburgh

2019

UNIVERSITY OF PITTSBURGH

SCHOOL OF MEDICINE

This dissertation was presented

by

Helen Eva Adams Rich

It was defended on

June 11, 2019

and approved by

Jennifer M. Bomberger
Associate Professor, Department of Microbiology & Molecular Genetics

Sarah L. Gaffen
Gerald P. Rodnan Professor, Department of Medicine

Saumendra N. Sarkar
Associate Professor, Department of Microbiology & Molecular Genetics

John V. Williams
Associate Professor, Department of Pediatrics

Dissertation Director: John F. Alcorn
Associate Professor, Department of Pediatrics

Controlling Bacterial Super-infection During Influenza

Helen Eva Adams Rich, PhD

University of Pittsburgh, 2019

Bacterial super-infection during influenza increases morbidity and mortality from the viral infection. Current therapies for influenza and bacterial super-infection are limited and inadequate, and rising multi-drug resistance in bacteria underscores the need for new therapies. Administration of an engineered antimicrobial peptide, WLBU2, reduced methicillin-resistant *Staphylococcus aureus* burden during pulmonary bacterial infection, but failed to reduce *S. aureus* burden during influenza super-infection. Immunopathology is a strong driver of mortality in bacterial super-infection during influenza, so I investigated the underlying dysfunction in antibacterial immunity caused by preceding influenza. Type I interferon induced in response to influenza infection had been previously shown to be a broad suppressor of antibacterial immunity. Type III interferons had been described much more recently, and were shown to be produced in response to influenza at even higher levels than type I interferon. Thus, I interrogated the role of type III interferon in the pathogenesis of bacterial super-infection during influenza. To do this, I compared super-infection outcomes between wild-type mice and mice lacking IFNλ3, one of the two murine type III interferons. However, total IFNλ was not markedly reduced in these mice, so I instead decided to test the effect of IFNλ treatment during influenza on outcomes of bacterial super-infection, as it had been recently published that IFNλ treatment ameliorated morbidity and mortality from influenza. It had also been recently shown that mice lacking the type III interferon receptor had increased burden in *S. aureus* super-infection during influenza, which mimicked data from mice lacking the type I interferon receptor. Adenoviral overexpression of IFNλ3 one day prior to

bacterial super-infection induced neutrophil dysregulation, with lower binding and uptake of both *S. aureus* and *Streptococcus pneumoniae* in the lungs of mice during influenza super-infection with each of these bacteria. These results suggest that, while new therapeutics for bacterial super-infection during influenza need to be discovered, neither IFNλ nor WLBU2 should be considered. WLBU2 may be effective for bacterial pneumonia alone, but IFNλ should not be used as a treatment for influenza due to the high risk of mortality and morbidity from bacterial super-infection.

Table of Contents

List of Tables

List of Figures

Preface

I would like to take this time to thank the many people who made this work possible. First and foremost is my advisor John Alcorn, who has helped me become the scientist I am today. John has always provided me the perspective necessary to dig down and uncover the diamond in the rough, the exciting bit of data concealed in a set of experiments I might have assumed were worthless. Through his mentorship, I have learned how to not sweat the small stuff, to always consider physiological relevance, and to not throw myself blindly at a problem thinking that hard work will eventually uncover a useful answer. I am a better experimentalist, public speaker, and—most importantly—grant writer because of him.

I would also not be here today without the individual contributions of everyone in the Alcorn lab. Two people in particular, Michelle Manni and Keven Robinson, have been exceptional mentors to me, collaborating with me and teaching me while putting up with my endless questions. Michelle has pushed me to be a more rigorous scientist and I hope to emulate her careful consideration of all aspects of science, from logical inconsistencies in written arguments down to testing individual lots of reagents to ensure the accuracy of an experiment. Keven has been a fount of medical knowledge and the practice of pulmonary medicine, and like John, has showed me that problems may not be as important as I perceive them in the moment—"Is somebody dying? No? Then you're doing okay." Each member of the lab has helped me learn techniques, new ways to approach experiments, talked with me about the theories and hypotheses underlying my science, and listened to me rant when experiments were going poorly. My eternal thanks to everyone in the lab for supporting me through this long and arduous process.

My thesis committee has always been a source of support and new perspectives during this journey. I first encountered Saumen Sarkar's teaching when I signed up for his elective course on innate immunity during the spring semester of my first year in graduate school. I found out on the first day that I was more junior than all the other students, and considered dropping the course, but Saumen encouraged me to stay in and be challenged. I will always appreciate his encouragement, honesty, and continual drive to comprehensively understand science. While John would always tell me to add more background after a presentation, Saumen would readily stop me during discussions to make me explain the basics of my experiments, always concerned with the minutiae of an assay and understanding my data from the ground up. I will always hear both Saumen and Michelle's voices in the back of my head during experimental design, and I am so grateful for their continued assistance. John Williams, the MD on my committee, provided me his invaluable perspective as a virologist and practicing pediatric infectious disease specialist. He is the author of the most terrifying email I have ever received, in which he told me in no uncertain terms to only ever call him John and not Dr. Williams. His geniality and kindness have underscored every interaction I have had with him, from signing my TB test forms so I could access the animal facility to answering my virology questions at Rangos happy hours. I have felt supported by Jen Bomberger ever since she agreed to let me advance to PhD candidacy as part of my comprehensive examination committee, and have always admired her organization and mentorship as she led me and my fellow graduate students in teaching microbiology to medical students. Finally, I want to emphasize the role that Sarah Gaffen has had in my development as a scientist. From interviewing with her for this graduate program to getting advice on potential postdoctoral mentors, she has supported me through every step of my development in graduate school. At the "Circle Seventeen Investigators" monthly meeting, she would ask some of the most insightful questions to help

trainees with their experiments, showing her expertise as an exacting scientist with the breadth of knowledge to match. She has always taken time out of her busy schedule to give me advice, encouraging me to reach higher and believe in myself more. Sarah, Jen, John, and Saumen, you have my deepest gratitude.

My cohort of immunology PhD students has been there for me since the beginning, even before I joined John's lab. Through first-year classes and seminars on seminars, they have provided friendship, support, and an enthusiastic willingness to always attend happy hour afterward. Commiserating over beers has been the perfect antidote to feeling hopeless after long days, weeks, and months of failure. Thank you so, so much, Nicole, Adolfo, and Hiroshi.

As well, I would like to extend my thanks to all the staff who have helped me along the way, including the DLAR and administrative assistants without whom our institutions would not function.

Last but certainly not least, I would like to thank the people in my life outside of the scientific bubble who have helped me through this experience. I met Dave at the now-shuttered mainstay of Pittsburgh's Oakland neighborhood, Peter's Pub, during an evening of blues dancing. Since that night, he has given me nothing but support and comfort, always ready to let me talk science at him or turn my brain off and relax with a movie, whichever I need more in the moment. And finally, my family—Mum, Dad, and my sister Nina—who have cheered me on from afar through this entire process. Fortunately, Boston has only been a short flight away, and I have cherished spending my holidays surrounded by their unconditional love and support. Thank you all, from the bottom of my heart.

Abbreviations

AMs: alveolar macrophages

AMPs: antimicrobial peptides

BAL: bronchoalveolar lavage

BPIFA1: BPI-fold containing group A member 1

CD: cluster of differentiation

CFU: colony-forming units

cGAS: cytosolic GMP-AMP synthase

CLRs: C-type lectin receptors

CVV: candidate vaccine virus

DC: dendritic cell

DMFO: dimethylformamide

dsRNA: double-stranded ribonucleic acid

EGFR: epidermal growth factor receptor

EPCAM: epithelial cell adhesion molecule

FITC: fluorescein isothiocyanate

FPR2: formyl peptide receptor 2

G-CSF: granulocyte-colony stimulating factor

HA: hemagglutinin

hCAP: human cathelicidin antimicrobial protein

IFN: interferon

IL: interleukin

IRF: interferon regulatory factor

ISG: interferon-stimulated gene

ISGF: interferon-stimulated gene factor

ISRE: interferon-stimulated response element

JAK: Janus kinase

KC: keratinocyte chemoattactant

LAIV: live attenuated influenza vaccine

MAVS: mitochondrial antiviral signaling protein

MCP-1: monocyte chemoattractant protein-1

MDCK: Madin-Darby canine kidney cells

MHC: major histocompatibility complex

MRSA: methicillin-resistant *Staphylococcus aureus*

MSSA: methicillin-sensitive *Staphylococcus aureus*

NA: neuraminidase

NF-κB: nuclear factor kappa B

NGAL: neutrophil gelatinase-associated lipocalin, also named lipocalin 2 (lcn2)

NLRs: nucleotide-binding oligomerization domain-like receptors

OPA: oropharyngeal aspiration

PCR: polymerase chain reaction

PR8: the common laboratory strain influenza H1N1 A/Puerto Rico/8/34

PRRs: pattern recognition receptors

RLRs: RIG-1 like receptors

RNPs: ribonucleoproteins

RSV: respiratory syncytial virus

STAT: signal transducer and activator of transcription

STING: stimulator of interferon genes

ssRNA: single-stranded ribonucleic acid

TLRs: Toll-like receptors

TSLP: thymic stromal lymphopoietin

TYK: tyrosine kinase

WT: wild-type

1.0 Introduction

1.1 Interferons

While type I interferons have been known since 1957 as cell-secreted antiviral factors (1), and were in fact the first cytokines discovered, type III interferons (IFNλ, IL-28/29) were only first described in 2003. Their simultaneous discovery by two different groups led to their many names, with Paul Sheppard's paper calling them interleukins (IL)-29 and IL-28A/B (2), while Sergei Kotenko's paper named them interferon lambda (IFNλ1/2/3, respectively) (3). While IFNλ1 is only found in humans, both mice and humans express IFNλ2 and IFNλ3. On the other hand, IFNλ4 is polymorphically expressed in humans and is more strongly associated with hepatitis C virus clearance in populations of African descent (4). It is likely that all IFNλ genes share a common evolutionary ancestor (5). While IFNλ is functionally an interferon, it shares little structural similarity with type I interferon. Rather, IFNλ structurally parallels members of the IL-10 family, and is most similar in structure to the type 17 cytokine IL-22, which protects mucosal tissues against bacterial infection (6).

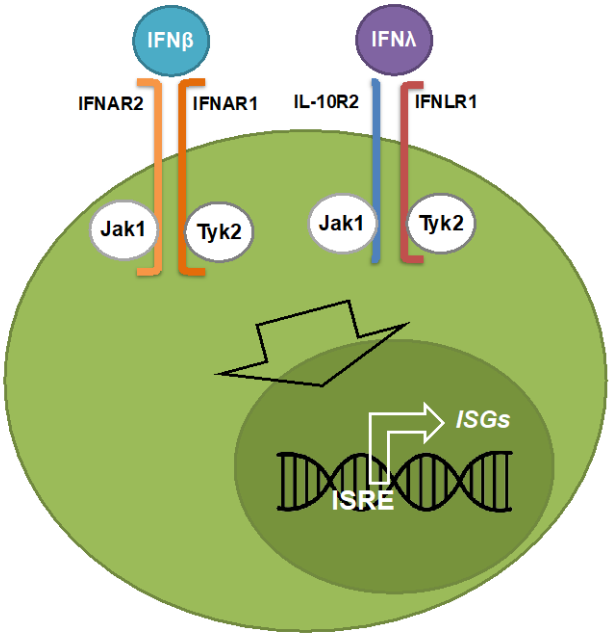

Figure 1: Type I and III interferon signaling.

Type I and III interferons, though structurally dissimilar, converge at the beginning of their signal cascades to induce the transcription of a highly overlapping complement of interferon-stimulated genes (ISGs). Type I interferons (thirteen human and fourteen murine IFNα subtypes, and a single IFNβ in both mouse and human) bind to the ubiquitously expressed heterodimeric receptor of IFNαR1 and IFNαR2. Type III interferon binds to the specific IFNλR1 and the broadly expressed IL-10R2, which is shared with many IL-10 family members including both IL-10 and IL-22. Binding of these interferons to their receptors causes phosphorylation of Janus kinase 1 (JAK1) and tyrosine kinase 2 (TYK2), resulting in phosphorylation of signal transducer and activator of transcription (STAT) proteins STAT1 and STAT2. These proteins bind to form a STAT1/STAT2 heterodimer, which then binds IRF9 to become the interferon-stimulated gene factor 3 (ISGF3) transcription factor complex. ISGF3 translocates to the nucleus, where it binds

the interferon-stimulated response element (ISRE) to activate the transcription of interferon stimulated genes (ISGs).

1.2 Influenza

While influenza is often thought to be a seasonal nuisance, estimates extrapolating from data collected between 2010 and 2013 demonstrate its lethality: approximately 4,915-27,174 deaths each year in the United States were attributable to influenza, along with 18,491-95,390 ICU admissions and 113,192-624,435 hospitalizations (7). The estimated annual direct costs of influenza are $4.6 billion, with an additional $7 billion from employees' sick days and lost productivity (8). The impact of influenza infection skyrockets during pandemics. The infamous 1918 "Spanish Flu" was estimated to have killed 50 million people worldwide (9), while the most recent influenza pandemic in 2009 was estimated to have infected 60.8 million people in the U.S. and hospitalized approximately 275,000 (10).

The seasonality of influenza has been the subject of much debate, and virus survival and transmission are now thought to be mainly influenced by temperature and relative humidity (11). The influenza virus is thought to spread from person to person via droplet, either by coughing, sneezing, or physical contact. Once inhaled, the influenza virus preferentially infects the first cells it comes in contact with: epithelial cells of the respiratory tract. Using these epithelial cells as factories, the influenza virus replicates rapidly using the host cell machinery to produce more virions.

There are four categories of influenza viruses: influenza A, B, C and D. Influenza D was first isolated from pigs in 2011 and is thought to only infect livestock (12). It is unable to reassort with its closest relative, influenza C, which is a seven-segmented virus that causes only mild respiratory disease in children. Only two of the four, influenza A and B, cause significant illness in humans. These are both viruses with eight segments of negative-sense, single-stranded RNA (ssRNA), which encode the machinery needed to infect host cells and replicate their genetic material to generate more virus. This genetic material is packaged inside a protein capsid (Figure 1.1, shown in purple) and enveloped by a lipid bilayer (Figure 1.1, shown in brown), which is acquired from the host cell membrane during budding.

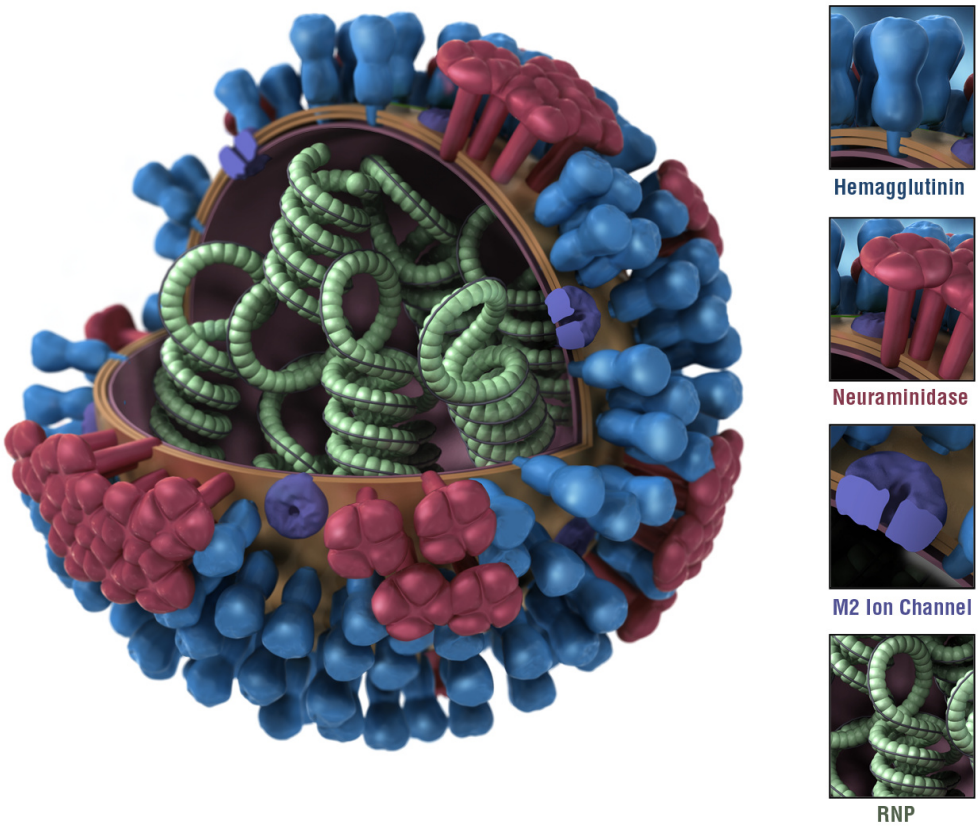

Figure 2: Influenza A virion structure.

CDC/Doug Jordan, M.A. Public Health Image Library.
Reproduced here under public domain licensing.

The influenza virus attaches to the host cell by recognizing sialic acids on the cell surface, binding them with the hemagglutinin (HA) protein expressed on the surface of the viral capsid (Figure 1.1, shown in blue), which triggers endocytosis. Once inside the endosome, the lowered pH induces a conformational change in HA that exposes a portion at its N-terminus termed the "fusion peptide". The viral envelope then fuses with the endosomal membrane, while the M2 ion channel pumps protons into the interior of the virion, allowing complexes of viral RNA polymerase, nucleoprotein, and RNA termed ribonucleoproteins (RNPs, shown in Figure 1.1 in green) to be released from the M1 matrix protein and escape into the cytoplasm of the host cell

(13). These RNPs display a nuclear localization signal, which directs host cell proteins in the cytoplasm to traffic the RNPs to the nucleus. Once inside, the viral RNA segments are disguised by "stealing" of 5' capped primers from host pre-mRNA, allowing for replication of viral RNA by host cell machinery inside the nucleus. Once its eight segments of single-stranded RNA have been translated into protein and packaged into the viral capsid, the fully-fledged virus buds off from the host cell. HA viral proteins continue to bind sialic acids, tethering the virus to the host cell membrane, until viral neuraminidase (NA, shown in Figure 1.1 in maroon) cleaves the sialic acid residues from host cell-surface glycoproteins and the mature virus is released, retaining the host cell lipid bilayer as its envelope (14).

The pandemic potential of influenza comes from its ability to reassort. Reassortment is the process by which different influenza strains exchange segments of genetic material, and is made possible when a single host cell is infected by more than one different influenza virus. This process has been co-opted to make the seasonal influenza vaccine: chicken eggs are dually infected with the high-growth laboratory strain influenza H1N1 A/PR/8/34 (PR8) and a "donor" strain that is predicted to be most widely circulating during the next influenza season. Reassortment of genome segments between the two influenza strains takes place *in ovo*, and antiserum against the H1 and N1 antigens of PR8 is added to select for the surface HA and NA antigens of the donor strain. The reassorted virus retains the high-growth internal machinery of PR8 while expressing the surface antigens of the donor strain (15). This new virus, termed a candidate vaccine virus (CVV), is then inactivated or attenuated, purified, and administered along with adjuvant either by intramuscular injection (of inactivated virus) or by intranasal spray (of live attenuated virus).

Historically, CVV production has occurred in fertilized chicken eggs, but in 2016 the use of vaccines using CVVs made in Madin-Darby canine kidney (MDCK) cells was approved by the

Food and Drug Administration (FDA). MDCK cells are considered safe cell substrates and are useful for large-scale, rapid replication of CVVs (16), which allows more time for researchers at the World Health Organization (WHO) and the FDA to choose donor strains for the upcoming influenza season's vaccines (17). Both trivalent and quadrivalent inactivated influenza vaccines are currently available, made from two influenza A CVVs and either one or two influenza B CVVs, respectively (18). While significant effort was put into developing a live attenuated influenza vaccine (LAIV), which more naturally mimics influenza infection route and immune response, the LAIV has shown no correlate of protection (19). Use of LAIV was discontinued during the 2016-2017 influenza season, but was reinstated in the 2017-2018 season and continues to be available. However, the American Academy of Pediatrics still recommends use of the inactivated influenza vaccine for its target population (2-17 years of age) (20). Vaccine coverage and protection is woefully inadequate as demonstrated each year by the prevalence and spread of influenza, however, treatment options are equally ineffective. While neuraminidase inhibitors such as oseltamivir (Tamiflu) have shown efficacy in reducing the duration of influenza symptoms, oseltamivir must be taken within 48 hours of symptom onset to be effective. There is some suggestion that oseltamivir may also reduce hospital admissions, duration of hospitalization, and risk of lower respiratory tract complications (21), however there are significant disparities between the conclusions drawn from meta-analyses (22, 23).

1.2.1 Pulmonary immune response to influenza

The lung has many defenses against viral infection. The first is a physical defense termed the mucociliary elevator: ciliated cells rhythmically beat their hair-like appendages to clear pathogens and debris from airspaces by moving the particle-entrapping mucus that coats the

airway, protecting the epithelium from pathogen attachment. Alveolar macrophages (AMs) comprise its second defense, patrolling the airspaces and protecting the alveoli where the crucial gas exchange of oxygen for carbon dioxide occurs. When these AMs encounter foreign particles above 0.5 μM in diameter, they engulf them via the process of phagocytosis, digesting and presenting any protein antigens to passing immune cells. AMs can also be considered the first immunological line of defense against infection. Upon sensing bacterial and viral pathogens via pattern recognition receptors (PRRs), AMs execute an immunological signaling cascade specific to the offending pathogen. The epithelium expresses an overlapping complement of PRRs and is also involved in pathogen sensing. PRRs are divided into four families: Toll-like receptors (TLRs) and C-type lectin receptors (CLRs) extend from the cell surface and into endosomes and recognize extracellular pathogens, while RIG-1 like receptors (RLRs) and nucleotide-binding oligomerization domain-like receptors (NLRs) are located in the cytoplasm and recognize intracellular pathogens.

Once alerted to invading pathogens, AMs and airway epithelial cells become activated and produce chemokines and other cytokines to mount an effective, pathogen-specific immune response. During influenza infection, viral double-stranded RNA (dsRNA) and single-stranded RNA are sensed in endosomes of epithelial cells, plasmacytoid dendritic cells, and AMs by TLR3 and TLR7. Viral RNA with its "stolen" 5' cap is recognized by the RLRs MDA5 and RIG-1. Both these pathways converge on the ISGF3 complex, which includes the phosphorylated interferon regulatory factors (IRFs) IRF3 and IRF7, which induce the transcription of type I and III interferons (IFNs). TLR signaling also activates NF-κB signaling, leading to the production of IL-1β and other pro-inflammatory cytokines (24).

1.2.2 Interferon signaling in response to influenza

When viral dsRNA is sensed by RIG-1 and MDA5, these RLRs associate with the mitochondrial antiviral signaling protein (MAVS) found on the membranes of mitochondria, peroxisomes, and the endoplasmic reticulum, inducing an antiviral response dependent on the location of MAVS inside the cell. When localized to mitochondria, MAVS engagement induces the expression of type I IFNs and their ISGs. However, peroxisome-attached MAVS instead drives type III IFN production without inducing type I IFNs, and IFNλ expression is amplified upon peroxisome proliferation (25). Unlike type I interferons, IFNλ has been shown to activate JAK2 signaling (25, 26), and its antiviral effects can be blocked by MAP kinase inhibitors (27). And unlike IFNλ, IFNα has been shown to activate STAT3 (28), which is also known to negatively regulate the type I interferon response (29). The kinetics of these interferon responses differ as well, with IFN III inducing most IFN I ISGs with increasing similarity as with increased dose, suggesting that IFN I is more potent while IFN III is more sustained (30). Additionally, IFNλ has been shown to induce some ISGs more highly than type I IFN, including CXCL10 and CXCL11 (31). While differences in IFN I and III signaling were originally thought to be due to differential receptor expression between cell types, as IFNλR1 expression was thought to be confined to mucosal barrier surfaces (32), more recent work shows that these differences may be independent of receptor abundance and instead intrinsic to their signaling pathways (33).

Both type I and III interferons are important for antiviral defense in the lung. Treatment with either IFN I or IFN III restricts viral replication in respiratory epithelial cells and mice (34), and there appears to be significant redundancy between type I and III interferons in the respiratory tract (35). Mice lacking either IFNαR1 or IFNλR1 are more susceptible to influenza infection, but both are important for limiting mortality during influenza (36). Importantly, type III interferon is

even more highly produced in response to influenza A infection than type I interferon in mice (37). It is commonly thought that type III IFN is less inflammatory than type I IFN. Mice lacking either IFNλR1 or both IFNαR1 and IFNλR1 had increased immunopathology as shown by both histology and BAL cellularity during influenza infection, but IFNαR1 deletion alone did not increase immunopathology (36). Epithelial cells ($EPCAM^+$) produce IFNλ in the first days after influenza infection, with parenchymal $CD45^+CD11c^+MHCII^+Siglec\ F^-$ dendritic cells (DCs) producing a small amount by day three. Epithelial cells express high basal IFNλR1 which was downregulated upon influenza infection, while neutrophils express the second highest basal IFNλR1 but upregulate it upon influenza infection to become the highest IFNλR1 expressers (36). Importantly, IFNα but not IFNλ induces inflammatory cytokines in neutrophils (36), which are a driver of immunopathology during influenza. Moreover, IFNλ induced by enteric virus infection reduces reactive oxygen species (ROS) generation and suppresses degranulation in neutrophils, suggesting this mechanism is not exclusive to the lung (38). Overall, type I IFN induces a higher inflammatory response that is important for influenza control, but control of immunopathology seems to be the task of IFNλ.

1.3 Bacterial Super-infection

In 1918—before the advent of antibiotics ten years later—over 95% of tissue specimens from pandemic victims later tested positive for bacterial infection. Even as recently as the 2009 pandemic, bacterial super-infection was found in 25-50% of severe cases (39). This phenomenon is not specific to pandemic influenza; the Center for Disease Control tracks all pediatric deaths from influenza and consistently reports that almost half of children who die from influenza have a

bacterial co-infection. On average during the last three influenza seasons (2016-2019), 47.8% of pediatric deaths were associated with bacterial co-infection. 25.4% of these bacterial co-infections were identified as *S. pneumoniae,* while 41.4% of bacterial co-infections were *S. aureus*, of which 20% were methicillin-resistant *S. aureus* (MRSA) (40). The prevalence of MRSA increases during pandemic years, with 71% of *S. aureus* co-infections typed as methicillin-resistant in 2009 (41), underscoring the need for an in-depth understanding of the phenomenon of bacterial super-infection. Many groups have shown that this susceptibility to secondary bacterial infection during influenza is due to immune dysregulation, and understanding of this underlying pathology is necessary for a more comprehensive view of this phenomenon.

Approximately one week into influenza infection, the inflammatory response is maximal and interferon response peaks around this time in both humans and mice. IFNλ and IFNα expression in the lung are highest 5-7 days after infection with 10 PFU influenza, and IFNβ is also highest at day 7. During high-dose infection with 100 PFU influenza, IFNα and IFNβ expression peak on day 5 while IFNλ expression peaks from days 3-5 (36). The epithelial barrier has eroded by this time, leading to disrupted gas exchange and poor blood oxygenation. Both Gram positive and Gram negative extracellular bacteria now take advantage of exposed adherence sites (42) and begin secondary infection in a nutrient-rich environment (43). When these pathogens enter the influenza-infected lung, antibacterial immune responses are blunted. The lung is now “primed” by influenza for a secondary bacterial infection.

1.3.1 Bacterial infection of the lung

While most respiratory tract infections are caused by viruses, many of these are mild to moderate upper respiratory tract infections including “the common cold”. Lower respiratory tract infections, bronchitis/bronchiolitis and pneumonia, are much more severe and a higher percentage are fatal. The most common bacteria that cause pneumonia are Gram positive, namely *Staphylococcus aureus* and *Streptococcus pneumoniae*, with Gram negative bacteria also common including *Klebsiella pneumoniae*, *Pseudomonas aeruginosa, Escherichia coli,* and *Enterobacter* species (44). Immune responses differ in specific ways between bacterial strains, although many commonalities exist (45).

1.3.2 Pulmonary immune response to bacteria

The lung has robust immunity to pathogenic bacteria, which are introduced by every breath into the lungs. The first layer of defense against infection is barrier function: mucus and cilia work together to clear the airway of debris and pathogens, and surfactant proteins bind bacteria to improve clearance. AMs patrol alveoli, eliminating extracellular bacteria and displaying antigen to T cells. When pathogenic bacteria enter the lung, recognition by pattern recognition receptors occurs in and on cells at barrier sites. Epithelial cells produce antimicrobial peptides (AMPs), which can directly lyse bacteria. Both epithelial cells and AMs make interferons and inflammatory cytokines, resulting in neutrophil and monocyte activation and homing to the lung. When unimpaired, this influx of phagocytes provides bacterial phagocytosis and killing to control the infection, including generation of reactive oxygen species. Bacteria induce variable chemokine responses, but overall cytokine responses are often conserved. The influx of cells into the lung

brings fluid through the damaged epithelial/endothelial barrier, which can lead to acute respiratory distress syndrome (ARDS) and significant mortality if unresolved.

Influenza infection leads to the production of inflammatory chemokines by lung-resident cells (epithelial cells and AMs), which recruit granulocytes as well as other immune cells to the lung. Neutrophils recruited to fight pulmonary bacteria during influenza have reduced bactericidal capacity, yet retain their inflammatory functions, leading to increased immunopathology. It has been shown that neutrophils from influenza-infected mouse lungs display reduced bacterial phagocytosis and intracellular ROS production upon bacterial challenge (46). Macrophages also display decreased bacterial phagocytosis when infected with influenza virus (47). This suppression of neutrophils is recapitulated in humans, where influenza infection lead to a defect in lysozyme secretion by sputum neutrophils (48). However, the presence of these neutrophils in the lung is still required, as antibody depletion of Ly6G+ cells resulted in increased bacterial burden during MRSA challenge seven days post-influenza (49). In fact, increased neutrophil numbers can aid bacterial clearance, when combined with an increase in function (50).

Not only cellular responses but molecular responses are also blunted by preceding influenza. Antimicrobial peptides (AMPs) are made by epithelial cells and neutrophils, as well as alveolar macrophages, as direct killing mechanisms against bacteria (51). These peptides can also recruit neutrophils and act as chemokines (52). Prior influenza infection suppresses this antimicrobial peptide response, especially through inhibiting production of neutrophil gelatinase-associated lipocalin (NGAL, also termed lipocalin 2). Restoration of antibacterial immunity can be achieved when NGAL is given exogenously (53). Cytokine and chemokine production is also altered by prior influenza infection.

Type 17 cytokines are crucial to antibacterial defense. Type 17 cytokines are predominantly produced during bacterial super-infection by gamma delta T cells (54), which are present in or quickly recruited to tissue, in contrast to conventional CD4+ T helper (Th)17 cells. Mice lacking receptors for the type 17 cytokines IL-17 and IL-22, respectively IL-17RA and IL-22R1, had significantly increased lung bacterial burden during primary *S. aureus* infection. In mice that received influenza six days prior to *S. aureus* challenge, type I IFNs inhibited the induction of IL-17, IL-22, and IL-23, a potent inducer of type 17 cytokines. Exogenous IL-23 rescued the production of both IL-17 and IL-22 and increased bacterial clearance during *S. aureus* super-infection (55). Many other cytokines have been implicated in this immune dysregulation from preceding influenza, including both type 1 cytokines (interferon gamma (56) and tumor necrosis factor alpha (57)) and type 2 cytokines (IL-27 (58), IL-33 (50), IL-10 (59), and IL-13 (60)). Type I interferon seems to be a broad dysregulator of antibacterial immunity, as mice lacking the IFN I receptor IFNαR1 do not display an influenza-induced increase in bacterial burden during bacterial challenge.

1.3.3 Interferon signaling in response to bacterial infection and super-infection

Macrophages and dendritic cells (DCs) in the lung produce type I IFNs in response to infection with certain bacteria (61, 62). *S. aureus* infection leads to IFNβ production via stimulator of interferon genes (STING) protein and the cytosolic DNA sensor cyclic GMP-AMP synthase (cGAS). Importantly, this production of IFNβ is pathogenic to the host, as mice lacking STING effectively clear cutaneous *S. aureus* infection (63). Influenza induces production of type I and significantly more type III IFN (37, 64), with expression peaking three to five days after infection (36). While wild-type mice show an increase in bacterial burden when influenza precedes

pulmonary *S. aureus* infection, mice lacking the type I IFN receptor (IFNαR1$^{-/-}$ mice) show no such increase (55). This effect is not specific to *S. aureus*, and has been shown for *S. pneumoniae* (65) as well as Gram-negative bacteria including *Escherichia coli* and *Pseudomonas aeruginosa* (66). Mice lacking the IFN induced transcription factors STAT1 or STAT2 (67) also exhibit reduced susceptibility to secondary bacterial infection (68). These findings were recapitulated in mice lacking the type III IFN receptor, suggesting that both type I and III IFNs increase bacterial burden during influenza super-infection (69).

Interestingly, wild-type mice are surprisingly less susceptible than IFNαR1$^{-/-}$ mice to bacterial super-infection early during influenza infection. This resistance to bacterial super-infection tracks with an increase in the type I IFN family member IFNβ, whereas later susceptibility correlates with increased IFNα. Importantly, antibody inhibition of IFNβ one day post-viral infection increased bacterial burden in the lung, while antibody inhibition of IFNα five days post-viral infection reduced lung bacterial burden. Mice treated with recombinant IFNα one day before lung infection with MRSA increased bacterial burden in the lung, suggesting that increased IFNα is critical to enhancing susceptibility to super-infection (49).

1.3.4 Treating bacterial super-infection during influenza

As lung function is critical to life, development of new antimicrobial therapies to fight bacterial pneumonias is necessary. Pneumococcal vaccination has drastically reduced streptococcal pneumonia since the initial licensing of the vaccine in 1977 (70). Vaccines against *S. aureus* have not yet cleared phase III clinical trials, but many are currently being developed (71). Neutralizing antibodies against staphylococcal toxins, namely alpha-toxin, have been successful in a variety of trials (72, 73). Many other therapeutic strategies against bacterial pore-

forming toxins have been developed over the past few decades including pore-forming toxin receptor blockade, pore blocking agents, toxoid vaccines, liposomes to capture pore-forming toxins, and small molecules that bind pore-forming toxins to prevent their oligomerization (74).

One path towards creating effective therapies is examining factors that affect patient survival. Many therapeutics that show promise in mice do not ameliorate disease in humans. Importantly, mice and humans differ significantly in their immunity to *S. aureus* infection, as demonstrated by the fact that humanized mice show increased susceptibility to *S. aureus* skin infection (75) as well as lung infection (76). Children displayed increased antibody titer to the bicomponent pore-forming toxin LukAB upon seroconversion from acute-phase to convalescent-phase during invasive *S. aureus* infection, and sera containing anti-LukAB antibodies was able to neutralize the cytotoxicity of *S. aureus* isolates (77). Thomsen *et al.* were able to generate three hybridomas from a pediatric patient with *S. aureus* osteomyelitis that produce monoclonal antibodies with anti-LukAB activity, which were effective against cytotoxicity and together were able to reduce colony counts in a murine model of *S. aureus* sepsis (78). LukAB has now been shown to kill not only neutrophils and macrophages but also human dendritic cells (79), suggesting this toxin is a prime candidate for therapeutic targeting. The possibility remains that neutralizing only one toxin may not be not effective as others become more highly expressed to take its place in the phenomenon of "counter inhibition" (80). To address this, a single human monoclonal antibody has been developed with the ability to neutralize alpha-hemolysin as well as four other bicomponent leukocidins, and more recently a combination therapy of two human monoclonal antibodies which together can neutralize six *S. aureus* cytotoxins (81, 82). Many new antibacterial therapies are currently being developed, which are absolutely crucial to the treatment of bacterial

super-infection as current measures against influenza are limited and bacterial resistance to antibiotics is ever-increasing.

2.0 The Engineered Antimicrobial Peptide WLBU2 Does Not Reduce Bacterial Burden During Influenza Super-infection

2.1 Summary

With the current increase in antibiotic resistance, development of new therapeutics against multi-drug resistant bacteria is necessary. WLBU2 is a novel engineered antimicrobial peptide, built on the scaffold of the endogenous cathelicidin LL-37. LL-37 is a short, α-helical protein formed from the cleavage of hCAP18, which is effective at killing a wide range of pathogens. LL-37 also binds host cellular receptors and modulates the immune response, increasing pro-inflammatory cytokines such as IL-1β along with neutrophil and macrophage/monocyte chemokines. Overactivation of the immune system can lead to significant immunopathology during bacterial lung infection, as immune cell recruitment to the lung can result in pulmonary edema. Excess fluid in the lung disrupts the crucial gas exchange in the alveoli that allows blood to be oxygenated, and can lead to acute respiratory distress syndrome. Thus, treatments for pulmonary bacterial infection must balance bacterial killing while limiting immunopathology.

While the engineered WLBU2 retains the short helical structure of LL-37, it is composed only of three amino acids: valine, arginine, and tryptophan. I show that WLBU2 does not have the same immunomodulatory properties as LL-37, but retains the ability to kill bacteria in an *in vivo* model of methicillin-resistant *Staphylococcus aureus* (MRSA) lung infection. However, WLBU2 is unable to reduce pulmonary bacterial burden in a model of MRSA super-infection during influenza. While WLBU2 may not be effective against bacterial super-infection during influenza, it has been shown to be effective in models of bacterial sepsis, biofilm formation, and pulmonary

bacterial infection, and may become an important tool in the fight against bacterial infection in an era of rapidly increasing multi-drug resistance.

2.2 Introduction

Current treatments for bacterial super-infection are limited to treatment of the underlying influenza infection, with the addition of antibiotics against the super-infecting pathogen. With the rise of multi-drug resistance, especially in methicillin-resistant *S. aureus* strains, it is crucial that new antibacterial compounds be developed. One such avenue of discovery is the engineering of antimicrobial peptides: small (12-50 amino acid) proteins which directly kill a wide range of invading pathogens, including viruses, bacteria, and fungi. Antimicrobial peptides are naturally produced by the innate immune system and have myriad mechanisms by which they kill microbes, but commonly display an amphipathic tertiary structure which allows their passage through the microbial phospholipid membrane, allowing for membrane disruption as well as binding of intracellular molecules.

The most abundant antimicrobial peptides in the lung are alpha-defensins, beta-defensins, and cathelicidins. These peptides are expressed by cells of the innate immune system, including epithelial cells, neutrophils, and alveolar macrophages. While these classes of peptides differ structurally, all are amphipathic with both hydrophobic and positively charged surfaces. α- and β-defensins have a triple-stranded β-sheet structure formed by three intramolecular disulfide bridges, while cathelicidins have an α-helical structure (83). The single human cathelicidin, LL-37, is a 37 amino acid peptide formed by proteolytic cleavage of the C-terminus from the human cathelicidin antimicrobial protein 18 (hCAP18). LL-37 has a broad spectrum of direct antimicrobial activity,

but also binds host cellular receptors (formyl peptide receptor 2 (FPR2) (84, 85), P2X7 (86), and epidermal growth factor receptor (EGFR) (87)) and stimulates immune pathways.

The simpler α-helical structure of cathelicidins constitutes a prime scaffold for designing novel antimicrobial peptides. Deslouches *et al.* began by optimizing this structure, creating a 12-residue amphipathic helix consisting only of hydrophobic valine residues on one face and cationic arginine residues on the other, termed the "lytic base unit" (LBU). Many variations on length of this peptide were tested, with the 24-residue LBU2 peptide producing optimal killing of both *Pseudomonas aeruginosa* and *Staphylococcus aureus*. A second series included the addition of tryptophan residues, often found in membrane-disrupting peptides, termed the WLBU series. Again, the 24-residue peptide proved most potent, with the WLBU2 peptide displaying the lowest minimal bactericidal concentration (88). Importantly, WLBU2 retained its bacterial-killing properties in the presence of human serum, unlike the endogenous cathelicidin LL-37, and was able to rescue mice from fatality in a model of *P. aeruginosa* sepsis. The maximum tolerable dose for intravenous injection was determined to be 12 mg/kg by Kaplan-Meier survival curve, with LD50 estimated to be between 12-16 mg/kg. Mice treated with 3 mg/kg WLBU2 intravenously 30 minutes after intraperitoneal infection with *P. aeruginosa* survived sepsis and were rescued from bacteremia, while all PBS-treated mice perished within 36 hours (89).

Many groups have since published that WLBU2 has broad efficacy against many pathogens, both *in vitro* and *in vivo*. Most recently, WLBU2 has been shown to prevent biofilm formation by commonly multidrug-resistant respiratory pathogens *K. pneumoniae, P. aeruginosa,* and *S. aureus* (90). Moreover, WLBU2 has also been shown to have simultaneous antiviral and antibacterial activity, in a model of *P. aeruginosa* biofilm growth on bronchial epithelial cells infected with respiratory syncytial virus (RSV) (91). Due to its tolerability, high potency, and wide

range of antimicrobial activity, I hypothesized that WLBU2 might be a useful therapeutic for bacterial super-infection during influenza.

2.3 Materials and Methods

2.3.1 Antimicrobial peptides

LL-37 (LLGDFFRKSKEKIGKEFKRIVQRIKDFLRNLVPRTES) and the engineered antimicrobial peptide WLBU2 (RRWVRRVRRWVRRVVRVVRRWVRR) were generous gifts of Berthony Deslouches (88).

2.3.2 Mice

Six- to eight-week old male C57BL/6J mice were purchased from Taconic Biosciences (Hudson, NY) and maintained under pathogen-free conditions. All studies were performed on age- and sex-matched mice. All animal studies were conducted with approval from the University of Pittsburgh Institutional Animal Care and Use Committee.

2.3.3 Murine infections

All mouse infections were administered by oropharyngeal aspiration (OPA) after inhaled isoflurane anesthesia. Methicillin-resistant *Staphylococcus aureus* (MRSA) USA300 was grown to stationary phase overnight shaking at 37°C in *S. aureus*-specific media (appendix section A.5), using a second tube of uninoculated broth to ensure broth sterility. The next morning, the optical

density of the culture was measured at 660 nm, and colony-forming units (CFU) were estimated by multiplying the OD660 by the previously calculated extinction coefficient of 1.48×10^9. The culture was centrifuged at 10,000×g for five minutes, broth was aspirated, and the bacterial pellet was resuspended in enough PBS to deliver 5×10^7 CFU in 50 µl per mouse. Influenza H1N1 A/PR/8/34 was prepared by diluting frozen virus stock between 1:15,000 and 1:150,000 with PBS, to deliver enough virus in 50 µl per mouse to cause 10-15% weight loss by sacrifice on day 7.

2.3.4 Animal harvest

At harvest, mouse lungs were lavaged with 1 ml sterile PBS. This bronchoalveolar lavage (BAL) fluid was centrifuged at 10,000×g for 5 min to pellet cells, and the supernatant was aspirated and frozen at −80°C for later protein and cellular damage analysis. Cell pellets from lavage fluid were resuspended in 500 µl sterile PBS and counted on a hemocytometer to enumerate infiltrating cells. The right upper lobe of each lung was mechanically homogenized and plated for bacterial CFU counting, with the excess frozen at −80°C for later analysis.

2.3.5 Analysis of lung inflammation

Cytokine levels in bronchoalveolar lavage fluid and lung homogenate were analyzed with the Bio-Plex Pro mouse cytokine 23-plex array (Bio-Rad, Hercules, CA). Total protein in bronchoalveolar lavage was measured by Bradford assay (Thermo Scientific Pierce Coomassie Protein Assay kit; ThermoFisher, Waltham, MA).

2.3.6 Statistical analysis

Data were analyzed using GraphPad Prism 7 (GraphPad, La Jolla, CA). Analyses comparing two groups were performed by an unpaired t test with Welch's correction, unless data were not parametrically distributed, in which case Mann-Whitney analysis was used. Mortality data were analyzed by a log-rank (Mantel-Cox) test. All figures show combined data from multiple replicate studies as means ± standard errors of the means (SEM). The indicated *n* values are numbers of animals per group in each independent experiment. Statistical significance is reported as follows: * $p < 0.05$, ** $p < 0.01$, *** $p < 0.001$. P-values between 0.05 and 0.1 are displayed numerically.

2.4 Results

To establish a therapeutic dose of WLBU2 for pulmonary bacterial infection, I tested two doses of WLBU2 peptide by intravenously injecting mice two hours after bacterial infection with either 5 or 50 μg WLBU2 (approximately 0.2-0.25 mg/kg and 2-2.5 mg/kg, respectively). Respiratory distress upon oropharyngeal installation of 3.5-7 μg WLBU2 was previously observed by others in the laboratory, while IV treatment with 3 mg/kg was well-tolerated as previously published (89). Mice were sacrificed four hours following treatment, at six hours post-bacterial infection. This four-hour window was chosen to assess the killing of bacteria in the lung without inordinate influence of bacterial replication post-WLBU2 treatment. Deslouches *et al.* showed that WLBU2 required only 20 minutes in human serum to achieve complete killing of *P. aeruginosa in vitro* (89). I compared the effect of WLBU2 treatment on pulmonary bacterial burden with that

of the endogenous cathelicidin LL-37, which has been previously shown to ameliorate MRSA pneumonia when perfused intratracheally (92).

Intravenous injection of 50 μg WLBU2 two hours after pulmonary MRSA infection reduced bacterial burden in the lung, while a dose of 5 μg WLBU2 failed to show any reduction in lung bacterial burden (Figure 2.1B). The effect of 50 μg WLBU2 was comparable to that of 50 μg LL-37 (Figure 2.1C), suggesting that the engineered WLBU2 reduced lung bacterial burden as effectively as LL-37. LL-37 is known to activate many pathways of the immune system, including stimulating inflammasomes to cleave IL-1β to its active form (86), as well as binding FPR2 to induce neutrophil chemotaxis (84). LL-37 has been shown to induce production of the neutrophil chemoattractant IL-8 in human keratinocytes (93) and the macrophage/monocyte chemoattractant MCP-1 from a murine macrophage cell line (94). While phagocyte chemotaxis to the site of infection is necessary for bacterial killing and to limit bacterial spread, overabundant immune cell recruitment to the lung can cause immunopathology and acute respiratory distress syndrome (ARDS) (95, 96). ARDS is characterized by pulmonary edema, which limits gas exchange in the lungs and has high mortality rates ranging from 35-46% depending on ARDS severity (97). Limiting immunopathology during treatment of bacterial pneumonia may be an effective strategy to reduce mortality. I hypothesized that due to its dissimilar amino acid sequence, WLBU2 treatment would not activate immune signaling, and reduce mortality from pulmonary MRSA infection as compared to LL-37.

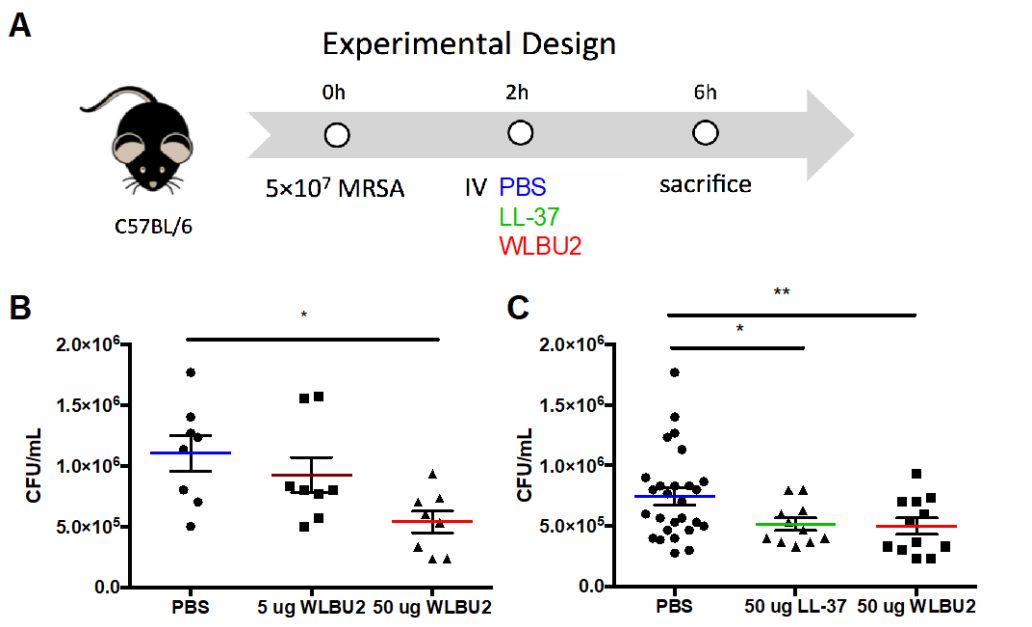

Figure 3: Treatment with the engineered antimicrobial peptide WLBU2 reduces MRSA pulmonary burden.

S. aureus pneumonia was modeled by infecting six- to eight-week old male C57BL/6J mice with 5×10^7 CFU USA300 MRSA by oropharyngeal aspiration. Two hours later, mice were injected intravenously in the tail vein with either WLBU2, LL-37, or PBS vehicle as control, and sacrificed four hours following antimicrobial peptide or vehicle treatment. **(A)** Timeline of infection, treatment, and sacrifice. **(B)** Comparison of bacterial burden between treatment with PBS, 5 µg WLBU2, and 50 µg WLBU2. n = 4, two independent experiments. **(C)** Comparison of bacterial burden between treatment with PBS, 50 µg WLBU2, and 50 µg LL-37. n = 2-4, seven independent experiments. Statistics were calculated by one-way ANOVA and graphical summary statistics are displayed as mean ± SEM.

The number of BAL-infiltrating cells and BAL protein as a measure of lung leakage were unchanged (Figure 2.2A-B), suggesting that overall lung inflammation was not significantly altered. Mortality was also unchanged (Figure 2.2D). However, LL-37 did significantly increase levels of the pro-inflammatory cytokine IL-1β, as well as neutrophil and macrophage/monocyte chemokines G-CSF, CXCL1, and CCL2. WLBU2 altered none of these except KC, which it significantly reduced (Figure 2.2C). This suggests that WLBU2 does not provoke immune activation, unlike LL-37, and may not contribute to immunopathology. Immunopathology is made

even worse with preceding influenza infection due to cytokine storm, so I tested if WLBU2 would similarly limit immunopathology while decreasing bacterial burden during influenza super-infection.

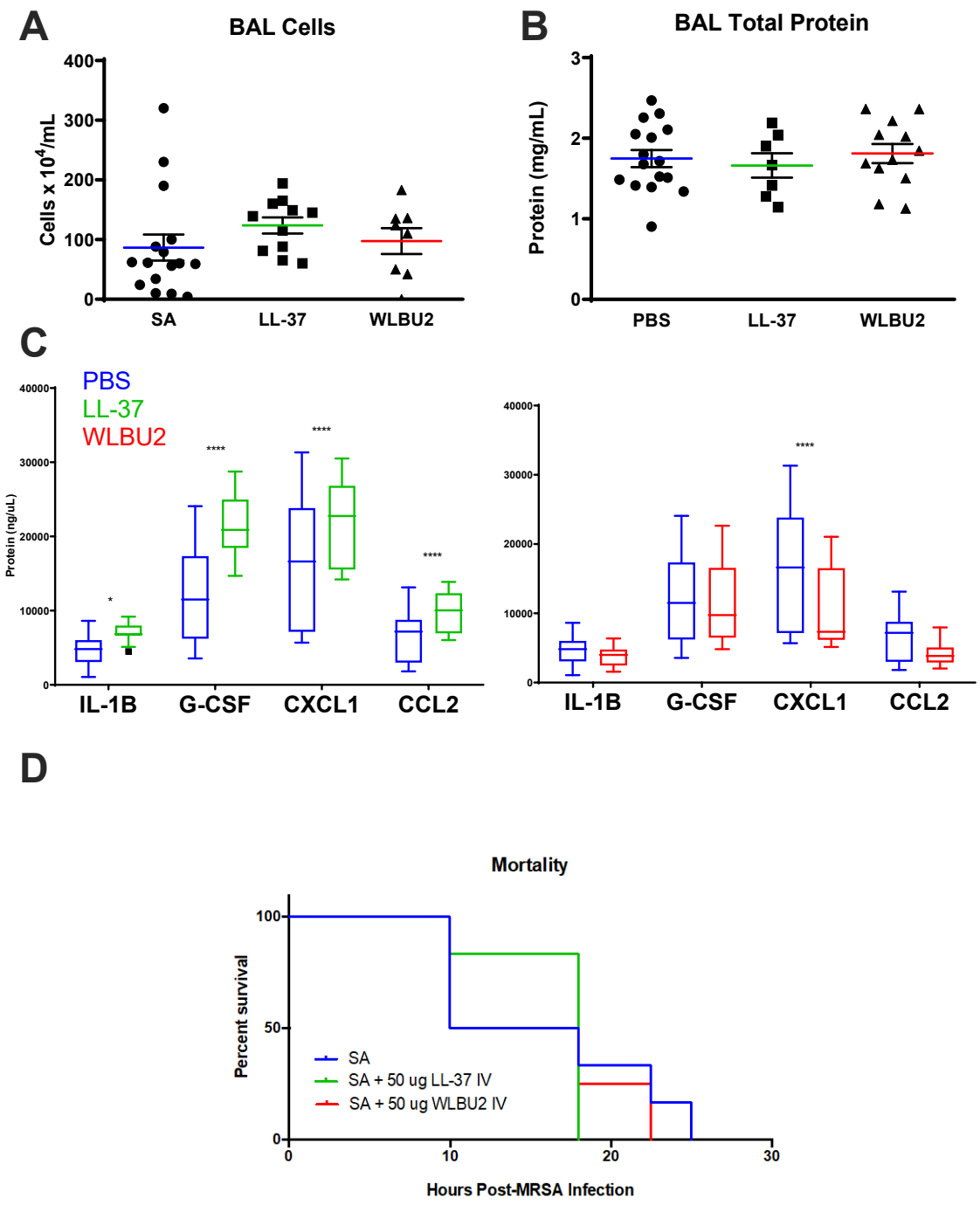

Figure 4: Unlike LL-37, WLBU2 does not alter inflammation in the lung during MRSA infection.

Mice were infected and treated as described in Figure 2.1. **(A)** Total cells in bronchoalveolar lavage fluid were quantified by counting on a hemocytometer. n = 3-4, four independent experiments. **(B)** Total protein in

bronchoalveolar lavage was determined by Bradford assay. n = 3-4, four independent experiments. **(C)** Homogenized lung tissue was assayed by cytokine multiplex for pro-inflammatory cytokines and chemokines. n = 4, five independent experiments. **(D)** Mice were challenged with 2.5×10^8 CFU MRSA. n = 6, one experiment. Statistics were calculated by **(A-B)** one-way ANOVA, **(C)** two-way ANOVA, or **(D)** Mantel-Cox log-rank test. Graphical summary statistics are displayed as **(A-B)** mean ± SEM, **(C)** box-and-whisker plot with median, 25%, and 75% percentile values marked, or **(D)** Kaplan-Meier survival curve.

WLBU2 treatment did not reduce bacterial burden in MRSA super-infection during influenza or change levels of pro-inflammatory cytokines (Figure 2.3D-E). Total infiltrating cells and lung leak as measured by total protein in BAL were also unchanged (Figure 2.3B-C). Together, these results suggest that while WLBU2 may be an effective treatment for MRSA lung infection alone, it is not effective in the situation of MRSA super-infection during influenza.

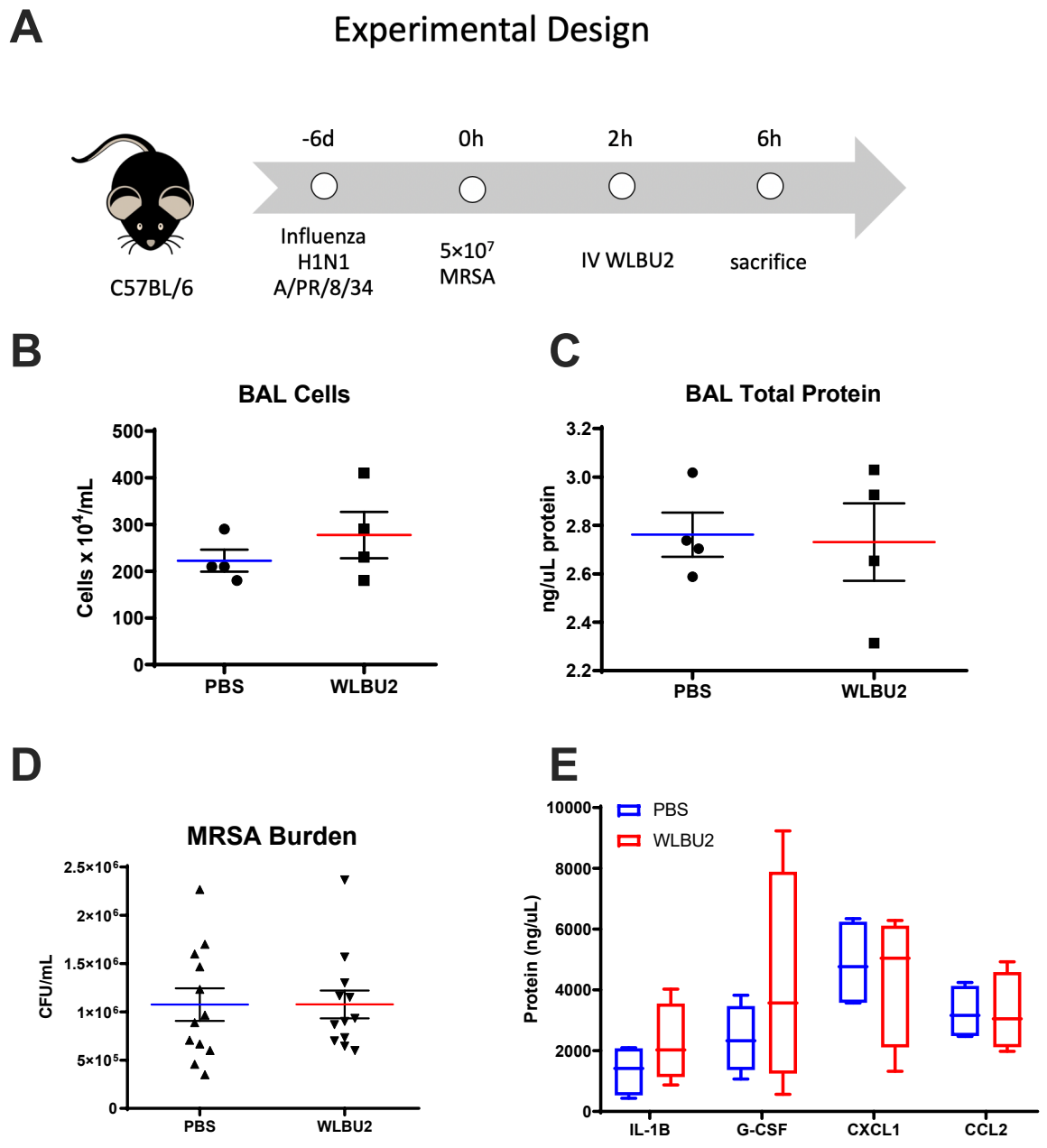

Figure 5: WLBU2 does not reduce disease in MRSA super-infection during influenza.

Bacterial super-infection during influenza was modeled by infecting six- to eight-week old male C57BL/6 mice with influenza H1N1 A/PR/8/34 to cause 10-15% weight loss by sacrifice. Six days post-influenza, mice were challenged with 5×10^7 CFU USA300 MRSA by oropharyngeal aspiration. Two hours later, mice were injected intravenously in the tail vein with either WLBU2 or PBS vehicle as control, and sacrificed four hours following treatment. **(A)** Timeline of infection, treatment, and sacrifice. **(B-C)** n = 4, one representative experiment. **(B)** Total cells in

bronchoalveolar lavage fluid were quantified by counting on a hemocytometer. **(C)** Total protein in bronchoalveolar lavage was determined by Bradford assay. **(D)** Comparison of bacterial burden between treatment with PBS and 50 µg WLBU2. n = 4, three independent experiments. **(E)** Homogenized lung tissue was assayed by cytokine multiplex for pro-inflammatory cytokines and chemokines. n = 4, one experiment. Statistics were calculated by **(B-D)** t test with Welch's correction or **(E)** two-way ANOVA and graphical summary statistics are displayed as **(B-D)** mean ± SEM or **(E)** box-and-whisker plot with median, 25%, and 75% percentile values marked.

2.5 Discussion

Since these data were generated, more research from other groups into the antimicrobial activities of WLBU2 has been published. WLBU2 has now been shown to be more effective than LL-37 at preventing biofilm formation of multidrug-resistant pathogens including both *P. aeruginosa* and *S. aureus* (90). This study and others *in vitro* have shown great promise for WLBU2 in preventing biofilms, suggesting that its best use may not be direct delivery to an infected patient but instead being used in a coating on implants before procedures such as joint replacement. However, it was shown in 2018 that oropharyngeal installation of WLBU2 at a much lower dose of 1 µg (0.05 mg/kg) was well-tolerated by mice (98). This was welcome but surprising, as we had previously observed respiratory distress when mice were administered doses of 3.5 µg and 7 µg administered by the same route. Chen *et al.* published that oropharyngeal installation of WLBU2 reduced *P. aeruginosa* burden and bacterial-driven inflammation in the lung 24 hours post-treatment, while installation of LL-37 increased bacterial burden as well as inflammatory cytokines (98). It appears that oropharyngeal installation of 1 µg WLBU2 is below the threshold required to cause respiratory distress in mice, which may be due to the strong cationic charge of the peptide. However, that hypothesis has not been experimentally interrogated, and it is possible

that the murine lung may react differently to delivery of antimicrobial peptide during *S. aureus* versus *P. aeruginosa* lung infection. These bacteria differ in many ways: foremost, the Gram positive *S. aureus* lacks an outer cell membrane and has an exposed cell wall high in peptidoglycan, whereas the Gram negative *P. aeruginosa* shields its cell wall with an outer membrane. Moreover, current guidelines for antibiotic treatment differ between these two bacteria, with pneumonias caused by *P. aeruginosa* requiring antipseudomonal cephalosporins or β lactam antibiotics, while pneumonias without pseudomonal risk factors can be instead treated with fluoroquinolones (99).

From these data, it seems that oropharyngeal installation of much lower therapeutic doses of WLBU2 directly to the site of infection is much more effective than intravenous treatment. This reasoning also supports the strong findings from Deslouches *et al.* that WLBU2 was able to save mice from lethal *P. aeruginosa* sepsis, as in that model the AMP was directly encountering pathogen in the blood. This underscores the fact that antibiotic treatment requires correct drug delivery and effective killing of bacteria. However, at its core the phenomenon of bacterial super-infection during influenza happens due to immune dysregulation, and mortality is thought to also be highly influenced by immunopathology, suggesting that the host response is the most crucial factor in outcomes during bacterial super-infection. Thus, I decided to look into the underlying immunopathology of this disease by understanding the role of individual cytokines. As discussed previously, type I interferon seemed to be a strong suppressor of immunity to bacteria commonly found during influenza super-infection. Although much was known about type I IFNs, type III IFNs were only just beginning to be explored.

3.0 IFNλ3 Knockout Does Not Reduce Total IFNλ In Bacterial Super-infection During Influenza

3.1 Introduction

Type I IFNs were the first cytokines to be described, and have been known as antiviral signaling molecules since their discovery in 1957. While type I IFNs have potent antiviral properties, they are also strong promoters of inflammation and have ceased to be used in first-line treatment for most viral infections. Conversely, type III IFNs were only first described in 2003, and share antiviral properties of type I IFNs while being less inflammatory overall (100). Moreover, type III IFN was shown to be even more highly produced in response to flu than type I interferon (37). The lung expresses high levels of the specific IFNλ receptor IFNλR1, which is not ubiquitously expressed, unlike the type I IFN receptor IFNαR1. As type I IFN treatment has many off-target effects, type III IFN treatment appeared promising due to the receptor restriction to mucosal barriers (and later neutrophils). Moreover, while corticosteroids do not reduce morbidity or mortality during pulmonary bacterial infection, immunopathology drives ARDS and negative patient outcomes, and thus dampening overall inflammation is still promising in treatment of bacterial super-infection during influenza.

Due to the novelty of type III IFN, there have been few reagents available for its investigation *in vivo* murine models. Only recently have the first knockout mice, which lack one of the two murine type III IFNs, become commercially available. Thus, I decided to test the hypothesis that IFNλ3$^{-/-}$ mice would display reduced bacterial burden and immunopathology in bacterial super-infection during influenza. Herein, the use of IFNλ3$^{-/-}$ mice to investigate the role

of type III interferon in bacterial super-infection during influenza is described. Surprisingly, IFNλ3$^{-/-}$ mice do not display reduced IFNλ when measured by ELISA, possibly due to upregulation of IFNλ2, which shares 96% amino acid similarity with IFNλ3 (5). These findings demonstrate that IFNλ3$^{-/-}$ mice are a poor model for the *in vivo* investigation of IFNλ.

3.2 Materials and Methods

3.2.1 Mice

IFNλ3$^{tm1.1(KOMP)Vlcg}$ mice were a generous gift from Dr. Jieru Wang, and wild-type C57BL/6NJ controls were purchased from The Jackson Laboratory. IFNλ3$^{tm1.1(KOMP)Vlcg}$ mice were bred in a homozygous fashion with wild-type C57BL/6NJ mice purchased as controls, and co-housed for one to two weeks before experimental use. To cohouse mice in order to limit variability from differences in intestinal microbiota, female mice were placed in cages containing at least one mouse of the opposing genotype, while male mice had their bedding swapped daily between cages due to risk of injury from fighting. To generate littermate controls, male wild-type C57BL/6NJ mice were bred with IFNλ3$^{tm1.1(KOMP)Vlcg}$ females and the resulting F1 offspring were used experimentally at six to eight weeks old. All studies were performed on age- and sex-matched mice. All animal studies were conducted with approval from the University of Pittsburgh Institutional Animal Care and Use Committee.

3.2.2 Murine infections

All mouse infections were administered by oropharyngeal aspiration (OPA) after inhaled isoflurane anesthesia. Methicillin-resistant *Staphylococcus aureus* (MRSA) USA300 and influenza H1N1 A/PR/8/34 were grown and administered as described in section 2.3.3.

3.2.3 Analysis of lung inflammation

At harvest, mouse lungs were lavaged with 1 ml sterile PBS. This lavage fluid was centrifuged at 10,000×g for 5 min to pellet cells, and the supernatant was frozen for cytokine measurement by an enzyme-linked immunosorbent assay (ELISA) for IFNλ (IFNλ2/3 DuoSet; R&D Systems, Minneapolis, MN). Cell pellets from lavage fluid were resuspended in 500 µl sterile PBS and counted on a hemocytometer to enumerate infiltrating cells. These cells were then either processed by cytospin and stained for differential counting or centrifuged again at 10,000×g for 5 min and then immediately frozen at −80°C for RNA extraction.

The right upper lobe of each lung was mechanically homogenized and plated for bacterial CFU counting. The right middle and lower lobes of each lung were snap-frozen in liquid nitrogen for RNA extraction.

3.2.3.1 Real-time PCR

RNA was isolated from whole lung lobes snap-frozen in liquid nitrogen using the Absolutely RNA miniprep kit (Agilent Technologies, Santa Clara, CA), and its concentration was analyzed by spectrophotometry (NanoDrop ND-1000; Thermo Fisher Scientific). RNA was

reverse transcribed into cDNA using the iScript cDNA synthesis kit (Bio-Rad, Hercules, CA), which was assayed by real-time PCR for gene expression with Assay on Demand TaqMan primer and probe sets (Life Technologies, Grand Island, NY).

3.2.4 Statistical analysis

Data were analyzed using GraphPad Prism 7 (GraphPad, La Jolla, CA). Analyses comparing two groups were performed by an unpaired t test with Welch's correction, unless data were not parametrically distributed, in which case Mann-Whitney analysis was used. Mortality data were analyzed by a log-rank (Mantel-Cox) test. All figures show combined data from multiple replicate studies as means ± standard errors of the means (SEM). The indicated *n* values are numbers of animals per group in each independent experiment. Statistical significance is reported as follows: * $p < 0.05$, ** $p < 0.01$, *** $p < 0.001$. P-values between 0.05 and 0.2 are displayed numerically.

3.3 Results

I interrogated the role of IFNλ in bacterial super-infection during influenza by using the only commercially available mouse strain at the time, IFNλ3$^{tm1.1(KOMP)Vlcg}$ mice, hereafter referred to as IFNλ3$^{-/-}$ mice. These animals lack the IFNλ3 gene, but not the other murine type III interferon IFNλ2. Thus, these IFNλ3$^{-/-}$ mice were expected to display reduced total IFNλ. Surprisingly, total BAL IFNλ was not significantly reduced in IFNλ3$^{-/-}$ mice compared to wild-type mice (Figure

3.1A). Both BAL IFNλ (Figure 3.1A) and bacterial burden (Figure 3.2B) trended to decrease in IFNλ3$^{-/-}$ mice, which supported the hypothesis that type III IFN acted similarly to type I IFN and promoted increased bacterial burden during influenza super-infection. Paradoxically, weight loss was significantly decreased in IFNλ3$^{-/-}$ mice as compared to WT mice (Figure 3.2D), and importantly on days 5 and 6 post-influenza, before mice received the bacterial challenge. This suggested that IFNλ3$^{-/-}$ mice had decreased morbidity from viral infection. However, these mice did not display reduced viral burden (Figure 3.4A). Additionally, bronchoalveolar lavage (BAL) cellularity was unchanged (Figure 3.1C), suggesting that there was no difference in immunopathology. However, there was significant variability in each of these measures, and both male and female mice were used in experiments (which were sex-matched and age-matched) as the IFNλ3$^{-/-}$ mice were propagated in-house. Thus, I asked if sex was a variable in these data.

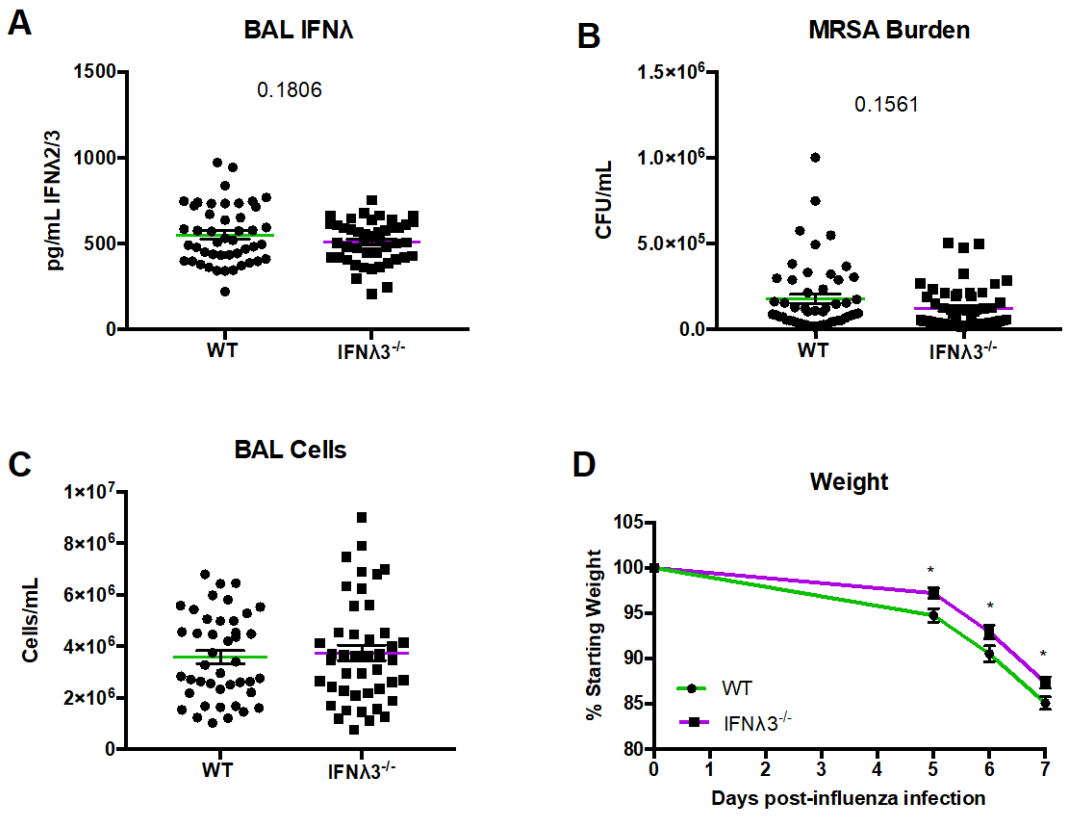

Figure 6: IFNλ3-/- mice lose less weight during bacterial super-infection than WT mice.

IFNλ3$^{tm1.1(KOMP)Vlcg}$ mice (IFNλ3$^{-/-}$ mice) and wild-type C57BL/6NJ controls were co-housed for one to two weeks before influenza infection. Bacterial super-infection during influenza was modeled by infecting six- to eight-week old mice with influenza H1N1 A/PR/8/34 to cause 10-15% weight loss by sacrifice on day 7. On day 6, one day prior to sacrifice, mice were challenged with 5×10^7 CFU USA300 MRSA by oropharyngeal aspiration. n = 3-5, nine independent experiments. **(A)** Protein levels of IFNλ in bronchoalveolar lavage (BAL) were measured by ELISA. **(B)** MRSA burden was quantified by bacterial plating. **(C)** BAL cells were quantified by counting on a hemocytometer. **(D)** Mice were weighed at the time of influenza infection (day 0), day 5, day 6 directly prior to MRSA challenge, and day 7 directly prior to sacrifice. Statistics were calculated by **(A,C)** t test with Welch's correction, **(B)** Mann-Whitney test due to non-Gaussian distribution of data, or **(D)** two-way ANOVA. Graphical summary statistics are displayed as mean ± SEM.

Inflammation, and specifically the antiviral response to influenza, differ between the sexes. Importantly, the sex hormone estradiol is pro-inflammatory while testosterone is

immunosuppressive. Females mount both a higher innate and adaptive immune response to viral infection, and males are more likely to get gastrointestinal and respiratory infections, while females are more likely to have autoimmune disorders including asthma. In influenza, progesterone treatment in female mice is protective against immunopathology during influenza by increasing type 17 immunity and upregulating the epidermal growth factor amphiregulin (101). Treatment of female mice with the oral contraceptive hormone levonorgestrel paradoxically protects against influenza mortality while decreasing serum antibodies (102). In male mice, testosterone treatment protects against influenza mortality but viral titer, antibody production, and immunopathology were unchanged (103). As both influenza and pulmonary infection differ between sexes, I interrogated the effect of sex on the pathogenesis of bacterial super-infection during influenza.

In total, nine experiments were performed: three using only female mice (n = 4-5), three using only male mice (n = 3-5), and three directly comparing sex as a variable within each experiment. Bacterial burden was significantly higher in female IFNλ3$^{-/-}$ mice than in male IFNλ3$^{-/-}$ mice ($p = 0.0322$), but only trended higher in female WT mice as compared to male WT mice (Figure 3.2B). Cell counts also trended to be lower in female WT mice than male WT mice (Figure 3.2C). While IFNλ3$^{-/-}$ mice trended to lose less weight than WT mice overall, there was no statistically significant difference in weight loss when sex was considered as a factor (Figure 3.2D). Again, no decrease in BAL IFNλ in IFNλ3$^{-/-}$ mice was seen as compared to WT (Figure 3.2A).

Very few disease endpoints were significantly changed by IFNλ3 knockout, even when sex was considered as a variable. There was wide variance in the difference in BAL IFNλ when comparing IFNλ3$^{-/-}$ to WT mice in individual experiments; some experiments even showed statistically significant higher BAL IFNλ in IFNλ3$^{-/-}$ mice. Some experiments showed a

statistically significant difference in weight loss while others did not, same with bacterial burden. Penetrance of each of these phenotypes (BAL cellularity, weight loss, bacterial burden) was widely varied with three or fewer individual experiments showing either statistically higher or lower outcomes. Moreover, phenotype penetrance was not segregated by sex, and no one phenotype correlated with any other between experiments. As there was such a range in phenotype penetrance, I decided to ask whether individual experiments that had shown statistically lower BAL IFNλ in IFNλ3$^{-/-}$ mice than WT mice, i.e. experiments which truly modeled a decrease in BAL IFNλ, had differences in disease outcome that were otherwise camouflaged.

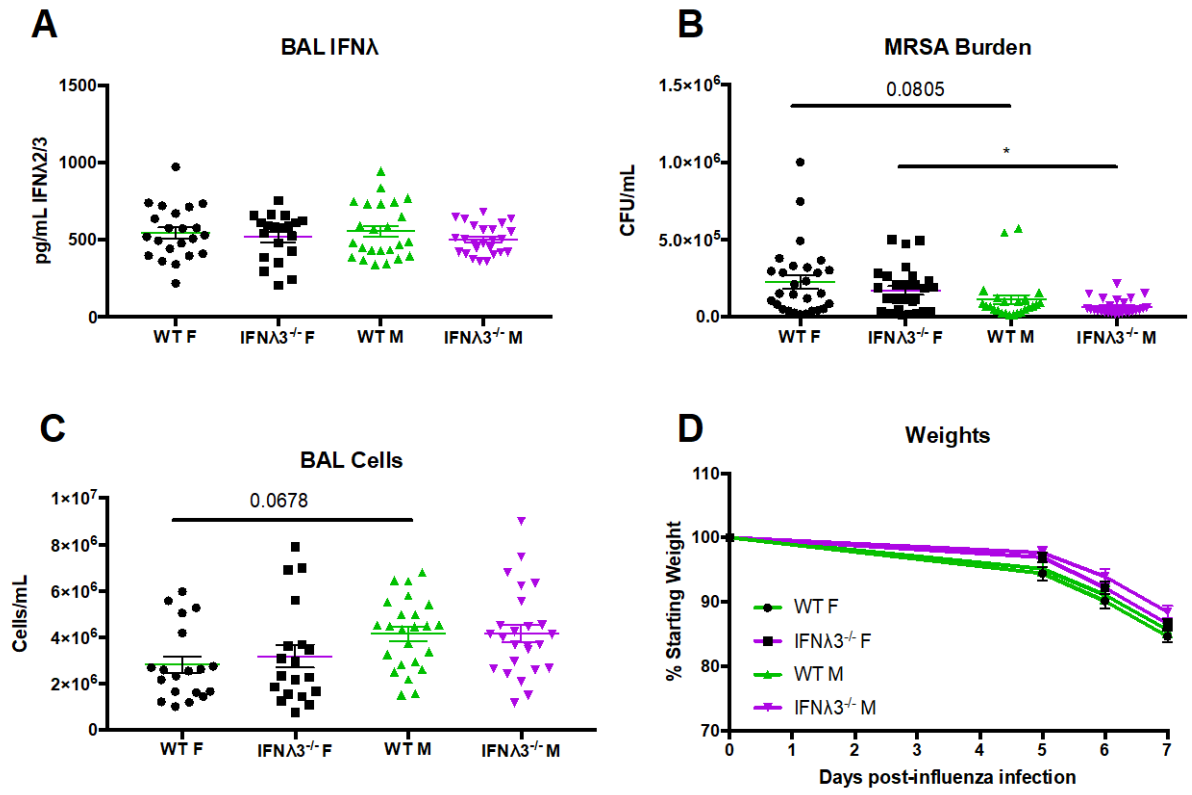

Figure 7: IFNλ3-/- mice exhibit small sex differences in bacterial burden during influenza super-infection.

Mice were treated as described in Figure 3.1. n = 3-5, nine independent experiments. **(A)** Protein levels of IFNλ in BAL were measured by ELISA. **(B)** MRSA burden was quantified by bacterial plating. **(C)** BAL cells were quantified by counting on a hemocytometer. **(D)** Mice were weighed on days 0, 5, 6 and 7. Statistics were calculated by **(A,C)** one-way ANOVA, **(B)** Kruskal-Wallis test due to non-Gaussian distribution of data, or **(D)** two-way ANOVA. Graphical summary statistics are displayed as mean ± SEM.

BAL IFNλ was only significantly reduced in IFNλ3$^{-/-}$ mice as compared with WT mice in 3 of 9 experiments, two of which were performed in male mice and one performed in female mice. Even though IFNλ3$^{-/-}$ mice had significantly lower BAL IFNλ in these experiments (Figure 3.3A), bacterial burden and BAL cellularity were unchanged (Figure 3.3B-C). Surprisingly, IFNλ3$^{-/-}$ mice again lost less weight than WT mice during influenza infection and bacterial super-infection (Figure 3.3D). As weight loss is commonly used as a proxy for influenza morbidity, these data

suggested that IFNλ3$^{-/-}$ mice would have lower influenza virus burden than WT mice. This contradicted my earlier hypothesis that IFNλ3$^{-/-}$ mice would have higher viral burden than WT mice, due to the reduction in antiviral cytokine. Thus, I investigated whether this decreased weight loss in IFNλ3$^{-/-}$ mice was due to decreased influenza burden.

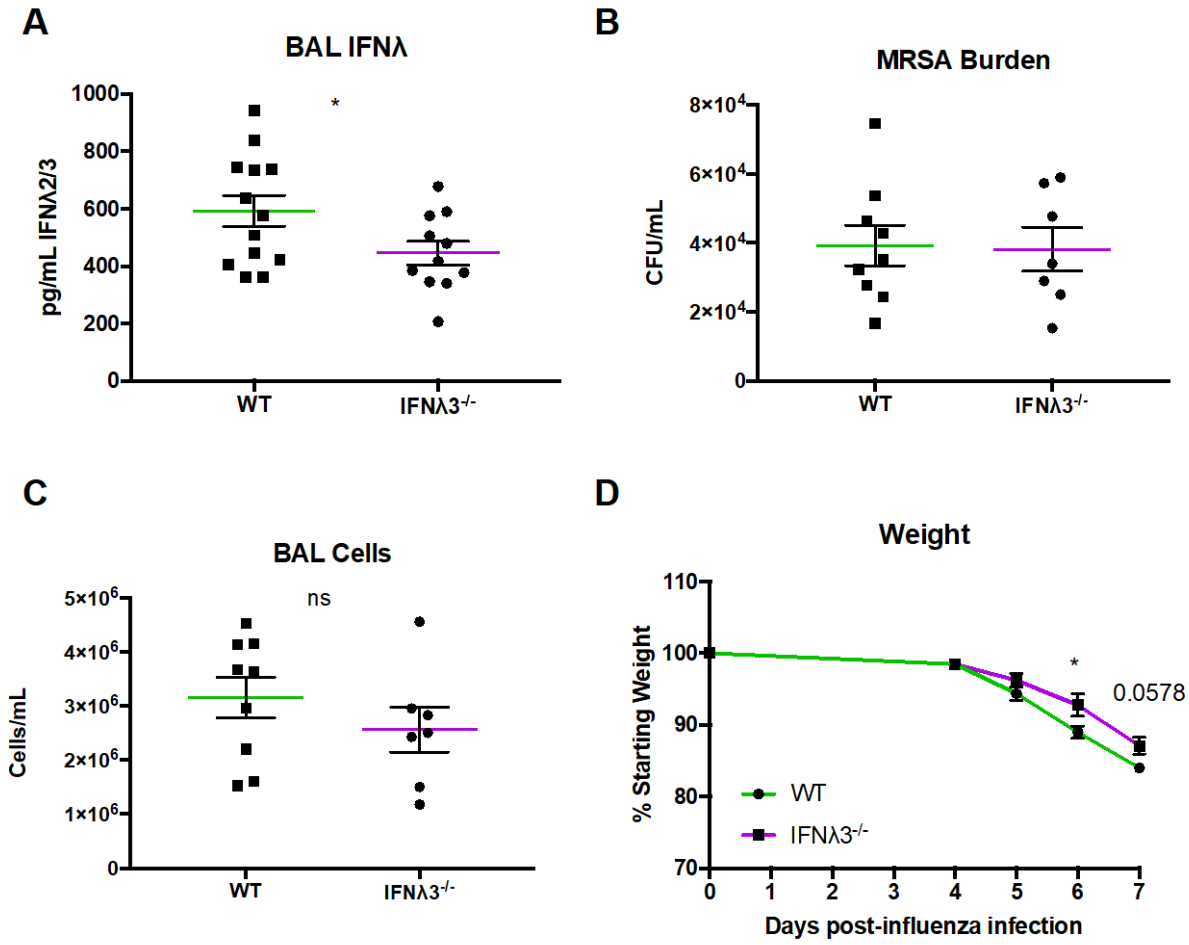

Figure 8: Reduced BAL IFNλ3 does not alter bacterial super-infection.

Mice were treated as described in Figure 3.1. **(A)** Protein levels of IFNλ in BAL were measured by ELISA. n = 3-5, three independent experiments. **(B)** MRSA burden was quantified by bacterial plating. n = 3-5, two independent experiments. **(C)** BAL cells were quantified by counting on a hemocytometer. n = 3-5, two independent experiments. **(D)** Mice were weighed on days 0, 5, 6 and 7. n = 3-5, three independent experiments. Statistics were calculated by **(A,C)** t test with Welch's correction, **(B)** Mann-Whitney test due to non-Gaussian distribution of data, or **(D)** two-way ANOVA. Graphical summary statistics are displayed as mean ± SEM.

IFNλ is well-known as an antiviral molecule, so I hypothesized that IFNλ3$^{-/-}$ mice would have higher viral burden than WT mice. As measured by real-time PCR for influenza M protein expression, viral burden in whole lung tissue was not significantly different in IFNλ3$^{-/-}$ mice than

in the WT mice (Figure 3.4A). Surprisingly, viral burden positively correlated with total IFNΛ protein in BAL in both IFNλ3$^{-/-}$ and WT mice (Figure 3.4B), regardless of genotype (Figure 3.4C). BAL IFNλ also positively correlated with BAL cellularity (Figure 3.4F) and bacterial burden (Figure 3.4E) in all mice, but not with weight loss from the time of influenza infection to sacrifice (Figure 3.4D).

I hypothesized that the wide variability in phenotypic penetrance was due to the variation introduced by ordering and co-housing wild-type controls instead of breeding littermate controls. To address this, I ordered male wild-type C57BL/6NJ mice and bred them in-house with female IFNλ3$^{tm1.1(KOMP)Vlcg}$ mice, using the entire F1 generation of offspring to assess the effect of both homozygous and heterozygous knockout of the IFNλ3 gene on bacterial super-infection in littermates.

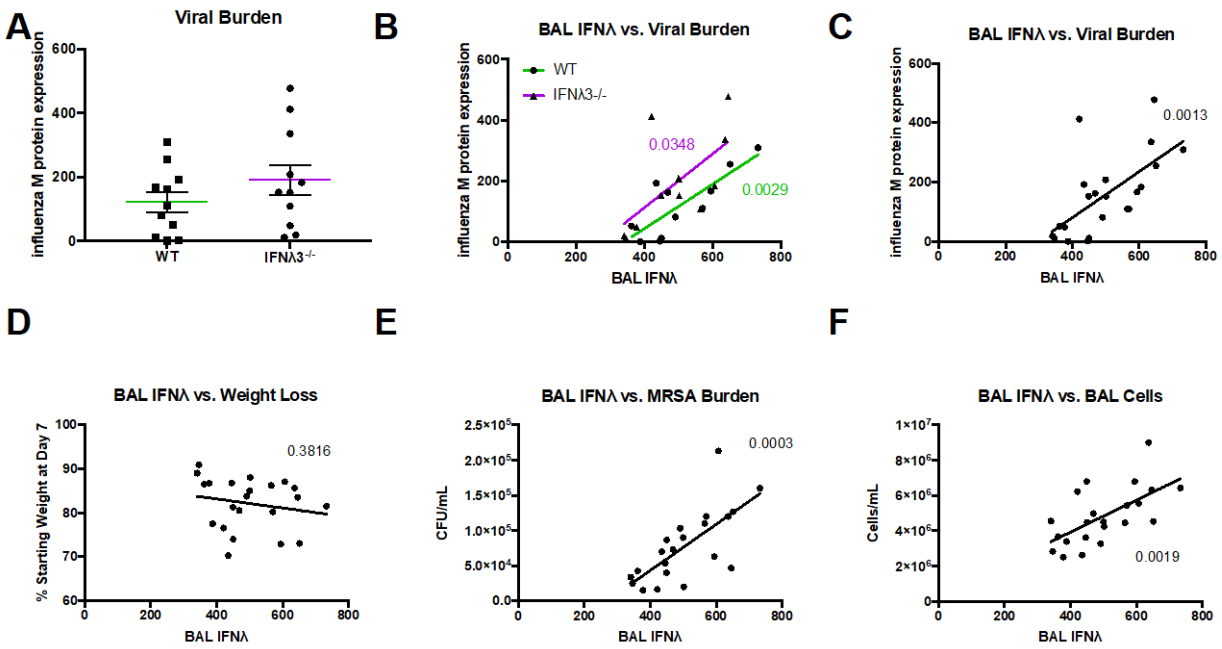

Figure 9: Total BAL IFNλ correlates positively with influenza severity.

Mice were treated as described in Figure 3.1. n = 3-5, three independent experiments. **(A)** Influenza M protein expression was quantified by real-time PCR. **(B)** Linear regression of BAL IFNλ and influenza M protein expression, segregated by mouse genotype. **(C)** Linear regression of BAL IFNλ and influenza M protein expression including all mice, regardless of genotype. **(D)** Linear regression of BAL IFNλ and mouse weight seven days after influenza infection, displayed as percentage of starting weight. **(E)** Linear regression of BAL IFNλ and pulmonary MRSA burden. **(F)** Linear regression of BAL IFNλ and BAL cellularity. Statistics were calculated by **(A)** t test with Welch's correction or **(B-F)** linear regression, in which p-values are displayed numerically. **(A)** Graphical summary statistics are displayed as mean ± SEM.

Littermates showed no difference in weight loss at any timepoint, total number of BAL cells, or bacterial burden in the lung during influenza super-infection (Figure 3.5B-D). Levels of total IFNλ in BAL were significantly different when assessed by Welch's t test with $p = 0.0461$ (Figure 3.5A), but when analyzed by one-way ANOVA with multiple comparisons including the group of IFNλ3$^{+/-}$ mice, were not statistically significant. While this difference is technically

statistically significant, these IFNλ3$^{-/-}$ mice show a mild reduction in total IFNλ at best. Moreover, bacterial burden and BAL cellularity, which were both significantly correlated with BAL IFNλ regardless of genotype (Figure 3.4E-F), were unchanged between genotype in littermates.

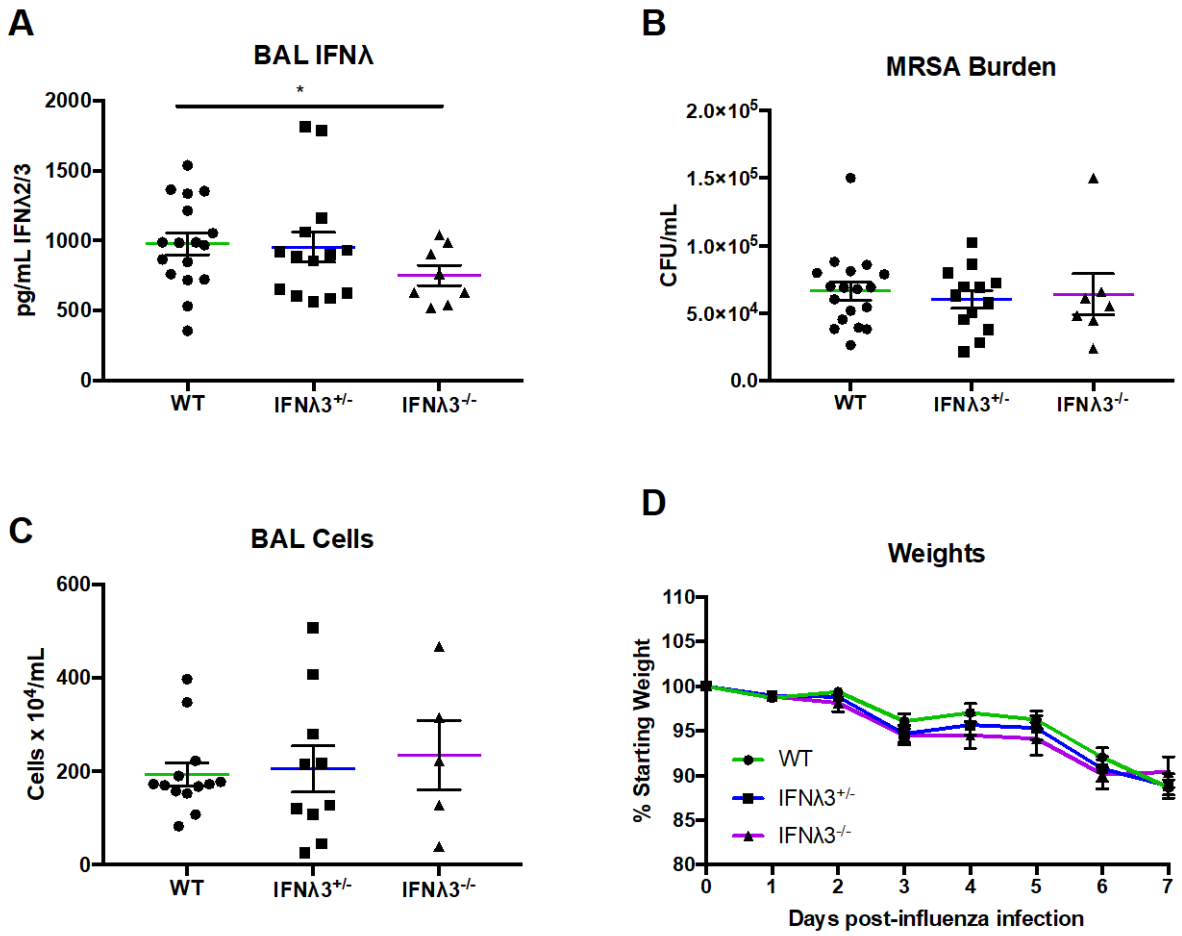

Figure 10: IFNλ3-/- mice do not display a different response to bacterial super-infection than WT littermates. Female IFNλ3$^{tm1.1(KOMP)Vlcg}$ mice were bred with male wild-type C57BL/6NJ mice to produce F1 offspring, which were used experimentally at six to eight weeks old. Bacterial super-infection during influenza was modeled by infecting six- to eight-week old mice with influenza H1N1 A/PR/8/34 to cause 10-15% weight loss by sacrifice on day 7. On day 6, one day prior to sacrifice, mice were challenged with 5×10^7 CFU USA300 MRSA by oropharyngeal aspiration. n = 4-13, two independent experiments. **(A)** Protein levels of IFNλ in BAL were measured by ELISA. **(B)** MRSA burden was quantified by bacterial plating. **(C)** BAL cells were quantified by counting on a hemocytometer. **(D)** Mice were weighed at influenza infection (day 0) and daily thereafter until sacrifice on day 7. Statistics were calculated by **(A-C)** t test between WT and IL-28B$^{-/-}$ groups with Welch's correction or **(D)** two-way ANOVA. Graphical summary statistics are displayed as mean ± SEM.

3.4 Discussion

IFNλ3$^{-/-}$ mice are a poor *in vivo* model for assessing the role of IFNλ in bacterial super-infection during influenza. ELISA detection of IFNλ in BAL measured both IFNλ2 and IFNλ3, as the proteins have 96% amino acid similarity and are both detected by the assay antibody. Levels of BAL IFNλ were strikingly similar between IFNλ3$^{-/-}$ mice and their wild-type littermates. Moreover, variability between experiments was quite high, and when the individual experiments were analyzed separately this difference became insignificant. Together, this suggests that IFNλ2 may be upregulated in response to IFNλ3 knockout in IFNλ3$^{-/-}$ mice, resulting in a minimal if at all present decrease in IFNλ3 in IFNλ3$^{-/-}$ mice. However, these experiments only assessed levels of IFNλ3 in bacterial super-infection during influenza, and these mice may show a larger reduction in total IFNλ in other disease settings.

Although IFNλ3$^{-/-}$ mice and co-housed C57BL/6NJ mice displayed differences in weight loss during influenza infection as well as bacterial super-infection, this phenotype was not observed in littermates, underscoring the necessity for littermate controls in experiments. These results also suggest that this paradoxical decrease in weight loss in mice that lack the antiviral cytokine IFNλ3 may be due to other possible underlying genetic differences between IFNλ3$^{-/-}$ mice and the background C57BL/6NJ strain. Alternatively, IFNλ2 may be upregulated in these IFNλ3$^{-/-}$ mice and may even protect them from influenza morbidity, however viral burden was unchanged so this hypothesis appears to hold little merit. Importantly, these data demonstrate that while weight loss is commonly used as a proxy for influenza morbidity, weight loss does not imply increased viral burden. The intestinal microbiome has been shown to influence the pulmonary immune response (104), so 16S sequencing on fecal samples was performed to assess the ability of co-housing to equalize intestinal microbiota. While the microbiota of non-littermate but co-

housed WT and IFNλ3$^{-/-}$ mice did not overlap perfectly in a principal component analysis, co-housing worked to shift the microbiome closer between the two groups (appendix Figure 5.2). Importantly, while these co-housed non-littermates showed sex differences in bacterial burden during influenza super-infection, littermates did not recapitulate this phenotype (appendix Figure 5.1). The method of co-housing is a likely culprit for this: female mice that were not weaned together can be housed together without issue, but male mice will often fight, occasionally to the point of death but generally inducing wounds which require immune processes to heal. To co-house male mice, I switched bedding between cages each day, which should be effective at altering the microbiome as mice are coprophagic. However, it is plausible that this difference in co-housing method for male mice was less able to equalize their intestinal microbiota, and that this differentially influenced pulmonary immunity.

The positive correlation between influenza viral burden in the lung and BAL IFNλ suggested that pulmonary IFNλ production increases with higher viral load. This interpretation was bolstered by the positive correlation shown between BAL IFNλ and BAL cellularity, as more severe influenza infection can lead to cytokine storm and overexuberant immune cell recruitment to the lung. Similarly, the positive correlation between BAL IFNλ and bacterial burden suggested that more severe influenza increases the susceptibility of the lung to bacterial super-infection. However, these correlations are unable to imply causation, so it became necessary to experimentally manipulate IFNλ. At the same time, IFNλR1$^{-/-}$ mice were first published. As the type III IFN receptor IFNλR1 knocks out both IFNλ2 and IFNλ3 signaling, the use of these IFNλ3$^{-/-}$ mice was rendered unnecessary. Planet *et al.* showed that IFNλR1$^{-/-}$ mice have reduced *Staphylococcus aureus* burden during influenza super-infection (69), suggesting that my hypothesis was correct that IFNλ inhibited antibacterial immunity during influenza infection. A

few months later, Galani *et al.* suggested that IFNλ be used as treatment for flu, as experimental treatment with exogenous IFNλ reduced viral burden along with morbidity and mortality from influenza infection (36). However, both the work by Planet *et al.* on type III IFN and the work by Kudva *et al.* on type I IFN suggested that additional IFNλ would make bacterial super-infection worse. Thus, I tested the hypothesis that "treating" super-infection with IFNλ would increase bacterial burden during influenza super-infection, which also let me experimentally test the role of IFNλ in this system to get answers on causation and not simply correlation.

4.0 IFNλ Inhibits Bacterial Clearance During Influenza Super-infection

4.1 Summary

Several groups have recently proposed the use of the antiviral cytokine interferon lambda (IFNλ) as a therapeutic for influenza, as administration of pegylated IFNλ improves lung function and survival during influenza by reducing the overabundance of neutrophils in the lung. However, our data suggest that therapeutic IFNλ impairs bacterial clearance during influenza super-infection. Specifically, mice treated with an adenoviral vector to overexpress IFNλ during influenza infection exhibited increased bacterial burdens upon super-infection with either MRSA or *Streptococcus pneumoniae*. Surprisingly, adhesion molecule expression, antimicrobial peptide production, and reactive oxygen species activity were not altered by IFNλ treatment. However, neutrophil uptake of both MRSA and *S. pneumoniae* were significantly reduced upon IFNλ treatment during influenza super-infection *in vivo*. Together, these data support the theory that IFNλ decreases neutrophil motility and function in the influenza-infected lung, thereby increasing bacterial burden during super-infection. Thus, we believe that caution should be exercised in the possible future use of IFNλ as therapy for influenza.

4.2 Introduction

Galani *et al.* treated mice with pegylated IFNλ2 two days after influenza infection, which resulted in a striking reduction in morbidity and mortality. Neutrophilia in the lung was decreased,

alleviating immunopathology, and IFNλ treatment was also able to increase lung function during the influenza infection. These findings corroborated other data from models of IFNλ treatment during inflammation in models of collagen-induced arthritis (105) and dextrate sulfate sodium-induced colitis (38). Together, these data point to a neutrophil-mediated alleviation of immunopathology, through *in vivo* data that fewer neutrophils arrive at sites of inflammation when mice are treated with IFNλ, and *in vitro* that IFNλ decreases neutrophil chemotaxis. Supported by the findings of Planet *et al.* that IFNλR1$^{-/-}$ mice had lower bacterial burden during influenza super-infection, I hypothesized that IFNλ treatment would increase bacterial burden during influenza super-infection. I also hypothesized that this would be due to lower neutrophil infiltration into the airspaces, which causes immunopathology during influenza but is also necessary for bacterial clearance.

The following study was published April 23, 2019 in Infection & Immunity. "Interferon Lambda Inhibits Bacterial Uptake during Influenza Superinfection" by Helen E. Rich, Collin C. McCourt, Wen Quan Zheng, Kevin J. McHugh, Keven M. Robinson, Jieru Wang, and John F. Alcorn.

4.3 Materials and Methods

4.3.1 Mice

Six- to eight-week old male wild-type C57BL/6J mice were purchased from Taconic Biosciences (Hudson, NY) and maintained under pathogen-free conditions. All studies were performed on age- and sex-matched mice. All animal studies were conducted with approval from the University of Pittsburgh Institutional Animal Care and Use Committee.

4.3.2 Murine infections

All murine treatments (influenza virus, adenovirus, *S. aureus*, and *S. pneumoniae*) were administered by oropharyngeal aspiration. Mice were infected with 25 PFU of influenza H1N1 A/PR/8/34 (106) or phosphate-buffered saline (PBS). Five days later, mice were treated with 1×10^{10} viral particles (VP) of an adenoviral vector overexpressing mIFNλ3/IL-28B (Vector BioLabs, Malvern, PA) or the enhanced GFP (eGFP) control in 50 µl of PBS (Genome Editing, Transgenic, and Virus Core, University of Pittsburgh). One day later, mice were challenged with 5×10^{7} CFU MRSA USA300 in 50 µl of PBS and harvested an additional 24 hours later, or mice were challenged with 1×10^{3} CFU *Streptococcus pneumoniae* serotype 3 (ATCC 6303) in 50 µl of PBS and harvested 48 hours later.

4.3.3 FITC labeling of bacteria

4.3.3.1 *Staphylococcus aureus*

S. aureus was grown overnight to stationary phase with shaking at 37°C in *S. aureus* media (appendix section A.5). After measurement of the optical density at 660 nm (OD660), 10 µl of 10 mg/ml FITC in dimethylformamide (DMFO) was added to 1 ml of bacteria and incubated with shaking at room temperature for 1 hour. Following incubation, bacteria were centrifuged at 10,000×g for 5 min and washed with PBS twice. FITC-labeled bacteria were resuspended in PBS to bring the concentration to 5×10^7 CFU per 50 µl.

4.3.3.2 *Streptococcus pneumoniae*

S. pneumoniae was grown for 6 hours with shaking at 37°C in Todd-Hewitt broth (BD Biosciences, Franklin Lakes, NJ). Next, 100 µl of this culture was used to inoculate a 100-ml flask of Todd-Hewitt broth and grown for an additional 12 hours with continued shaking at 37°C. After measurement of the culture at OD600, 10 µl of 10 mg/ml FITC in DMFO was added to 1 ml of bacteria, and the mixture was incubated with shaking at room temperature for 1h. Following incubation, bacteria were centrifuged at 10,000×g for 5 min and washed with PBS twice. FITC-labeled bacteria were resuspended in PBS to bring the concentration to 1000 CFU per 50 µl.

4.3.4 Analysis of lung inflammation

At harvest, mouse lungs were lavaged with 1 ml sterile PBS. This lavage fluid was centrifuged at 10,000×g for 5 min to pellet cells, and the supernatant was frozen for cytokine measurement by an enzyme-linked immunosorbent assay (ELISA) for IFNβ and IFNλ (mouse

IFNβ or IFNλ2/3 DuoSet; R&D Systems, Minneapolis, MN). Cell pellets from lavage fluid were resuspended in 500 μl sterile PBS and counted on a hemocytometer to enumerate infiltrating cells. These cells were then either processed by cytospin and stained for differential counting or centrifuged again at 10,000×g for 5 min and then immediately frozen at −80°C for RNA extraction.

The right upper lobe of each lung was mechanically homogenized and plated for bacterial CFU counting, and cytokines in lung homogenates were analyzed with the Bio-Plex Pro mouse cytokine 23-plex array (Bio-Rad, Hercules, CA). The right middle and lower lobes of each lung were snap-frozen in liquid nitrogen for RNA extraction.

4.3.4.1 Real-time PCR

RNA was isolated from whole lung lobes snap-frozen in liquid nitrogen using the Absolutely RNA miniprep kit (Agilent Technologies, Santa Clara, CA), and its concentration was analyzed by spectrophotometry (NanoDrop ND-1000; Thermo Fisher Scientific) or isolated from −80°C frozen bronchoalveolar lavage cell pellets using the MagMax-96 total RNA isolation kit (Invitrogen, Carlsbad, CA). RNA was reverse transcribed into cDNA using the iScript cDNA synthesis kit (Bio-Rad, Hercules, CA), which was assayed by real-time PCR for gene expression with Assay on Demand TaqMan primer and probe sets (Life Technologies, Grand Island, NY).

4.3.4.2 Flow cytometry

To obtain a single-cell suspension, lungs were mechanically dissected and then incubated at 37°C with shaking for 30 min in Dulbecco's modified Eagle's medium (DMEM) containing 10% fetal bovine serum (FBS) and 1 mg/ml collagenase. After collagenase treatment, tissue was forced through a 70 μm filter and treated with ACK buffer to lyse erythrocytes. The resulting single-cell suspension was pretreated with anti-CD16/32 for 5 min to block Fc receptor binding

before incubation with fixable viability dye and fluorochrome-conjugated anti-surface marker monoclonal antibodies for 30 min at 4°C. The following antibodies were used: anti-CD45, anti-CD11b, anti-CD11c, anti-Ly6G). Live/Dead fixable aqua stain (Life Technologies, Carlsbad, CA) was used to determine cell viability. Samples were collected using an LSRFortessa flow cytometer (BD Biosciences, San Jose, CA) and analyzed using FlowJo software (vX.0.7; TreeStar, Ashland, OR). Flow gating began with doublet exclusion by comparing forward light-scatter area versus height and then debris exclusion by comparing forward versus side light scatter. Dead cells were excluded based on viability dye staining. Neutrophils were identified as CD45+ Ly6G+ cells.

4.3.4.3 Blood cell quantification

Blood was taken from the heart via cardiac puncture at harvest, placed into K_2-EDTA tubes, and assayed within 30 min of recovery using a Hemavet 950FS hematology system (Drew Scientific, Miami Lakes, FL).

4.3.4.4 Myeloperoxidase assay

For assessment of myeloperoxidase (MPO) activity, the left lobe of each lung was perfused with PBS until white, snap-frozen in liquid nitrogen, and then mechanically homogenized for MPO activity assessment (MPO activity assay kit [colorimetric]; Abcam, Cambridge, UK).

4.3.5 Statistical analysis

Data were analyzed using GraphPad Prism 7 (GraphPad, La Jolla, CA). Analyses comparing two groups were performed by an unpaired t test with Welch's correction, unless data were not parametrically distributed, in which case Mann-Whitney analysis was used. *S.*

pneumoniae CFU data were log transformed before statistical analysis due to their distribution. Two-way analysis of variance (ANOVA) was used to compare repeated measures over time. All figures show combined data from multiple replicate studies as means ± standard errors of the means (SEM). The indicated n values are numbers of animals per independent experiment. Statistical significance is reported as follows: * $p < 0.05$, ** $p < 0.01$, *** $p < 0.001$. P values of between 0.05 and 0.1 are displayed numerically.

4.4 Results

To test the effect of IFNλ therapy on bacterial super-infection during influenza, we treated mice with an adenoviral vector to overexpress IFNλ (Ad-IFNλ) or control green fluorescent protein (GFP) (Ad-GFP) in the lung. Twenty-four hours following adenoviral treatment, mice were challenged with 5×10^7 CFU MRSA USA300 and harvested 24 hours later or challenged with 1×10^3 CFU *Streptococcus pneumoniae* and harvested 48 hours later (Fig. 4.1A). While mice quickly clear *S. aureus* from the lung and will survive this inoculum of MRSA, *S. pneumoniae* will replicate in the murine lung, eventually causing death. Moreover, both bacteria have been important causes of secondary bacterial infection during influenza throughout history and are still relevant today. Thus, we assessed the effect of Ad-IFNλ treatment on both influenza/MRSA and influenza/*S. pneumoniae* super-infection. In mice given either bacterial challenge, Ad-IFNλ treatment significantly increased the bacterial burden in the lung 24 hours after bacterial infection (Fig. 4.1B). The influenza viral burden was unchanged (appendix Figure 5.3). Together, these data suggest that IFNλ therapy has negative consequences for bacterial super-infection due to modulation of the immune response to influenza.

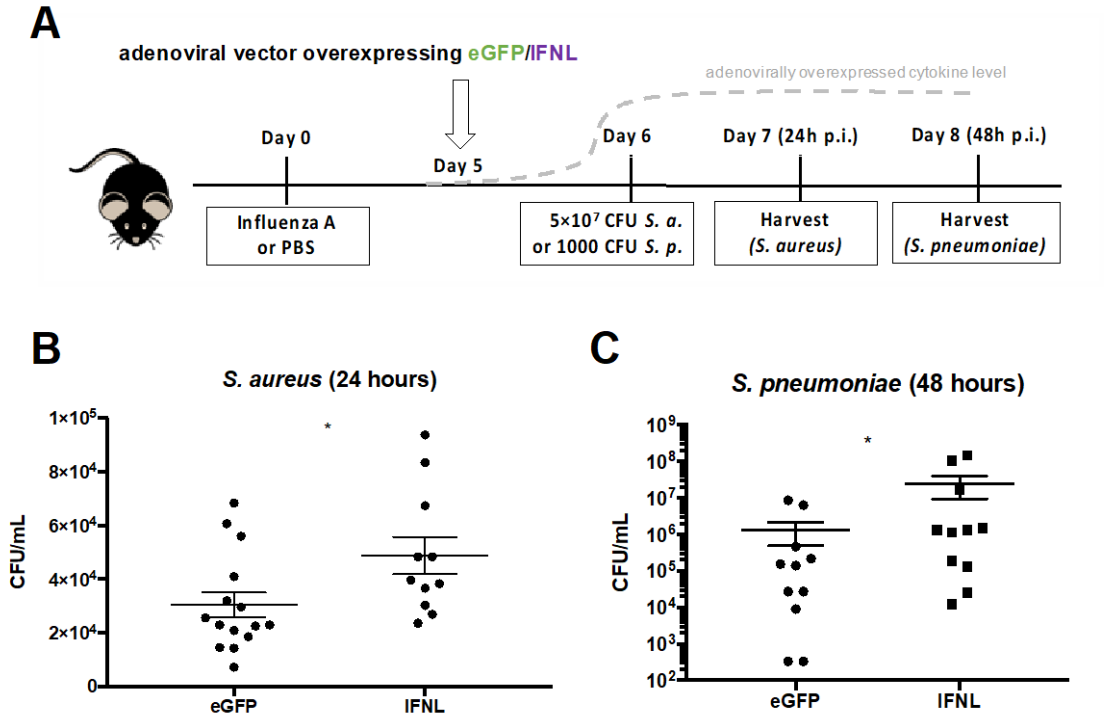

Figure 11: IFNλ treatment increases bacterial burden during influenza super-infection.

Mice were infected with 25 PFU influenza A/PR/8/34 H1N1 or PBS as a control and 5 days later given 1×10^{10} VP of an adenoviral vector to overexpress IFNλ (Ad-IFNλ) or GFP (Ad-GFP). Twenty-four hours following adenoviral treatment, mice were challenged with 5×10^{7} CFU methicillin-resistant *Staphylococcus aureus* USA300 (n = 4; four independent experiments) and harvested 1 day later or challenged with 1×10^{3} CFU *Streptococcus pneumoniae*. *, $P < 0.05$. (A) Diagram showing the experimental design. (B) Lung bacterial burden of *S. aureus* 24 hours after *S. aureus* challenge and lung bacterial burden of *S. pneumoniae* 48 hours after *S. pneumoniae* challenge.

Type I IFN signaling has many positive feedback mechanisms (107) as well as negative feedback mechanisms to shut down the interferon response, which is thought to protect against immunopathology and other issues from sustained interferon signaling (108). In HLLR1-1.4 cells, both type I and III IFNs induce USP18 which negatively regulates IFNα (109). Type III IFNs induce SOCS proteins that work on type I IFN during influenza (64), and type I IFN has been

shown to be a significant controller of susceptibility to bacterial super-infection (55). Thus, I hypothesized that altering IFNL would alter type I interferon in bacterial super-infection during influenza. Ad-IFNλ treatment 5 days following influenza A/PR/8/34 H1N1 infection resulted in a 4-fold increase in the level of IFNλ protein in bronchoalveolar lavage fluid (BALF), from a mean of 740.9 ± 56.81 to $3{,}114 \pm 583.8$ pg/ml (Figure 4.2A). Surprisingly, levels of type I and II IFNs were unchanged by IFNλ treatment (Figure 4.2B).

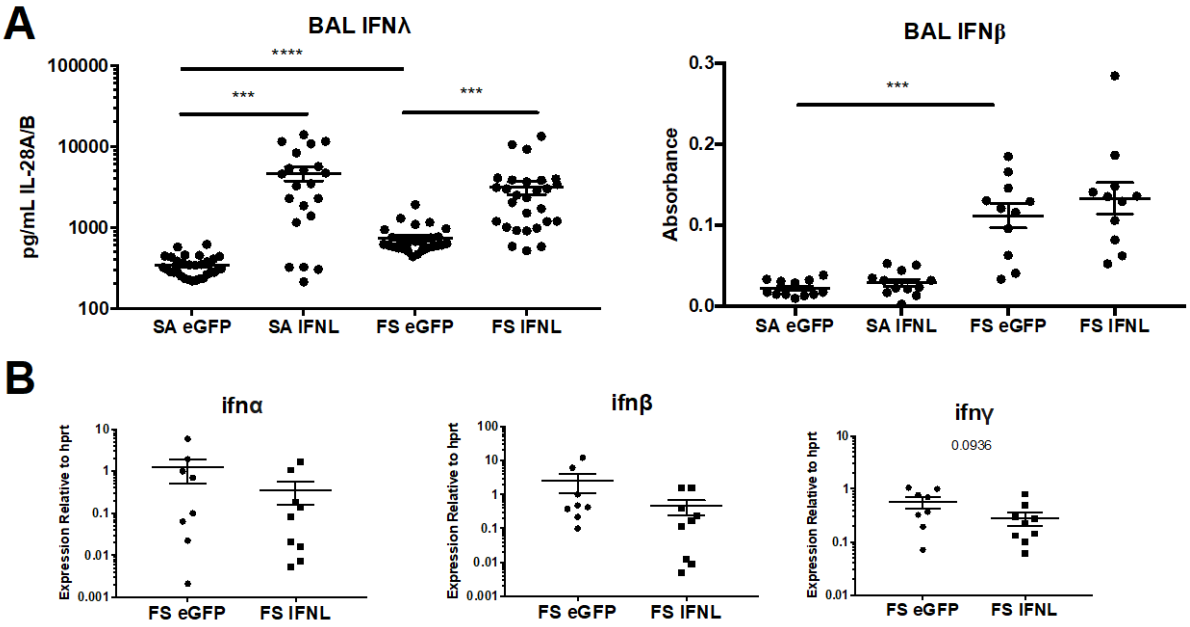

Figure 12: IFNλ overexpression does not alter other interferons.

Mice were infected with influenza (FS) or PBS vehicle (SA), five days later given adenovirus to overexpress IFNλ (Ad-IFNλ) or GFP (Ad-GFP), and twenty-four hours later challenged with 5×10^7 CFU MRSA as described in Figure 1. **(A)** ELISA for IFNλ or IFNβ in BAL (n = 4, three to eight independent experiments). **(B)** Real-time PCR for interferon genes in lung RNA (n = 4, three independent experiments *p < 0.05, **p < 0.01, *** p < 0.005, ns = not significant.

Little is known about the role of IFNλ in super-infection. It was previously reported that mice lacking the receptor for IFNλ have decreased bacterial burdens during both pulmonary MRSA infection and influenza/MRSA super-infection. This decrease in bacteria correlated with increased expression of IL-22 and its associated antimicrobial peptide NGAL (neutrophil gelatinase-associated lipocalin) (69). The release of antimicrobial peptides is a key bacterial defense mechanism for both myeloid cells and the lung epithelium during *S. aureus* infection (53, 110). Moreover, we have previously shown that administration of exogenous NGAL decreases the bacterial burden in influenza/MRSA super-infection (53). Thus, we tested the effect of IFNλ treatment on antimicrobial peptide expression during influenza/MRSA super-infection. IFNλ treatment did not alter the expression of NGAL in BALF cells or whole lung (Fig. 4.3) or the associated type 17 cytokine IL-17 (appendix Table 2) or IL-22 (Fig. 4.3). Expression levels of other lung antimicrobial peptides (regenerating islet-derived protein 3 gamma and cathelicidin antimicrobial peptide) and calprotectin (s100a8:s100a9 dimer), a neutrophil antimicrobial peptide which suppresses *S. aureus* growth (111), were also unchanged in both BALF cells and whole lung (Fig. 4.3). These results suggest that IFNλ does not increase the bacterial burden by inhibiting antimicrobial peptide expression.

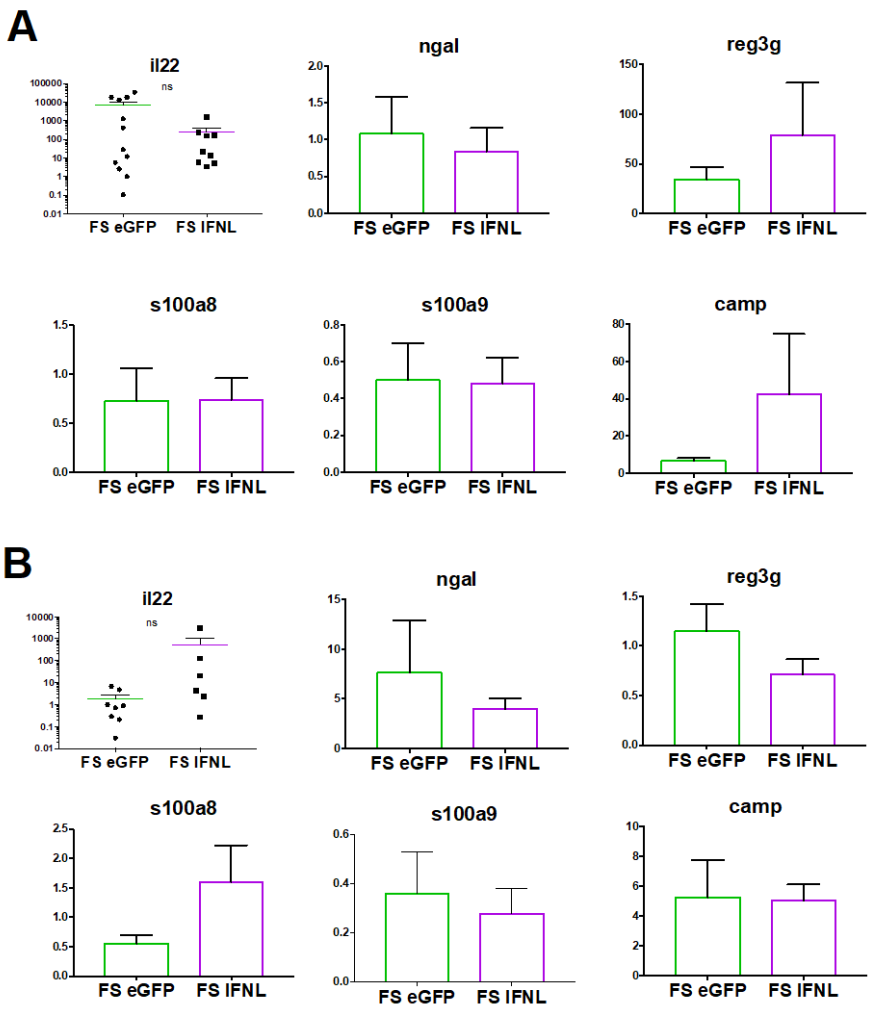

Figure 13: IFNλ treatment does not affect antimicrobial peptide expression in the lung.

Mice were infected with 25 PFU influenza virus A/PR/8/34 H1N1 or PBS as a control and 5 days later given 1×10^{10} VP of Ad-IFNλ or Ad-GFP. Twenty-four hours following adenoviral treatment, mice were challenged with 5×10^{7} CFU MRSA and harvested 1 day later. **(A)** Whole lung lobes were snap-frozen in liquid nitrogen, and RNA was extracted and assayed by real-time PCR for expression of IL-22 and the antimicrobial peptides ngal, reg3g, s100a8, s100a9, and camp (n = 4, two to three independent experiments). **(B)** Bronchoalveolar lavage fluid was centrifuged to pellet cells. The supernatant was removed, and the cell pellet was frozen at −80°C for RNA extraction and subsequent real-time PCR. FS, MRSA infection preceded by influenza virus infection for 6 days. ns, not significant.

No other reported data were available for how IFNλ affects infection with bacteria that commonly complicate influenza. Thus, we examined the known role of IFNλ in influenza infection alone as well as in other immunopathological diseases to hypothesize how it may affect influenza/bacterial super-infection. IFNλ has been shown to be a potent suppressor of neutrophil trafficking and function in murine models of collagen-induced arthritis, colitis, and, most importantly, influenza infection (36, 38, 105). To our knowledge, the role of IFNλ in neutrophil recruitment toward sites of bacterial infection is unknown. To assess the effect of IFNλ on neutrophils responding to pulmonary MRSA infection (with and without preceding influenza infection), we characterized infiltrating cells in the BALF by differential counting. Although the total number of cells in BALF was not significantly changed by IFNλ treatment, a trend of reduced cell numbers was apparent (Fig. 4.4A). Specifically, neutrophil recruitment to the airway was significantly reduced (Fig. 4.4B). During MRSA pneumonia alone, IFNλ treatment did not alter the bacterial burden or BALF cell numbers (appendix Figures 5.4 and 5.5). These data suggest that IFNλ increases the bacterial burden during influenza/MRSA super-infection by suppressing neutrophil recruitment to the airway.

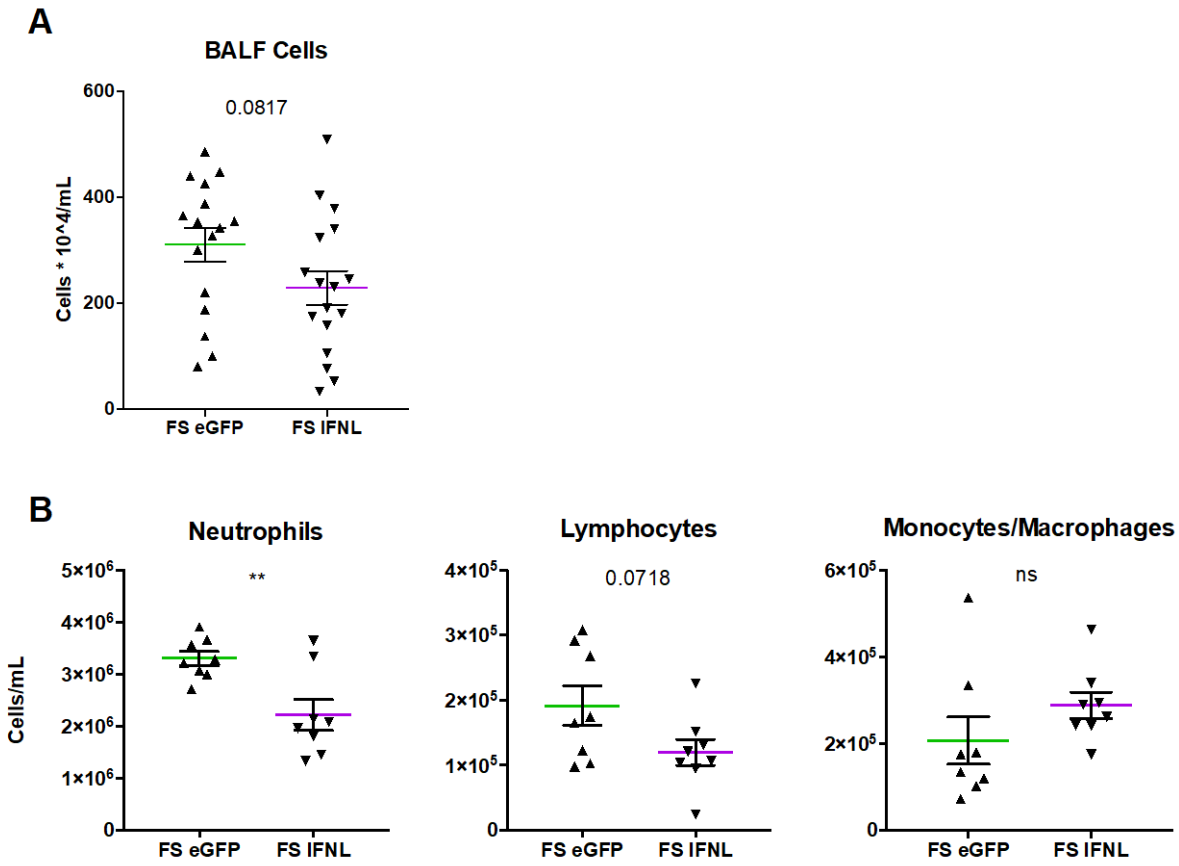

Figure 14: IFNλ treatment decreases neutrophils in BAL fluid during influenza/MRSA super-infection.

Mice were infected with influenza, given Ad-IFNλ or Ad-GFP 5 days later, and challenged with 5×10^7 CFU MRSA 24 h later, as described in the legend of Fig. 4.1. **(A)** Total cell counts from bronchoalveolar lavage fluid (n = 4; four independent experiments). **(B)** Differential counting of BALF cells (n = 4; two independent experiments). **, $P < 0.01$; ns, not significant.

We sought to determine the mechanism by which IFNλ treatment suppresses airway neutrophil recruitment. First, we measured levels of inflammatory cytokines in the lung. IFNλ treatment significantly increased the levels of only 3 of the 23 assayed cytokines, CXCL1/keratinocyte chemoattractant (KC), granulocyte colony-stimulating factor (G-CSF), and IL-1α (Fig. 4.5A and appendix Table 2). All three are neutrophil chemokines, suggesting a "frustrated" granulocyte chemokine release by the lung in response to a defect in neutrophil

production or trafficking. Neutropenia is a common side effect of type I IFN administration (112, 113), which led us to think that IFNλ might decrease numbers of circulating neutrophils as well. To test for a defect in neutrophil production, we assayed blood from mice with an automated hematology instrument. IFNλ treatment did not result in decreases in total leukocyte or neutrophil counts in whole blood (Fig. 4.4B), confirming that the reduction of neutrophils in BALF upon IFNλ treatment is not due to leukopenia or neutropenia.

To test if IFNλ treatment alters neutrophil trafficking to the lung, we assessed the expression of adhesion molecules in the BALF cell pellet, which is mainly composed of neutrophils (80 to 90%) (Fig. 4.4B). For successful emigration from capillaries into the lung, neutrophils must first tether to the lung endothelium by binding integrin α4β1 to endothelial vascular cell adhesion molecule 1 (VCAM-1) (114). Firm binding and adhesion are established by CD11/CD18 binding to endothelial intracellular adhesion molecule 1 (ICAM-1). Importantly, CD18 blockade reduces neutrophil migration to pulmonary S. aureus infection, as the dependence on CD18 for neutrophil emigration to the lung is highly stimulus specific (115). IFNλ treatment did not alter the expression of the genes encoding the neutrophil trafficking receptor VLA-4 (heterodimer of igta4:itgb1) (Fig. 4.5C) or the expression of CD11b/c on the surface of Ly6G+ lung neutrophils (Fig. 4.5D), suggesting that IFNλ likely does not alter integrin/CD11-mediated neutrophil adhesion to the lung endothelium.

These data suggest that IFNλ therapy does not suppress neutrophil production in the bone marrow and does not inhibit neutrophil recruitment to the airway by altering adhesion molecule expression. Interestingly, neutrophils from IFNλ-treated mice exhibit reduced chemotaxis in both TAXIscan and Transwell assays toward leukotriene B4 (LTB4) (38, 105), suggesting a general defect in neutrophil movement. Patients with reduced neutrophil chemotaxis or oxidative burst

exhibit increased susceptibility to *S. aureus* infection (116). Moreover, to evade the immune system, *S. aureus* produces factors to inhibit both neutrophil chemotaxis and phagocytosis (117-119). As IFNλ has been shown to inhibit neutrophil chemotaxis both *in vivo* and *in vitro*, we asked if neutrophil phagocytosis of *S. aureus* was also reduced by IFNλ treatment.

To kill MRSA, neutrophils must first sense the bacteria through Toll-like receptor 2 (TLR2) recognition of peptidoglycan. Treatment with a TLR2 agonist reduces bacterial burden and mortality during MRSA pneumonia in mice (120), and mice lacking TLR2 have altered neutrophil recruitment and bacterial phagocytosis in various infection models (121). Additionally, neutrophil killing of *S. aureus* relies upon the intracellular generation of reactive oxygen species (ROS), and patients defective in ROS generation are more susceptible to *S. aureus* infection (116). Neither TLR2 expression (Fig. 4.5C) nor antimicrobial peroxidase activity (Fig. 4.5B) was affected by IFNλ overexpression. These data suggest that IFNλ treatment may not alter the killing of *S. aureus* by neutrophils. However, data from other models suggest that IFNλ treatment specifically impairs neutrophil movement (38, 105), demonstrating that IFNλ directly impairs neutrophil chemotaxis both *in vitro* and *ex vivo*.

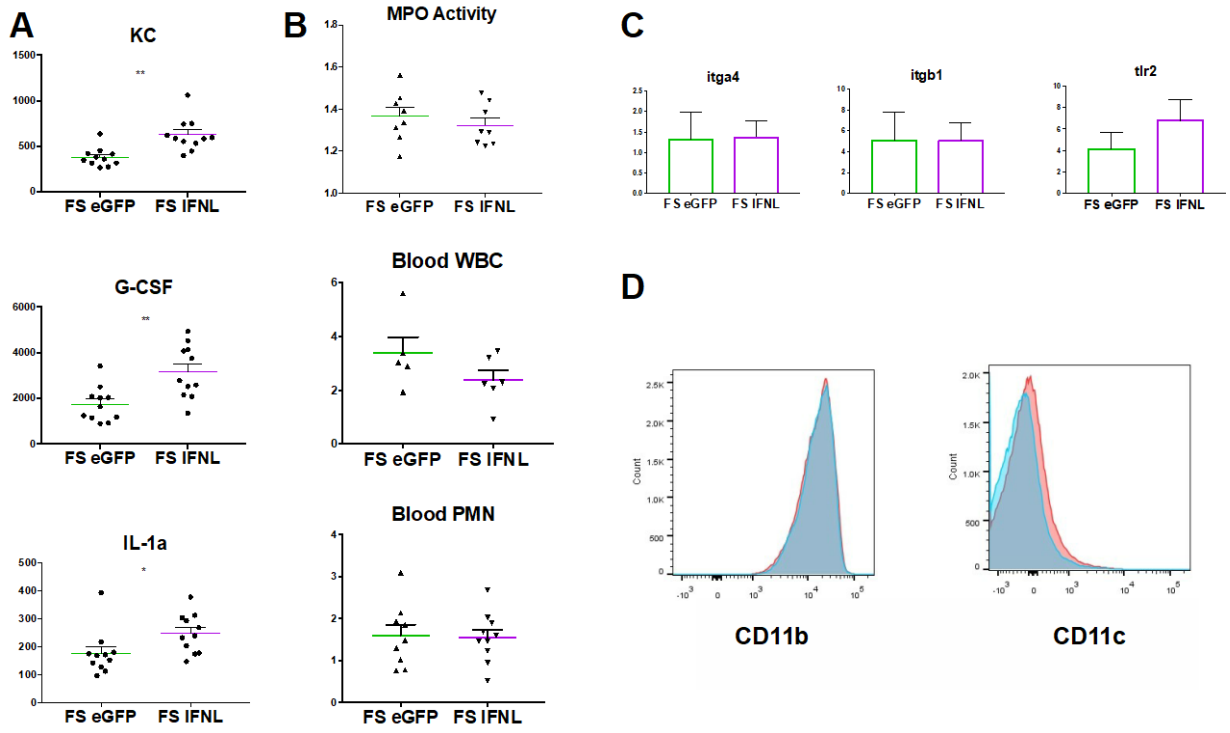

Figure 15: IFNλ treatment increases levels of granulocyte chemokines in the lung but does not affect neutrophil production, trafficking, or ROS generation.

Mice were infected with influenza, given Ad-IFNλ or Ad-GFP 5 days later, and challenged with 5×10^7 CFU MRSA 24 h later, as described in the legend of Fig. 4.1. **(A)** Cytokine production in lung homogenates (n = 4, three independent experiments**). (B)** Total white blood cell (WBC) counts and differential counting of blood neutrophils (n = 4; two independent experiments). The left lobe of the lung was perfused with PBS, homogenized, and assayed for myeloperoxidase (MPO) activity as a measure of reactive oxygen species generation (n = 4; three independent experiments). PMN, polymorphonuclear leukocytes. **(C)** Real-time PCR of the bronchoalveolar lavage cell pellet for neutrophil adhesion molecules and bacterial receptors (n = 4; three independent experiments). **(D)** Expression of CD11b on live CD45+ Ly6G+ lung neutrophils (n = 4; two independent experiments). Ad-IFNλ-treated samples are displayed in pink, and Ad-GFP-treated samples are in blue. *, $P < 0.05$; **, $P < 0.01$.

To assess the ability of neutrophils to phagocytose bacteria *in vivo*, we challenged influenza-infected mice with fluorescein isothiocyanate (FITC)-labeled MRSA or *S. pneumoniae* and analyzed lungs by flow cytometry 24 or 48 hours later, respectively. The percentage of FITC-

positive ($FITC^+$) neutrophils (defined as $FITC^+$ live $CD45^+$ $CD11b^+$ $Ly6G^+$ cells, for gating strategy see appendix Figure 5.6) in the lung decreased over 4-fold from 1.3% to 0.2% (Fig. 4.6A), implying that IFNλ decreases neutrophil phagocytosis of MRSA during super-infection. Moreover, when mice were challenged with FITC-labeled *S. pneumoniae*, neutrophil phagocytosis was also markedly decreased (Fig. 4.6B). While IFNλ overexpression impaired neutrophil infiltration into BALF (Fig. 4.4B), the percentage of neutrophils in lung tissue was not altered (Fig. 4.6A-B). However, flow cytometry analysis showed a striking decrease in neutrophil phagocytosis in vivo in IFNλ-treated mice (Fig. 4.6C). Together with data reported for models of sterile inflammation and influenza infection alone (36, 38, 105), these data suggest that IFNλ generally reduces neutrophil movement, preventing chemotaxis to and phagocytosis of bacteria during influenza/bacterial super-infection.

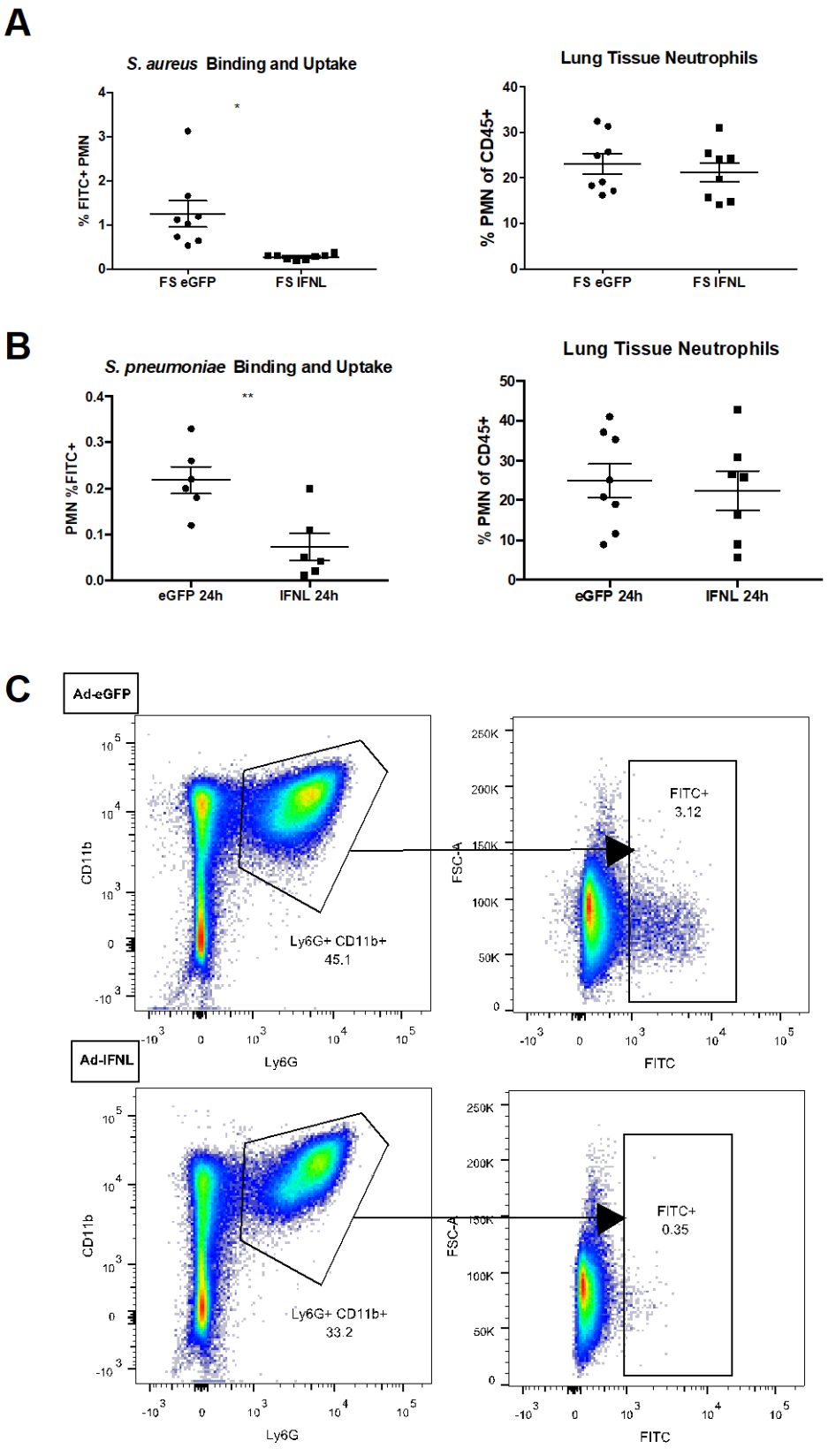
A
S. aureus Binding and Uptake
% FITC+ PMN
FS eGFP
FS IFNL
Lung Tissue Neutrophils
% PMN of CD45+
FS eGFP
FS IFNL
B
S. pneumoniae Binding and Uptake
PMN %FITC+
eGFP 24h
IFNL 24h
Lung Tissue Neutrophils
% PMN of CD45+
eGFP 24h
IFNL 24h
C
Ad-eGFP
CD11b
Ly6G
Ly6G+ CD11b+
45.1
FSC-A
FITC
FITC+
3.12
Ad-IFNL
CD11b
Ly6G
Ly6G+ CD11b+
33.2
FSC-A
FITC
FITC+
0.35

Figure 16: IFNλ inhibits bacterial phagocytosis during super-infection.

(A-B) Mice were infected with influenza and 5 days later given Ad-IFNλ or Ad-GFP as described in the legend of Fig. 1. Twenty-four hours later, mice were challenged with **(A)** 5×10^7 CFU FITC-labeled MRSA or **(B)** 1×10^3 CFU FITC-labeled *S. pneumoniae* and sacrificed 1 day later. The left lobe of the lung was digested to a single-cell suspension and stained for flow cytometry. The percentage of FITC+ neutrophils as analyzed by flow cytometry is reported (percentage of live CD45+ Ly6G+ CD11b+ cells that were FITC+) as well as the percentage of total immune cells in the lung that are neutrophils (percentage of live CD45+ cells that were Ly6G+ CD11b+) ($n = 4$; two independent experiments). **(C)** Representative flow cytometry plot showing the gating strategy for determining FITC positivity in neutrophils from mice treated with Ad-GFP or Ad-IFNλ during influenza/MRSA super-infection. *, $P < 0.05$; **, $P < 0.01$. FSC, forward scatter.

4.5 Discussion

IFNλ has recently been proposed as a potentially attractive therapy for influenza (36, 122). There is a dire need for more influenza therapeutics, as a broadly effective vaccine has not yet been developed, and current therapies are both time restricted and limited in effect (123). With the continual mismatch of influenza vaccines to circulating viral strains (124) and the ever-present threat of another influenza pandemic, more broadly effective treatments for influenza are certainly necessary. Galani *et al.* have shown that pegylated IFNλ (PEG-IFNλ) therapy during influenza reduces immunopathology and mortality by reducing cytokine storm and neutrophil infiltration (36). However, bacterial super-infection commonly complicates influenza, increasing morbidity and mortality. While reducing neutrophil recruitment to the lung ameliorates disease during influenza alone, these neutrophils are crucial for survival during *S. aureus* lung infection (125). Moreover, mice lacking the IFNλ receptor exhibit decreased bacterial burden during pulmonary MRSA infection as well as influenza/MRSA super-infection, suggesting that IFNλ contributes to

disease during bacterial infection of the lung (69). Especially with the rise of drug-resistant pathogens such as MRSA as secondary bacterial pathogens, considering the risk for super-infection when evaluating a therapeutic for influenza is critical.

I report that overexpression of IFNλ during influenza results in an increased lung bacterial burden upon super-infection with either MRSA or *Streptococcus pneumoniae*. These data support findings by Planet *et al.* showing that mice lacking the IFNλ receptor have lower bacterial burdens during pulmonary MRSA infection as well as influenza/MRSA super-infection (69). Specifically, Planet *et al.* found increases in the expression of IL-22 and its associated antimicrobial peptide NGAL in IFNλ receptor knockout mice. It has previously been shown that exogenous NGAL decreases the bacterial burden during influenza/MRSA super-infection (53). However, there was no change in IL-22 or NGAL expression upon IFNλ overexpression. However, IFNλ overexpression does not exactly recapitulate the phenotype of the total receptor knockout, as there is no difference in bacterial burdens during single *S. aureus* infection (appendix Figure 5.5), while in the IFNαR1$^{-/-}$ mice, the *S. aureus* burden is decreased. It is also likely that there is a differential requirement for IL-22 and the associated antimicrobial peptide expression during transient IFNλ overexpression versus constitutive IFNλ receptor knockout. Thus, I investigated what else might be responsible for the acute IFNλ-induced increase in the bacterial burden.

I demonstrate that IFNλ decreases BALF neutrophil accumulation during influenza/MRSA super-infection. Galani *et al.* also showed a decrease in BALF neutrophils as well as total BALF cells, along with reduced peribronchial and parenchymal cell infiltration, upon PEG-IFNλ administration during influenza infection alone. Notably, Galani *et al.* administered PEG-IFNλ at two days following viral infection, while I treated mice 5 days after viral infection, leading to a significant overexpression of IFNλ at harvest 2 days later. While weight loss from influenza virus

infection mimicked the weight loss reported by Galani *et al.* with similar inocula (36, 106), treatment with IFNλ 5 days after viral infection did not reproduce their reported reduction in viral burden. As current therapies for influenza decrease in effectiveness the later they are given during infection (123), the delay in treatment until 5 days after viral infection is likely responsible for this discrepancy. I did not observe a decrease in BALF neutrophil accumulation either 24 or 48 hours following influenza/*S. pneumoniae* super-infection (appendix Figure 5.5), which suggests that the decrease in BALF neutrophils during influenza/MRSA super-infection is not the cause of the increased bacterial burden.

Aside from differences in the timing of therapeutic intervention, bacterial super-infection drastically changes the immunological landscape of the lung. Interestingly, there was no increase in bacterial burden upon IFNλ treatment during MRSA pneumonia without preceding influenza (appendix Figure 5.4). This suggests that influenza-induced cytokines work in concert with IFNλ during bacterial super-infection to reduce antibacterial immunity. Type I IFN is also broadly produced in response to influenza and strongly contributes to super-infection susceptibility (55). It is likely that the high levels of type I IFN in the influenza-infected mouse may synergize with the administered IFNλ to produce this increase in bacterial burden during super-infection but not bacterial infection alone. Many other cytokines are induced by influenza and play significant roles in its pathogenesis, including type 17 cytokines (53) and IL-1 family members (50). There is likely an interactive role for these players in the complex cytokine environment of the influenza-infected lung.

During bacterial super-infection, IFNλ therapy produced no significant decrease in type I IFN expression or protein levels. There was also no decrease in tumor necrosis factor alpha (TNF-α), IFN-γ, CCL3, or CCL4 levels, which were reported by Galani *et al.* to be reduced by PEG-

IFNλ administration. Instead, IFNλ treatment during bacterial super-infection specifically increased neutrophil chemokines in the lung, while BALF neutrophils were decreased. This is consistent with previous findings that neutrophil depletion during *S. aureus* pulmonary infection increases lung KC and G-CSF levels (53), suggesting a "frustrated" chemokine production by the lung in response to a lack of neutrophils.

The reduction in BALF neutrophils implies that IFNλ induces a defect in neutrophil production or migration. However, upon assessment of circulating blood cells, there was no difference in neutrophils or total leukocytes. IFNλ has been shown to suppress neutrophil migration *in vitro* by Transwell and EZ-TAXIscan assays (38, 105), suggesting a defect in the migration of neutrophils into airspaces where MRSA aggregates reside (126). Surprisingly, while IFNλ treatment decreased BALF neutrophils, lung neutrophils were not altered, as measured by flow cytometry. It must be noted that this flow cytometry was performed on lavaged lungs, which may explain the disparity between these two measurements. Importantly, bronchoalveolar lavage samples only the epithelial surface of the respiratory tract (127), whereas flow cytometry was performed on a single-cell suspension digested from whole lung. Together, these data suggest that IFNλ may specifically impair neutrophil migration across the lung epithelium.

Although IFNλ treatment does not alter the number of neutrophils in the lung, it results in a marked decrease in neutrophil phagocytosis of MRSA *in vivo*. This effect of IFNλ appears to be specific, as it alters phagocytosis but not myeloperoxidase activity or the expression of adhesion molecules. As the cytoskeletal changes of a cell that allow for *in vivo* migration mimic those necessary for phagocytosis, including actin remodeling and microtubule assembly, these data suggest that IFNλ may be exerting a broader effect on neutrophil cellular motility and cytoskeletal rearrangement.

Together, these data strongly suggest that the use of IFNλ as a therapeutic for influenza may result in adverse outcomes for patients who contract a secondary bacterial infection. Neutrophils, which are essential for the control of superinfecting pathogens (54), were reduced in BALF following IFNλ treatment. Moreover, neutrophil binding and uptake of MRSA are reduced with IFNλ treatment, which correlates with an increase in the MRSA burden in the lung. Importantly, IFNλ administration also decreases binding and uptake of *S. pneumoniae* during influenza super-infection, which also correlates with an increase in the lung bacterial burden. Although IFNλ may reduce influenza severity, both our data and the findings of other groups show that it worsens bacterial super-infection (69). While new therapeutics targeting influenza are sorely needed, it is crucial that the risk of bacterial super-infection is considered when evaluating new treatments.

5.0 Conclusions and Future Directions

New therapeutics for super-infection need to be developed, but neither IFNλ nor WLBU2 should be considered for further development as therapies against bacterial super-infection during influenza. While WLBU2 was able to reduce bacterial burden during single lung infection with *S. aureus*, it was ineffective at reducing bacterial burden during influenza super-infection. While it may be that bacterial persistence due to preceding influenza overwhelmed the amount of WLBU2 delivered with high bacterial numbers, mice received up to 2.5 mg/kg of WLBU2 intravenously, whose LD_{50} is estimated to be between 12-16 mg/kg when administered intravenously (89). Highly reduced (0.01 mg/kg) dosing via oropharyngeal administration worked significantly better in a model of *P. aeruginosa* pneumonia, although influenza super-infection was not tested (98). It is likely that low-dose oropharyngeal instillation of WLBU2 would be effective against influenza/*P. aeruginosa* pneumonia, but it is still unclear whether its lack of efficacy in influenza/*S. aureus* pneumonia is due to delivery method, presence of influenza, or a special synergy between influenza and *S. aureus.*

Preceding influenza does alter lung factors other than antibacterial immunity. It is possible that the higher lung leak in the more damaged doubly-infected lung is interfering with the delivery of the drug to the airspaces, as edema blocks gas exchange in the alveoli and influenza is known to interfere with physical clearance of bacteria in the lung by altering mucus flow. Penetrance into the lung is a known issue with antibiotics, especially those effective against *S. aureus*. Specifically, vancomycin has worse lung penetrance than linezolid, contributing to its lack of efficacy against *S. aureus* (118). To test this, the WLBU2 peptide would have to be radiolabeled during synthesis to allow for imaging of the peptide inside the lung (128), as it is much too small of a molecule to

attach a fluorophore. However, radiolabeling the peptide would be extremely useful, as there is currently very little data on its mechanism of action, although it is assumed to blanket and disrupt bacterial membranes like other cathelicidins.

Other antibacterial agents are currently being developed that may be effective against bacterial super-infection during influenza. The current development of antibodies against *S. aureus* toxins is promising, especially since influenza and *S. aureus* toxins may specifically synergize to increase inflammation and promote cytotoxicity (129). Moreover, more research is being published each day on the immunological underpinnings of this disease. It was published in April 2019 that neutrophils express a new repertoire of chemokine receptors during influenza as compared with steady state (130). Rudd *et al.* show that while circulating blood neutrophils from healthy mice mostly express CXCR2, a broad set of both C-C and CXC chemokine receptors is expressed by neutrophils recruited to the lung during influenza infection, suggesting that all these receptors are possible targets for therapeutic intervention to limit neutrophilia during influenza infection. They remark on the possibility of bacterial super-infection, and suggest that these receptors may also be potential targets for modulation of neutrophil function during bacterial super-infection, as my data imply and others show that neutrophils are less bactericidal during influenza infection.

It is clear that IFNλ has become known as a neutrophil modulator as well as an antiviral cytokine (131). A new host of literature is also being published on type III interferon, and specifically how it influences neutrophils. It is beneficial to both the understanding of type III interferon biology and the pathogenesis of bacterial super-infection during influenza that neutrophils are in the spotlight, as neutrophilia is a main driver of immunopathology during influenza but neutrophils are crucial for bacterial clearance upon super-infection, and neutrophils

seem to be specifically targeted by type III interferon. In February 2019, Britto *et al.* published that neutrophil recruitment to the lung during acute inflammation is regulated by the airway-protective immunomodulatory host protein BPI-fold containing group A member 1 (BPIFA1). BPIFA1 was also shown by the authors to regulate type III interferon signaling, and interestingly type II interferon, as both IFNγ and IFNλ but not type I interferon expression were downregulated in Bpifa1$^{-/-}$ mice in an intranasal LPS model of acute lung inflammation. The neutrophil chemokines CXCL9 and CXCL10 were decreased, as well as their receptor CXCR3 (132), which was one of the neutrophil chemokine receptors shown to be upregulated in influenza-recruited lung neutrophils by Rudd *et al.*, suggesting that a CXCL9/10-CXCR3-IFNλ axis may also be involved in pulmonary regulation of neutrophilia during influenza.

Recent work also suggests that adaptive immunity may also be influenced by IFNλ. Ye *et al.* published in May 2019 that IFNλ stimulates production of thymic stromal lymphopoietin (TSLP) from upper airway M cells during influenza infection, stimulating CD103+ DC migration to draining lymph nodes and promoting germinal center B cell numbers (133). Even though human B cells express IFNλR1 while mouse B cells do not, perhaps IFNλ may influence mouse B cells after all. From the earlier literature focusing on the role of IFNλ in chronic viral infection that plasmacytoid dendritic cells (pDCs) express high levels of IFNλR1 (134), and when stimulated with IFNλ produce high amounts of CXCL10 (135). Together, these papers hint at a possible role for the putative CXCL9/10-CXCR3-IFNλ axis in adaptive immunity as well.

It is also important to contemplate the role of IFNλ in pulmonary inflammation in general when considering the immunology of bacterial super-infection during influenza. Insights from a neonatal mouse model of RSV bronchiolitis, a major risk factor in children for later development of asthma, have identified a new role for IFNλ. Blockade of the inflammatory prostaglandin D2

receptor DP2 increased IFNλ in the supernatant of airway epithelial cell cultures and in the BAL of neonatal mice given RSV bronchiolitis, which accelerated viral clearance (136). Taken together with the importance of lipids in influenza (137), these results suggest a role for lipids in mediating IFNλ as well. Won *et al.* show in a manuscript that will be published in July 2019 that IFNλ restricts type 2 inflammation in a murine model of allergic airway disease. Intranasal administration of a 1:1 ratio of recombinant IFNλ2/3 protein suppressed TSLP and IL-33 protein levels in BAL in an ovalbumin sensitization and challenge model in C57BL/6J mice (138). The Alcorn laboratory has previously showed that recombinant IL-33 treatment of *S. aureus* super-infection during influenza lowers bacterial burden and mortality, as well as pulmonary neutrophilia (50). Together, these studies suggest that IFNλ may have a role in this IL-33/neutrophil axis as well.

In conclusion, we are in the infancy of our knowledge about the role of IFNλ in the lung and in disease. New projects are being undertaken every day to understand the role of this novel interferon family during inflammation, and pegylated IFNλ is already being developed as a therapeutic for chronic viral infections, including phase II trials to become the first approved therapy for the most severe form of viral hepatitis in humans, hepatitis D. Our knowledge of the role of IFNλ in bacterial infection and allergic inflammation is much younger than its role in viral disease, and I expect that exciting and nuanced papers will continue to be published over the next decade, illuminating the function and therapeutic potential of IFNλ in these pulmonary diseases.

Appendix A -- Supplementary Figures

A.1 The Engineered Antimicrobial Peptide WLBU2 Does Not Reduce Bacterial Burden During Influenza Super-infection

Table 1: WLBU2 treatment does not alter other inflammatory chemokines.

Cytokine	PBS	WLBU2	p-value	LL-37	p-value
IL-1a	590.3 ± 62.4	461.7 ± 30.4	0.9872	700.9 ± 56.8	0.9910
IL-5	26.6 ± 4.7	14.5 ± 3.9	0.9999	40.2 ± 4.4	0.9999
IL-6	3325.2 ± 335.8	2570.9 ± 374.9	0.6425	4224.4 ± 318.0	0.5519
IL-10	21.9 ± 2.3	20.7 ± 2.9	>0.9999	38.1 ± 3.0	0.9998
IL-12p40	68.8± 9.6	42.1 ± 8.4	0.9994	112.1 ± 4.6	0.9986
IL-12p70	368.6 ± 29.1	289.9 ± 19.4	0.9952	463.6 ± 17.1	0.9934
IL-13	123.3 ± 16.6	119.1 ± 21.8	>0.9999	232 ± 17.1	0.9913
IL-17A	70 ± 12.4	54.3 ± 11.2	0.9998	125.3 ± 26.6	0.9977
Eotaxin	1803.0 ± 100.7	1512.7 ± 142.4	0.9365	2370.5 ± 158.4	0.7888
GM-CSF	661.6 ± 100.6	318.1 ± 81.2	0.9122	948.4 ± 87.9	0.9412
IFNg	131.5 ± 14.3	94.8 ± 17.9	0.9989	205 ± 7.9	0.9960
MIP-1a	2634.2 ± 315.5	1972.3 ± 257.7	0.7112	4421.8 ± 233	0.0973
MIP-1B	408.7 ± 51.6	306.4 ± 53.5	0.9919	657.6 ± 31.7	0.9553
RANTES	207.8 ± 33.3	98.4 ± 22.7	0.9907	333 ± 21.1	0.9885
TNFa	416.5 ± 78	308.1 ± 81.2	0.9818	785.8 ± 43.9	0.9254

Mice were infected with 5×10^7 CFU MRSA by oropharyngeal aspiration. Two hours later, mice were injected intravenously in the tail vein with either WLBU2, LL-37, or PBS vehicle as control, and sacrificed four hours later as described in Figure 2.1. Homogenized lung tissue was assayed by cytokine multiplex for pro-inflammatory cytokines and chemokines. n = 4, five independent experiments. Statistics were calculated by two-way ANOVA.

A.2 IFNλ3 Knockout Does Not Reduce Total IFNλ in Bacterial Super-infection During Influenza

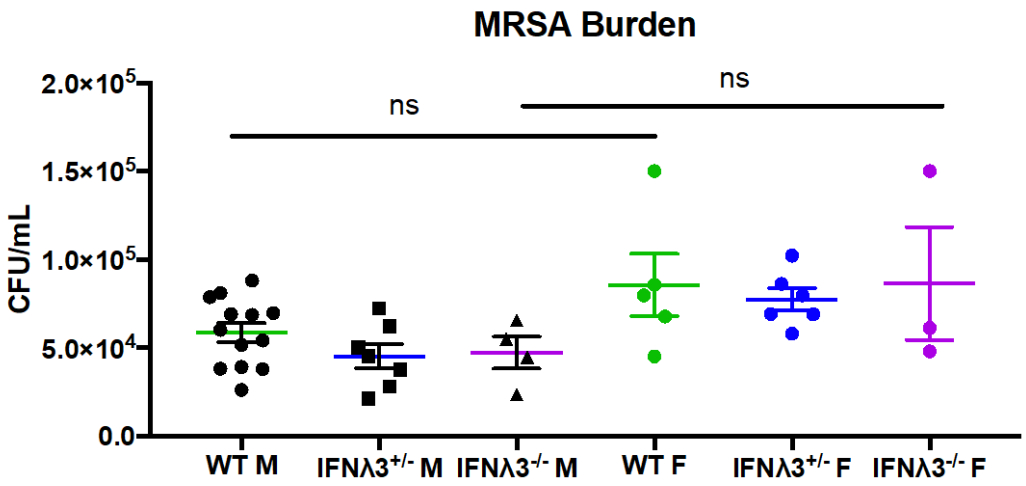

Figure 17: IFNλ3-/- littermates do not display sex differences in bacterial burden during influenza super-infection.

Mice were infected as described in Figure 3.5. Data were analyzed by student's t test with Welch's correction. n = 2-8, two independent experiments.

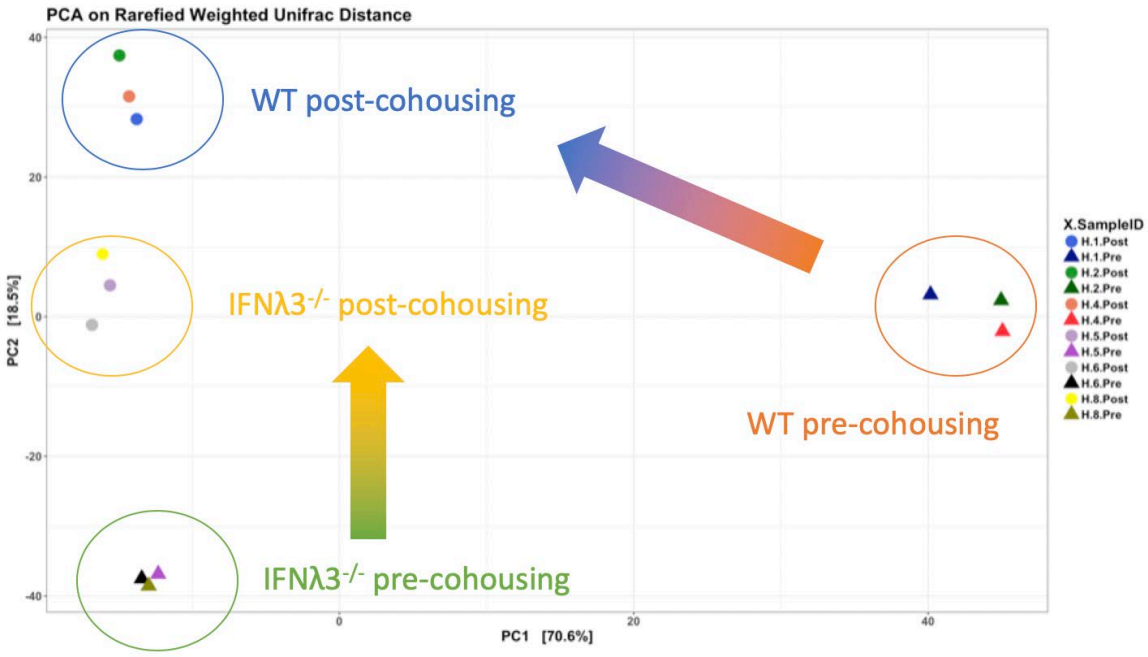

Figure 18: IFNλ3-/- mice co-housed with non-littermate WT mice have more similar intestinal microbiota.

Mice were infected as described in Figure 3.1. High-throughput sequencing of bacterial 16S rRNA gene amplicons encoding the V4 region40 (150 bp read length, paired-end protocol) was performed using a MiSeq Illumina Sequencer. The 16S rRNA gene sequences were analysed using the Quantitative Insights into Microbial Ecology (QIIME) pipeline for analysis of microbiome data and a principal component analysis based on rareified weighted UniFrac distance was performed using the software package R.

A.3 IFNλ Inhibits Bacterial Clearance During Influenza Super-infection

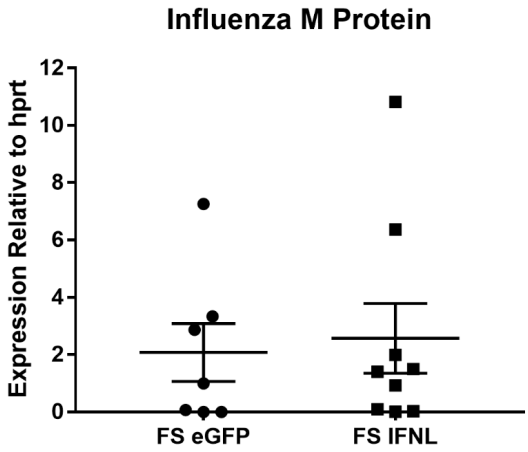

Figure 19: IFNλ overexpression does not alter influenza viral burden.

Mice were infected with influenza, five days later given adenovirus to overexpress IFNλ (Ad-IFNλ) or GFP (Ad-GFP), and twenty-four hours later challenged with 5×10^7 CFU MRSA as described in Figure 1. **(A)** RT-PCR for influenza A/PR/8/34 H1N1 M protein in lung RNA (n = 4, two independent experiments).

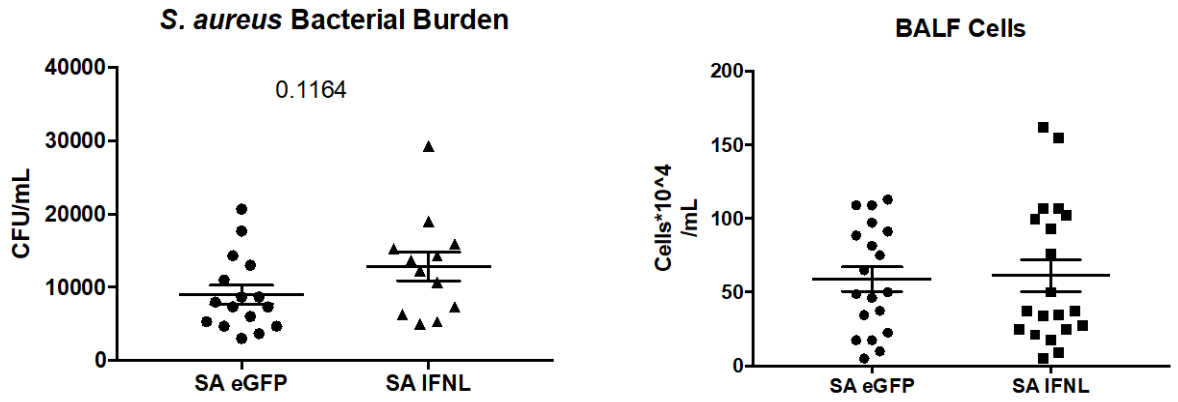

Figure 20: IFNλ overexpression does not alter bacterial burden during MRSA lung infection alone.

Mice were infected with influenza, five days later given adenovirus to overexpress IFNλ (Ad-IFNλ) or GFP (Ad-GFP), and twenty-four hours later challenged with 5×10^7 CFU MRSA. Bacterial burden was determined by counting CFU from plated lung homogenate. BALF cell number was determined by lavaging mouse lungs at time of sacrifice with 1 mL sterile PBS, performing red blood cell lysis, and resuspending in PBS and counting total cells on a hemocytometer.

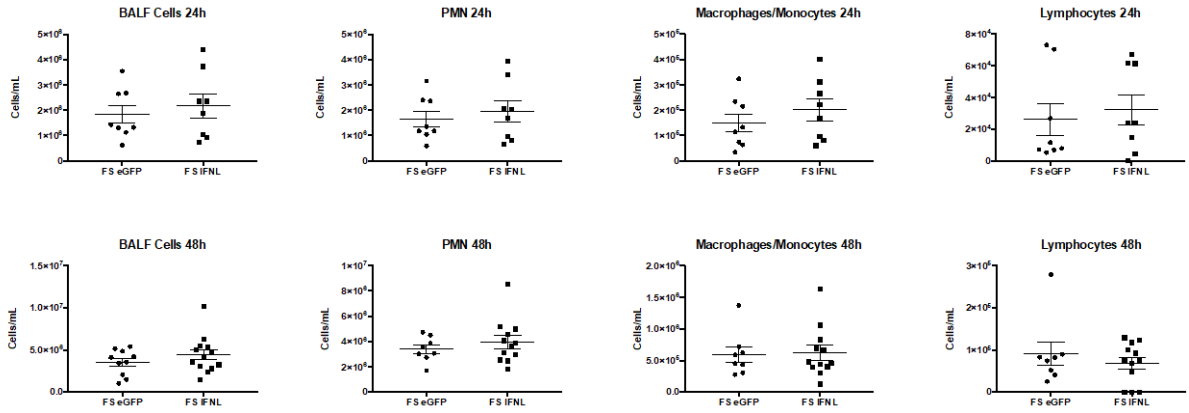

Figure 21: IFNλ overexpression does not alter bronchoalveolar lavage cells during influenza/S. pneumoniae super-infection.

Mice were infected with influenza, five days later given adenovirus to overexpress IFNλ (Ad-IFNλ) or GFP (Ad-GFP), and twenty-four hours later challenged with 1000 CFU *S. pneumoniae*. Mice were sacrificed either 24 or 48 hours later as indicated in the figure titles. Lungs were lavaged with 1 mL sterile PBS and the resulting bronchoalveolar lavage fluid (BALF) was processed by cytospin and BALF cells were differentially counted after staining (Diff-Quik).

Table 2: IFNλ overexpression does not alter other inflammatory chemokines.

Cytokine	FS eGFP	FS IFNL	significance	p-value
Eotaxin	2192 ± 602.9	2722 ± 780.4		0.5969
G-CSF	1734 ± 233.7	3172 ± 350.7	**	0.0032
GM-CSF	51.8 ± 4.484	54.31 ± 5.076		0.7153
IFNg	89.82 ± 15.33	87.61 ± 13.11		0.9139
IL-10	155.3 ± 36.67	100.6 ± 15.61		0.192
IL-12p40	129.2 ± 13.27	147 ± 21.05		0.4838
IL-12p70	186.4 ± 16.18	203.4 ± 16.14		0.4649
IL-13	52.41 ± 12.1	62.58 ± 13.65		0.5836
IL-17A	82.27 ± 15.97	82.54 ± 15.18		0.9901
IL-1a	176.3 ± 24.06	248.4 ± 21.25	*	0.0363
IL-1B	57.88 ± 4.573	74.5 ± 8.911		0.1181
IL-2	69.99 ± 13.24	76.65 ± 13.72		0.7305
IL-3	30 ± 6.312	29.3 ± 5.856		0.9367
IL-5	36.02 ± 6.619	32.38 ± 5.341		0.6733
IL-6	248.9 ± 30.36	285.5 ± 44.74		0.5069
IL-9	105.9 ± 17.06	111.5 ± 16.8		0.8198
KC	380.9 ± 31.37	625.4 ± 53.82	**	0.0012
MCP-1	4184 ± 893.5	3072 ± 563.6		0.3074
MIP-1a	2039 ± 277.9	2108 ± 338.6		0.8753
MIP-1B	1242 ± 146	1138 ± 158.6		0.6332
RANTES	2879 ± 423.5	2385 ± 517.1		0.4685
TNFa	207.1 ± 25.77	276.9 ± 36.97		0.1389

Mice were infected with influenza, five days later given adenovirus to overexpress IFNλ (Ad-IFNλ) or GFP (Ad-GFP), and twenty-four hours later challenged with 5×10^7 CFU MRSA as described in Figure 4.1. Lungs were snap-frozen, homogenized, and the supernatant assayed for inflammatory cytokines by multiplex (n=12, three independent experiments). Data are reported as mean +/- SEM, with significance and p-value calculated by Welch's t-test.

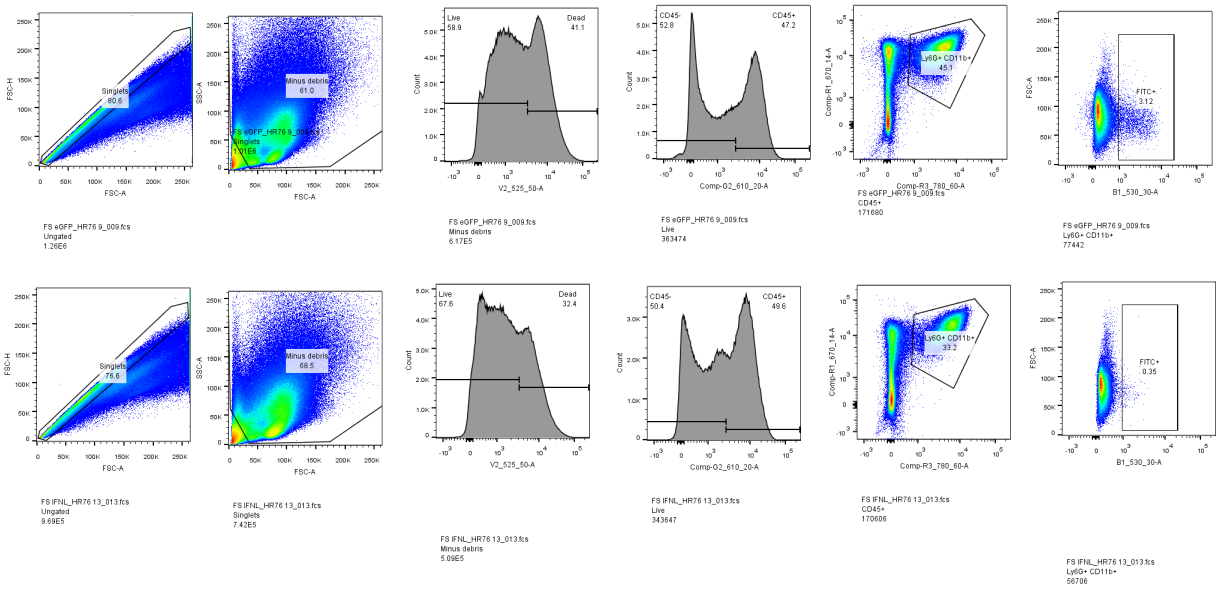

Figure 22: Gating strategy for identifying FITC+ neutrophils.

Mice were infected and flow cytometry was performed as described in Figure 5.6. Gating strategy for two representative mice is shown.

Appendix B -- Supplementary Materials and Methods

B.1 Real-Time PCR Primers

Mouse real-time PCR primers are listed below. They are proprietary primer and probe sets purchased from Life Technologies entitled TaqMan "Assay on Demand".

Table 3: List of mouse real-time PCR primers.

Gene Name	Assay ID
il22	Mm0044421_m1
ngal	Mm01324470_m1
reg3g	Mm00441127_m1
s100a8	Mm00496696_g1
s100a9	Mm00656925_m1
camp	Mm00438285_m1
itga4	Mm00439770_m1
itgb1	Mm01253230_m1
tlr2	Mm00442346_m1
ifna1	Mm03030145_gH
ifnb	Mm00439546_s1
ifng	Mm01168134_m1

B.2 *Staphylococcus aureus* Media Recipe

1) Mix the following in a 1L Erlenmeyer flask:

7.5 g	agar
15 g	yeast extract
10 g	casamino acids
1.24 g	Na_2HPO_4
0.205 g	KH_2PO_4
10 mg	$MgSO_4 \cdot 7H_2O$
3.75 mg	$MnSO_4 \cdot H_2O$
3.2 mg	$FeSO_4 \cdot 7H_2O$
3.2 mg	citric acid
450 ml	distilled water

2) pH to 7.3.

3) Autoclave.

4) Meanwhile, mix:

11.6 g	sodium pyruvate
50 ml	distilled water

5) Filter-sterilize sodium pyruvate mixture and add to autoclaved portion once it has cooled slightly.

6) Distribute 10 ml of media to sterile plates under cell culture hood, swirling to spread evenly and popping any bubbles with a sterile glass pipet tip.

To make broth, follow all above steps and exclude the addition of agar.

Bibliography

1. Isaacs A, Lindenmann J. 1957. Virus interference. I. The interferon. Proc R Soc Lond B Biol Sci 147:258-67.

2. Sheppard P, Kindsvogel W, Xu W, Henderson K, Schlutsmeyer S, Whitmore TE, Kuestner R, Garrigues U, Birks C, Roraback J, Ostrander C, Dong D, Shin J, Presnell S, Fox B, Haldeman B, Cooper E, Taft D, Gilbert T, Grant FJ, Tackett M, Krivan W, McKnight G, Clegg C, Foster D, Klucher KM. 2003. IL-28, IL-29 and their class II cytokine receptor IL-28R. Nat Immunol 4:63-8.

3. Kotenko SV, Gallagher G, Baurin VV, Lewis-Antes A, Shen M, Shah NK, Langer JA, Sheikh F, Dickensheets H, Donnelly RP. 2003. IFN-lambdas mediate antiviral protection through a distinct class II cytokine receptor complex. Nat Immunol 4:69-77.

4. Prokunina-Olsson L, Muchmore B, Tang W, Pfeiffer RM, Park H, Dickensheets H, Hergott D, Porter-Gill P, Mumy A, Kohaar I, Chen S, Brand N, Tarway M, Liu L, Sheikh F, Astemborski J, Bonkovsky HL, Edlin BR, Howell CD, Morgan TR, Thomas DL, Rehermann B, Donnelly RP, O'Brien TR. 2013. A variant upstream of IFNL3 (IL28B) creating a new interferon gene IFNL4 is associated with impaired clearance of hepatitis C virus. Nat Genet 45:164-71.

5. Hamming OJ, Terczynska-Dyla E, Vieyres G, Dijkman R, Jorgensen SE, Akhtar H, Siupka P, Pietschmann T, Thiel V, Hartmann R. 2013. Interferon lambda 4 signals via the IFNlambda receptor to regulate antiviral activity against HCV and coronaviruses. EMBO J 32:3055-65.

6. Gad HH, Dellgren C, Hamming OJ, Vends S, Paludan SR, Hartmann R. 2009. Interferon-lambda is functionally an interferon but structurally related to the interleukin-10 family. J Biol Chem 284:20869-75.

7. Reed C, Chaves SS, Daily Kirley P, Emerson R, Aragon D, Hancock EB, Butler L, Baumbach J, Hollick G, Bennett NM, Laidler MR, Thomas A, Meltzer MI, Finelli L. 2015. Estimating influenza disease burden from population-based surveillance data in the United States. PLoS One 10:e0118369.

8. Molinari NA, Ortega-Sanchez IR, Messonnier ML, Thompson WW, Wortley PM, Weintraub E, Bridges CB. 2007. The annual impact of seasonal influenza in the US: measuring disease burden and costs. Vaccine 25:5086-96.

9. Belser JA, Tumpey TM. 2018. The 1918 flu, 100 years later. Science 359:255.

10. Shrestha SS, Swerdlow DL, Borse RH, Prabhu VS, Finelli L, Atkins CY, Owusu-Edusei K, Bell B, Mead PS, Biggerstaff M, Brammer L, Davidson H, Jernigan D, Jhung MA, Kamimoto LA, Merlin TL, Nowell M, Redd SC, Reed C, Schuchat A, Meltzer MI. 2011. Estimating the burden of 2009 pandemic influenza A (H1N1) in the United States (April 2009-April 2010). Clin Infect Dis 52 Suppl 1:S75-82.

11. Marr LC, Tang JW, Van Mullekom J, Lakdawala SS. 2019. Mechanistic insights into the effect of humidity on airborne influenza virus survival, transmission and incidence. J R Soc Interface 16:20180298.

12. Su S, Fu X, Li G, Kerlin F, Veit M. 2017. Novel Influenza D virus: Epidemiology, pathology, evolution and biological characteristics. Virulence 8:1580-1591.

13. Alvarado-Facundo E, Gao Y, Ribas-Aparicio RM, Jimenez-Alberto A, Weiss CD, Wang W. 2015. Influenza virus M2 protein ion channel activity helps to maintain pandemic 2009 H1N1 virus hemagglutinin fusion competence during transport to the cell surface. J Virol 89:1975-85.

14. Bouvier NM, Palese P. 2008. The biology of influenza viruses. Vaccine 26 Suppl 4:D49-53.

15. Fulvini AA, Ramanunninair M, Le J, Pokorny BA, Arroyo JM, Silverman J, Devis R, Bucher D. 2011. Gene constellation of influenza A virus reassortants with high growth phenotype prepared as seed candidates for vaccine production. PLoS One 6:e20823.

16. Hegde NR. 2015. Cell culture-based influenza vaccines: A necessary and indispensable investment for the future. Hum Vaccin Immunother 11:1223-34.

17. Weir JP, Gruber MF. 2016. An overview of the regulation of influenza vaccines in the United States. Influenza Other Respir Viruses 10:354-60.

18. Harding AT, Heaton NS. 2018. Efforts to Improve the Seasonal Influenza Vaccine. Vaccines (Basel) 6.

19. Mohn KG, Smith I, Sjursen H, Cox RJ. 2018. Immune responses after live attenuated influenza vaccination. Hum Vaccin Immunother 14:571-578.

20. Piedra PA. 2019. Live Attenuated Influenza Vaccine: Will the Phoenix Rise Again? Pediatrics 143.

21. Dobson J, Whitley RJ, Pocock S, Monto AS. 2015. Oseltamivir treatment for influenza in adults: a meta-analysis of randomised controlled trials. Lancet 385:1729-1737.

22. Ebell MH, Call M, Shinholser J. 2013. Effectiveness of oseltamivir in adults: a meta-analysis of published and unpublished clinical trials. Fam Pract 30:125-33.

23. Qiu S, Shen Y, Pan H, Wang J, Zhang Q. 2015. Effectiveness and safety of oseltamivir for treating influenza: an updated meta-analysis of clinical trials. Infect Dis (Lond) 47:808-19.

24. Iwasaki A, Pillai PS. 2014. Innate immunity to influenza virus infection. Nat Rev Immunol 14:315-28.

25. Odendall C, Dixit E, Stavru F, Bierne H, Franz KM, Durbin AF, Boulant S, Gehrke L, Cossart P, Kagan JC. 2014. Diverse intracellular pathogens activate type III interferon expression from peroxisomes. Nat Immunol 15:717-26.

26. Lee SJ, Kim WJ, Moon SK. 2012. Role of the p38 MAPK signaling pathway in mediating interleukin-28A-induced migration of UMUC-3 cells. Int J Mol Med 30:945-52.

27. Pervolaraki K, Stanifer ML, Munchau S, Renn LA, Albrecht D, Kurzhals S, Senis E, Grimm D, Schroder-Braunstein J, Rabin RL, Boulant S. 2017. Type I and Type III Interferons Display Different Dependency on Mitogen-Activated Protein Kinases to Mount an Antiviral State in the Human Gut. Front Immunol 8:459.

28. Mahony R, Gargan S, Roberts KL, Bourke N, Keating SE, Bowie AG, O'Farrelly C, Stevenson NJ. 2017. A novel anti-viral role for STAT3 in IFN-alpha signalling responses. Cell Mol Life Sci 74:1755-1764.

29. Wang WB, Levy DE, Lee CK. 2011. STAT3 negatively regulates type I IFN-mediated antiviral response. J Immunol 187:2578-85.

30. Zhou Z, Hamming OJ, Ank N, Paludan SR, Nielsen AL, Hartmann R. 2007. Type III interferon (IFN) induces a type I IFN-like response in a restricted subset of cells through signaling pathways involving both the Jak-STAT pathway and the mitogen-activated protein kinases. J Virol 81:7749-58.

31. Caine EA, Scheaffer SM, Arora N, Zaitsev K, Artyomov MN, Coyne CB, Moley KH, Diamond MS. 2019. Interferon lambda protects the female reproductive tract against Zika virus infection. Nat Commun 10:280.

32. Kotenko SV, Durbin JE. 2017. Contribution of type III interferons to antiviral immunity: location, location, location. J Biol Chem 292:7295-7303.

33. Pervolaraki K, Rastgou Talemi S, Albrecht D, Bormann F, Bamford C, Mendoza JL, Garcia KC, McLauchlan J, Hofer T, Stanifer ML, Boulant S. 2018. Differential induction of interferon stimulated genes between type I and type III interferons is independent of interferon receptor abundance. PLoS Pathog 14:e1007420.

34. Wells AI, Coyne CB. 2018. Type III Interferons in Antiviral Defenses at Barrier Surfaces. Trends Immunol 39:848-858.

35. Klinkhammer J, Schnepf D, Ye L, Schwaderlapp M, Gad HH, Hartmann R, Garcin D, Mahlakoiv T, Staeheli P. 2018. IFN-lambda prevents influenza virus spread from the upper airways to the lungs and limits virus transmission. Elife 7.

36. Galani IE, Triantafyllia V, Eleminiadou EE, Koltsida O, Stavropoulos A, Manioudaki M, Thanos D, Doyle SE, Kotenko SV, Thanopoulou K, Andreakos E. 2017. Interferon-lambda Mediates Non-redundant Front-Line Antiviral Protection against Influenza Virus Infection without Compromising Host Fitness. Immunity 46:875-890 e6.

37. Jewell NA, Cline T, Mertz SE, Smirnov SV, Flano E, Schindler C, Grieves JL, Durbin RK, Kotenko SV, Durbin JE. 2010. Lambda interferon is the predominant interferon induced by influenza A virus infection in vivo. J Virol 84:11515-22.

38. Broggi A, Tan Y, Granucci F, Zanoni I. 2017. IFN-lambda suppresses intestinal inflammation by non-translational regulation of neutrophil function. Nat Immunol 18:1084-1093.

39. Rynda-Apple A, Robinson KM, Alcorn JF. 2015. Influenza and Bacterial Superinfection: Illuminating the Immunologic Mechanisms of Disease. Infect Immun 83:3764-70.

40. CDC. 2018. Influenza-Associated Pediatric Mortality. https://gis.cdc.gov/GRASP/Fluview/PedFluDeath.html. Accessed May 19.

41. Shang M, Blanton L, Brammer L, Olsen SJ, Fry AM. 2018. Influenza-Associated Pediatric Deaths in the United States, 2010-2016. Pediatrics 141.

42. Fainstein V, Musher DM, Cate TR. 1980. Bacterial adherence to pharyngeal cells during viral infection. J Infect Dis 141:172-6.

43. Siegel SJ, Roche AM, Weiser JN. 2014. Influenza promotes pneumococcal growth during coinfection by providing host sialylated substrates as a nutrient source. Cell Host Microbe 16:55-67.

44. Langelier C, Kalantar KL, Moazed F, Wilson MR, Crawford ED, Deiss T, Belzer A, Bolourchi S, Caldera S, Fung M, Jauregui A, Malcolm K, Lyden A, Khan L, Vessel K, Quan J, Zinter M, Chiu CY, Chow ED, Wilson J, Miller S, Matthay MA, Pollard KS, Christenson S, Calfee CS, DeRisi JL. 2018. Integrating host response and unbiased microbe detection for lower respiratory tract infection diagnosis in critically ill adults. Proc Natl Acad Sci U S A 115:E12353-E12362.

45. Eddens T, Kolls JK. 2012. Host defenses against bacterial lower respiratory tract infection. Curr Opin Immunol 24:424-30.

46. McNamee LA, Harmsen AG. 2006. Both influenza-induced neutrophil dysfunction and neutrophil-independent mechanisms contribute to increased susceptibility to a secondary Streptococcus pneumoniae infection. Infect Immun 74:6707-21.

47. Cooper GE, Pounce ZC, Wallington JC, Bastidas-Legarda LY, Nicholas B, Chidomere C, Robinson EC, Martin K, Tocheva AS, Christodoulides M, Djukanovic R, Wilkinson TM, Staples KJ. 2016. Viral Inhibition of Bacterial Phagocytosis by Human Macrophages: Redundant Role of CD36. PLoS One 11:e0163889.

48. Pang G, Clancy R, Cong M, Ortega M, Zhigang R, Reeves G. 2000. Influenza virus inhibits lysozyme secretion by sputum neutrophils in subjects with chronic bronchial sepsis. Am J Respir Crit Care Med 161:718-22.

49. Shepardson KM, Larson K, Morton RV, Prigge JR, Schmidt EE, Huber VC, Rynda-Apple A. 2016. Differential Type I Interferon Signaling Is a Master Regulator of Susceptibility to Postinfluenza Bacterial Superinfection. MBio 7.

50. Robinson KM, Ramanan K, Clay ME, McHugh KJ, Rich HE, Alcorn JF. 2018. Novel protective mechanism for interleukin-33 at the mucosal barrier during influenza-associated bacterial superinfection. Mucosal Immunol 11:199-208.

51. Scharf S, Zahlten J, Szymanski K, Hippenstiel S, Suttorp N, N'Guessan PD. 2012. Streptococcus pneumoniae induces human beta-defensin-2 and -3 in human lung epithelium. Exp Lung Res 38:100-10.

52. De Filippo K, Neill DR, Mathies M, Bangert M, McNeill E, Kadioglu A, Hogg N. 2014. A new protective role for S100A9 in regulation of neutrophil recruitment during invasive pneumococcal pneumonia. FASEB J 28:3600-8.

53. Robinson KM, McHugh KJ, Mandalapu S, Clay ME, Lee B, Scheller EV, Enelow RI, Chan YR, Kolls JK, Alcorn JF. 2014. Influenza A virus exacerbates Staphylococcus aureus pneumonia in mice by attenuating antimicrobial peptide production. J Infect Dis 209:865-75.

54. Li W, Moltedo B, Moran TM. 2012. Type I interferon induction during influenza virus infection increases susceptibility to secondary Streptococcus pneumoniae infection by negative regulation of gammadelta T cells. J Virol 86:12304-12.

55. Kudva A, Scheller EV, Robinson KM, Crowe CR, Choi SM, Slight SR, Khader SA, Dubin PJ, Enelow RI, Kolls JK, Alcorn JF. 2011. Influenza A inhibits Th17-mediated host defense against bacterial pneumonia in mice. J Immunol 186:1666-1674.

56. Sun K, Metzger DW. 2008. Inhibition of pulmonary antibacterial defense by interferon-gamma during recovery from influenza infection. Nat Med 14:558-64.

57. Small CL, Shaler CR, McCormick S, Jeyanathan M, Damjanovic D, Brown EG, Arck P, Jordana M, Kaushic C, Ashkar AA, Xing Z. 2010. Influenza infection leads to increased susceptibility to subsequent bacterial superinfection by impairing NK cell responses in the lung. J Immunol 184:2048-56.

58. Robinson KM, Lee B, Scheller EV, Mandalapu S, Enelow RI, Kolls JK, Alcorn JF. 2015. The role of IL-27 in susceptibility to post-influenza Staphylococcus aureus pneumonia. Respir Res 16:10.

59. van der Sluijs KF, van Elden LJ, Nijhuis M, Schuurman R, Pater JM, Florquin S, Goldman M, Jansen HM, Lutter R, van der Poll T. 2004. IL-10 is an important mediator of the enhanced susceptibility to pneumococcal pneumonia after influenza infection. J Immunol 172:7603-9.

60. Rynda-Apple A, Harmsen A, Erickson AS, Larson K, Morton RV, Richert LE, Harmsen AG. 2014. Regulation of IFN-gamma by IL-13 dictates susceptibility to secondary postinfluenza MRSA pneumonia. Eur J Immunol 44:3263-72.

61. Parker D, Martin FJ, Soong G, Harfenist BS, Aguilar JL, Ratner AJ, Fitzgerald KA, Schindler C, Prince A. 2011. Streptococcus pneumoniae DNA initiates type I interferon signaling in the respiratory tract. MBio 2:e00016-11.

62. Parker D, Cohen TS, Alhede M, Harfenist BS, Martin FJ, Prince A. 2012. Induction of type I interferon signaling by Pseudomonas aeruginosa is diminished in cystic fibrosis epithelial cells. Am J Respir Cell Mol Biol 46:6-13.

63. Scumpia PO, Botten GA, Norman JS, Kelly-Scumpia KM, Spreafico R, Ruccia AR, Purbey PK, Thomas BJ, Modlin RL, Smale ST. 2017. Opposing roles of Toll-like receptor and cytosolic DNA-STING signaling pathways for Staphylococcus aureus cutaneous host defense. PLoS Pathog 13:e1006496.

64. Wei H, Wang S, Chen Q, Chen Y, Chi X, Zhang L, Huang S, Gao GF, Chen JL. 2014. Suppression of interferon lambda signaling by SOCS-1 results in their excessive production during influenza virus infection. PLoS Pathog 10:e1003845.

65. Shahangian A, Chow EK, Tian X, Kang JR, Ghaffari A, Liu SY, Belperio JA, Cheng G, Deng JC. 2009. Type I IFNs mediate development of postinfluenza bacterial pneumonia in mice. J Clin Invest 119:1910-20.

66. Lee B, Robinson KM, McHugh KJ, Scheller EV, Mandalapu S, Chen C, Di YP, Clay ME, Enelow RI, Dubin PJ, Alcorn JF. 2015. Influenza-induced type I interferon enhances susceptibility to gram-negative and gram-positive bacterial pneumonia in mice. Am J Physiol Lung Cell Mol Physiol 309:L158-67.

67. Gopal R, Lee B, McHugh KJ, Rich HE, Ramanan K, Mandalapu S, Clay ME, Seger PJ, Enelow RI, Manni ML, Robinson KM, Rangel-Moreno J, Alcorn JF. 2018. STAT2 Signaling Regulates Macrophage Phenotype During Influenza and Bacterial Super-Infection. Front Immunol 9:2151.

68. Lee B, Gopal R, Manni ML, McHugh KJ, Mandalapu S, Robinson KM, Alcorn JF. 2017. STAT1 Is Required for Suppression of Type 17 Immunity during Influenza and Bacterial Superinfection. Immunohorizons 1:81-91.

69. Planet PJ, Parker D, Cohen TS, Smith H, Leon JD, Ryan C, Hammer TJ, Fierer N, Chen EI, Prince AS. 2016. Lambda Interferon Restructures the Nasal Microbiome and Increases Susceptibility to Staphylococcus aureus Superinfection. MBio 7:e01939-15.

70. Berical AC, Harris D, Dela Cruz CS, Possick JD. 2016. Pneumococcal Vaccination Strategies. An Update and Perspective. Ann Am Thorac Soc 13:933-44.

71. Redi D, Raffaelli CS, Rossetti B, De Luca A, Montagnani F. 2018. Staphylococcus aureus vaccine preclinical and clinical development: current state of the art. New Microbiol 41:208-213.

72. Ragle BE, Bubeck Wardenburg J. 2009. Anti-alpha-hemolysin monoclonal antibodies mediate protection against Staphylococcus aureus pneumonia. Infect Immun 77:2712-8.

73. Sause WE, Buckley PT, Strohl WR, Lynch AS, Torres VJ. 2016. Antibody-Based Biologics and Their Promise to Combat Staphylococcus aureus Infections. Trends Pharmacol Sci 37:231-241.

74. Escajadillo T, Nizet V. 2018. Pharmacological Targeting of Pore-Forming Toxins as Adjunctive Therapy for Invasive Bacterial Infection. Toxins (Basel) 10.

75. Tseng CW, Biancotti JC, Berg BL, Gate D, Kolar SL, Muller S, Rodriguez MD, Rezai-Zadeh K, Fan X, Beenhouwer DO, Town T, Liu GY. 2015. Increased Susceptibility of Humanized NSG Mice to Panton-Valentine Leukocidin and Staphylococcus aureus Skin Infection. PLoS Pathog 11:e1005292.

76. Prince A, Wang H, Kitur K, Parker D. 2017. Humanized Mice Exhibit Increased Susceptibility to Staphylococcus aureus Pneumonia. J Infect Dis 215:1386-1395.

77. Thomsen IP, Dumont AL, James DB, Yoong P, Saville BR, Soper N, Torres VJ, Creech CB. 2014. Children with invasive Staphylococcus aureus disease exhibit a potently neutralizing antibody response to the cytotoxin LukAB. Infect Immun 82:1234-42.

78. Thomsen IP, Sapparapu G, James DBA, Cassat JE, Nagarsheth M, Kose N, Putnam N, Boguslawski KM, Jones LS, Wood JB, Creech CB, Torres VJ, Crowe JE, Jr. 2017. Monoclonal Antibodies Against the Staphylococcus aureus Bicomponent Leukotoxin AB Isolated Following Invasive Human Infection Reveal Diverse Binding and Modes of Action. J Infect Dis 215:1124-1131.

79. Berends ETM, Zheng X, Zwack EE, Menager MM, Cammer M, Shopsin B, Torres VJ. 2019. Staphylococcus aureus Impairs the Function of and Kills Human Dendritic Cells via the LukAB Toxin. MBio 10.

80. Yoong P, Torres VJ. 2015. Counter inhibition between leukotoxins attenuates Staphylococcus aureus virulence. Nat Commun 6:8125.

81. Diep BA, Le VT, Visram ZC, Rouha H, Stulik L, Dip EC, Nagy G, Nagy E. 2016. Improved Protection in a Rabbit Model of Community-Associated Methicillin-Resistant Staphylococcus aureus Necrotizing Pneumonia upon Neutralization of Leukocidins in Addition to Alpha-Hemolysin. Antimicrob Agents Chemother 60:6333-40.

82. Rouha H, Weber S, Janesch P, Maierhofer B, Gross K, Dolezilkova I, Mirkina I, Visram ZC, Malafa S, Stulik L, Badarau A, Nagy E. 2018. Disarming Staphylococcus aureus from destroying human cells by simultaneously neutralizing six cytotoxins with two human monoclonal antibodies. Virulence 9:231-247.

83. Seiler F, Lepper PM, Bals R, Beisswenger C. 2014. Regulation and function of antimicrobial peptides in immunity and diseases of the lung. Protein Pept Lett 21:341-51.

84. Tjabringa GS, Ninaber DK, Drijfhout JW, Rabe KF, Hiemstra PS. 2006. Human cathelicidin LL-37 is a chemoattractant for eosinophils and neutrophils that acts via formyl-peptide receptors. Int Arch Allergy Immunol 140:103-12.

85. De Y, Chen Q, Schmidt AP, Anderson GM, Wang JM, Wooters J, Oppenheim JJ, Chertov O. 2000. LL-37, the neutrophil granule- and epithelial cell-derived cathelicidin, utilizes formyl peptide receptor-like 1 (FPRL1) as a receptor to chemoattract human peripheral blood neutrophils, monocytes, and T cells. J Exp Med 192:1069-74.

86. Elssner A, Duncan M, Gavrilin M, Wewers MD. 2004. A novel P2X7 receptor activator, the human cathelicidin-derived peptide LL37, induces IL-1 beta processing and release. J Immunol 172:4987-94.

87. Tjabringa GS, Aarbiou J, Ninaber DK, Drijfhout JW, Sorensen OE, Borregaard N, Rabe KF, Hiemstra PS. 2003. The antimicrobial peptide LL-37 activates innate immunity at the airway epithelial surface by transactivation of the epidermal growth factor receptor. J Immunol 171:6690-6.

88. Deslouches B, Phadke SM, Lazarevic V, Cascio M, Islam K, Montelaro RC, Mietzner TA. 2005. De novo generation of cationic antimicrobial peptides: influence of length and tryptophan substitution on antimicrobial activity. Antimicrob Agents Chemother 49:316-22.

89. Deslouches B, Islam K, Craigo JK, Paranjape SM, Montelaro RC, Mietzner TA. 2005. Activity of the de novo engineered antimicrobial peptide WLBU2 against Pseudomonas aeruginosa in human serum and whole blood: implications for systemic applications. Antimicrob Agents Chemother 49:3208-16.

90. Lin Q, Deslouches B, Montelaro RC, Di YP. 2018. Prevention of ESKAPE pathogen biofilm formation by antimicrobial peptides WLBU2 and LL37. Int J Antimicrob Agents 52:667-672.

91. Melvin JA, Lashua LP, Kiedrowski MR, Yang G, Deslouches B, Montelaro RC, Bomberger JM. 2016. Simultaneous Antibiofilm and Antiviral Activities of an Engineered Antimicrobial Peptide during Virus-Bacterium Coinfection. mSphere 1.

92. Hou M, Zhang N, Yang J, Meng X, Yang R, Li J, Sun T. 2013. Antimicrobial peptide LL-37 and IDR-1 ameliorate MRSA pneumonia in vivo. Cell Physiol Biochem 32:614-23.

93. Chen X, Takai T, Xie Y, Niyonsaba F, Okumura K, Ogawa H. 2013. Human antimicrobial peptide LL-37 modulates proinflammatory responses induced by cytokine milieus and double-stranded RNA in human keratinocytes. Biochem Biophys Res Commun 433:532-7.

94. Scott MG, Davidson DJ, Gold MR, Bowdish D, Hancock RE. 2002. The human antimicrobial peptide LL-37 is a multifunctional modulator of innate immune responses. J Immunol 169:3883-91.

95. Muller S, Wolf AJ, Iliev ID, Berg BL, Underhill DM, Liu GY. 2015. Poorly Cross-Linked Peptidoglycan in MRSA Due to mecA Induction Activates the Inflammasome and Exacerbates Immunopathology. Cell Host Microbe 18:604-12.

96. Wolf AJ, Liu GY, Underhill DM. 2017. Inflammatory properties of antibiotic-treated bacteria. J Leukoc Biol 101:127-134.

97. Siegel MD. March 28, 2019 2019. Acute respiratory distress syndrome: Prognosis and outcomes in adults. https://www.uptodate.com/contents/acute-respiratory-distress-syndrome-prognosis-and-outcomes-in-adults. Accessed May 19, 2019.

98. Chen C, Deslouches B, Montelaro RC, Di YP. 2018. Enhanced efficacy of the engineered antimicrobial peptide WLBU2 via direct airway delivery in a murine model of Pseudomonas aeruginosa pneumonia. Clin Microbiol Infect 24:547 e1-547 e8.

99. Mantero M, Tarsia P, Gramegna A, Henchi S, Vanoni N, Di Pasquale M. 2017. Antibiotic therapy, supportive treatment and management of immunomodulation-inflammation response in community acquired pneumonia: review of recommendations. Multidiscip Respir Med 12:26.

100. Lazear HM, Schoggins JW, Diamond MS. 2019. Shared and Distinct Functions of Type I and Type III Interferons. Immunity 50:907-923.

101. Hall OJ, Limjunyawong N, Vermillion MS, Robinson DP, Wohlgemuth N, Pekosz A, Mitzner W, Klein SL. 2016. Progesterone-Based Therapy Protects Against Influenza by Promoting Lung Repair and Recovery in Females. PLoS Pathog 12:e1005840.

102. Hall OJ, Nachbagauer R, Vermillion MS, Fink AL, Phuong V, Krammer F, Klein SL. 2017. Progesterone-Based Contraceptives Reduce Adaptive Immune Responses and Protection against Sequential Influenza A Virus Infections. J Virol 91.

103. Vom Steeg LG, Vermillion MS, Hall OJ, Alam O, McFarland R, Chen H, Zirkin B, Klein SL. 2016. Age and testosterone mediate influenza pathogenesis in male mice. Am J Physiol Lung Cell Mol Physiol 311:L1234-L1244.

104. Anand S, Mande SS. 2018. Diet, Microbiota and Gut-Lung Connection. Front Microbiol 9:2147.

105. Blazek K, Eames HL, Weiss M, Byrne AJ, Perocheau D, Pease JE, Doyle S, McCann F, Williams RO, Udalova IA. 2015. IFN-lambda resolves inflammation via suppression of neutrophil infiltration and IL-1beta production. J Exp Med 212:845-53.

106. Zhang H, Luo J, Alcorn JF, Chen K, Fan S, Pilewski J, Liu A, Chen W, Kolls JK, Wang J. 2017. AIM2 Inflammasome Is Critical for Influenza-Induced Lung Injury and Mortality. J Immunol 198:4383-4393.

107. Marie I, Durbin JE, Levy DE. 1998. Differential viral induction of distinct interferon-alpha genes by positive feedback through interferon regulatory factor-7. EMBO J 17:6660-9.

108. Ye J, Maniatis T. 2011. Negative regulation of interferon-beta gene expression during acute and persistent virus infections. PLoS One 6:e20681.

109. Francois-Newton V, Magno de Freitas Almeida G, Payelle-Brogard B, Monneron D, Pichard-Garcia L, Piehler J, Pellegrini S, Uze G. 2011. USP18-based negative feedback control is induced by type I and type III interferons and specifically inactivates interferon alpha response. PLoS One 6:e22200.

110. Rigby KM, DeLeo FR. 2012. Neutrophils in innate host defense against Staphylococcus aureus infections. Semin Immunopathol 34:237-59.

111. Corbin BD, Seeley EH, Raab A, Feldmann J, Miller MR, Torres VJ, Anderson KL, Dattilo BM, Dunman PM, Gerads R, Caprioli RM, Nacken W, Chazin WJ, Skaar EP. 2008. Metal chelation and inhibition of bacterial growth in tissue abscesses. Science 319:962-5.

112. Fried MW, Shiffman ML, Reddy KR, Smith C, Marinos G, Goncales FL, Jr., Haussinger D, Diago M, Carosi G, Dhumeaux D, Craxi A, Lin A, Hoffman J, Yu J. 2002. Peginterferon alfa-2a plus ribavirin for chronic hepatitis C virus infection. N Engl J Med 347:975-82.

113. Manns MP, McHutchison JG, Gordon SC, Rustgi VK, Shiffman M, Reindollar R, Goodman ZD, Koury K, Ling M, Albrecht JK. 2001. Peginterferon alfa-2b plus ribavirin compared with interferon alfa-2b plus ribavirin for initial treatment of chronic hepatitis C: a randomised trial. Lancet 358:958-65.

114. Tasaka S, Richer SE, Mizgerd JP, Doerschuk CM. 2002. Very late antigen-4 in CD18-independent neutrophil emigration during acute bacterial pneumonia in mice. Am J Respir Crit Care Med 166:53-60.

115. Ramamoorthy C, Sasaki SS, Su DL, Sharar SR, Harlan JM, Winn RK. 1997. CD18 adhesion blockade decreases bacterial clearance and neutrophil recruitment after intrapulmonary E. coli, but not after S. aureus. J Leukoc Biol 61:167-72.

116. Miller LS, Cho JS. 2011. Immunity against Staphylococcus aureus cutaneous infections. Nat Rev Immunol 11:505-18.

117. de Haas CJ, Veldkamp KE, Peschel A, Weerkamp F, Van Wamel WJ, Heezius EC, Poppelier MJ, Van Kessel KP, van Strijp JA. 2004. Chemotaxis inhibitory protein of Staphylococcus aureus, a bacterial antiinflammatory agent. J Exp Med 199:687-95.

118. Smith EJ, Visai L, Kerrigan SW, Speziale P, Foster TJ. 2011. The Sbi protein is a multifunctional immune evasion factor of Staphylococcus aureus. Infect Immun 79:3801-9.

119. Dossett JH, Kronvall G, Williams RC, Jr., Quie PG. 1969. Antiphagocytic effects of staphylococcal protein A. J Immunol 103:1405-10.

120. Chen YG, Zhang Y, Deng LQ, Chen H, Zhang YJ, Zhou NJ, Yuan K, Yu LZ, Xiong ZH, Gui XM, Yu YR, Wu XM, Min WP. 2016. Control of Methicillin-Resistant Staphylococcus aureus Pneumonia Utilizing TLR2 Agonist Pam3CSK4. PLoS One 11:e0149233.

121. Fournier B. 2012. The function of TLR2 during staphylococcal diseases. Front Cell Infect Microbiol 2:167.

122. Davidson S, McCabe TM, Crotta S, Gad HH, Hessel EM, Beinke S, Hartmann R, Wack A. 2016. IFNlambda is a potent anti-influenza therapeutic without the inflammatory side effects of IFNalpha treatment. EMBO Mol Med 8:1099-112.

123. Canini L, Conway JM, Perelson AS, Carrat F. 2014. Impact of different oseltamivir regimens on treating influenza A virus infection and resistance emergence: insights from a modelling study. PLoS Comput Biol 10:e1003568.

124. Sautto GA, Kirchenbaum GA, Ross TM. 2018. Towards a universal influenza vaccine: different approaches for one goal. Virol J 15:17.

125. Robertson CM, Perrone EE, McConnell KW, Dunne WM, Boody B, Brahmbhatt T, Diacovo MJ, Van Rooijen N, Hogue LA, Cannon CL, Buchman TG, Hotchkiss RS, Coopersmith CM. 2008. Neutrophil depletion causes a fatal defect in murine pulmonary Staphylococcus aureus clearance. J Surg Res 150:278-85.

126. Hook JL, Islam MN, Parker D, Prince AS, Bhattacharya S, Bhattacharya J. 2018. Disruption of staphylococcal aggregation protects against lethal lung injury. J Clin Invest 128:1074-1086.

127. Hunninghake GW, Gadek JE, Kawanami O, Ferrans VJ, Crystal RG. 1979. Inflammatory and immune processes in the human lung in health and disease: evaluation by bronchoalveolar lavage. Am J Pathol 97:149-206.

128. Schumacher TN, Tsomides TJ. 2001. In vitro radiolabeling of peptides and proteins. Curr Protoc Protein Sci Chapter 3:Unit 3 3.

129. Jeannoel M, Casalegno JS, Ottmann M, Badiou C, Dumitrescu O, Lina B, Lina G. 2018. Synergistic Effects of Influenza and Staphylococcus aureus Toxins on Inflammation Activation and Cytotoxicity in Human Monocytic Cell Lines. Toxins (Basel) 10.

130. Rudd JM, Pulavendran S, Ashar HK, Ritchey JW, Snider TA, Malayer JR, Marie M, Chow VTK, Narasaraju T. 2019. Neutrophils Induce a Novel Chemokine Receptors Repertoire During Influenza Pneumonia. Front Cell Infect Microbiol 9:108.

131. Rivera A. 2019. Interferon Lambda's New Role as Regulator of Neutrophil Function. J Interferon Cytokine Res doi:10.1089/jir.2019.0036.

132. Britto CJ, Niu N, Khanal S, Huleihel L, Herazo-Maya JD, Thompson A, Sauler M, Slade MD, Sharma L, Dela Cruz CS, Kaminski N, Cohn LE. 2019. BPIFA1 regulates lung neutrophil recruitment and interferon signaling during acute inflammation. Am J Physiol Lung Cell Mol Physiol 316:L321-L333.

133. Ye L, Schnepf D, Becker J, Ebert K, Tanriver Y, Bernasconi V, Gad HH, Hartmann R, Lycke N, Staeheli P. 2019. Interferon-lambda enhances adaptive mucosal immunity by boosting release of thymic stromal lymphopoietin. Nat Immunol 20:593-601.

134. Kelly A, Robinson MW, Roche G, Biron CA, O'Farrelly C, Ryan EJ. 2016. Immune Cell Profiling of IFN-lambda Response Shows pDCs Express Highest Level of IFN-lambdaR1 and Are Directly Responsive via the JAK-STAT Pathway. J Interferon Cytokine Res 36:671-680.

135. Finotti G, Tamassia N, Calzetti F, Fattovich G, Cassatella MA. 2016. Endogenously produced TNF-alpha contributes to the expression of CXCL10/IP-10 in IFN-lambda3-activated plasmacytoid dendritic cells. J Leukoc Biol 99:107-19.

136. Werder RB, Lynch JP, Simpson JC, Zhang V, Hodge NH, Poh M, Forbes-Blom E, Kulis C, Smythe ML, Upham JW, Spann K, Everard ML, Phipps S. 2018. PGD2/DP2 receptor activation promotes severe viral bronchiolitis by suppressing IFN-lambda production. Sci Transl Med 10.

137. Garcia-Sastre A. 2013. Lessons from lipids in the fight against influenza. Cell 154:22-3.

138. Won J, Gil CH, Jo A, Kim HJ. 2019. Inhaled delivery of Interferon-lambda restricts epithelial-derived Th2 inflammation in allergic asthma. Cytokine 119:32-36.